

EMS Lib

Q  
880  
N47  
1976  
v.1



## JOINT ORGANIZING COMMITTEE

GARP  
PUBLICATIONS  
SERIES

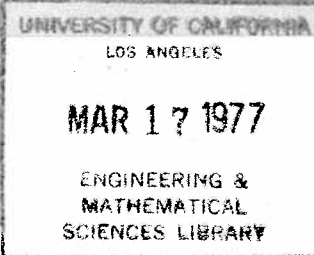
No. 17

NUMERICAL METHODS  
USED IN  
ATMOSPHERIC MODELS

ENGINEERING & MATHEMATICAL  
SCIENCES LIBRARY

UNIVERSITY OF CALIFORNIA  
LOS ANGELES, CALIF. 90024

VOLUME I



INTERNATIONAL COUNCIL  
OF SCIENTIFIC UNIONS

WORLD METEOROLOGICAL  
ORGANIZATION

GLOBAL ATMOSPHERIC RESEARCH PROGRAMME (GARP)

WMO-ICSU Joint Organizing Committee

## THE GLOBAL ATMOSPHERIC RESEARCH PROGRAMME

The Global Atmospheric Research Programme (GARP) is a programme for studying those physical processes in the troposphere and stratosphere that are essential for an understanding of:

- (a) The transient behaviour of the atmosphere as manifested in the large-scale fluctuations which control changes of the weather; this would lead to increasing the accuracy of forecasting over periods from one day to several weeks;
- (b) The factors that determine the statistical properties of the general circulation of the atmosphere which would lead to better understanding of the physical basis of climate.

This programme consists of two distinct parts, which are, however, closely inter-related:

- (i) The design and testing by computational methods of a series of theoretical models of relevant aspects of the atmosphere's behaviour to permit an increasingly precise description of the significant physical processes and their interactions;
- (ii) Observational and experimental studies of the atmosphere to provide the data required for the design of such theoretical models and the testing of their validity.

## NUMERICAL METHODS USED IN ATMOSPHERIC MODELS

By F. Mesinger and A. Arakawa

VOLUME I

### JOINT ORGANIZING COMMITTEE (JOC)

Prof. B. Bolin	Dr. C. Leith
Dr. P. K. Das	Prof. P. Morel
Acad. E. K. Fedorov	Acad. A. M. Oboukhov
Prof. K. Gambo	Prof. J. Smagorinsky ( <i>Chairman</i> )
Prof. K. Hasselmann	Prof. R. W. Stewart
Dr. J. T. Houghton	Dr. G. B. Tucker ( <i>Vice-chairman</i> )

### JOINT PLANNING STAFF (JPS)

Prof. B. R. Döös (*Director*)

GARP PUBLICATIONS SERIES No. 17

August 1976

## SUMMARY

This publication is discussing methods that are used for the solution of hydrodynamic governing equations in numerical models of the atmosphere. The number of methods in use in these models is, one might find, surprisingly great; thus, in addition to analysis of problems involved and techniques used for investigation of properties of various schemes, a discussion is included only of schemes which are more widely used, or which are expected by the authors to become more widely used in the near future.

The present volume is restricted to grid point finite difference methods, and, furthermore, to problems and methods used for time and horizontal space differencing. One remaining topic of the horizontal space differencing, that of the numerical solution of the advection equation with *two* dependent variables (advection terms of the two-dimensional primitive equations) will be included in the Volume II of the publication.

In Chapter I of this volume, following a short historical introduction on the development and use of numerical methods in atmospheric models, available methods for numerical solution of the differential equations governing the atmosphere are briefly reviewed. Then, basic elements of the finite difference method for solving these equations are introduced. Finally, the concept of stability of finite difference equations, and methods for testing the stability of these equations, are considered at some length.

Chapter II presents a discussion of time differencing schemes which are elementary enough so that they can be defined using a simple ordinary differential equation, with *one* dependent variable. After defining a number of such schemes, behaviour of numerical solutions is investigated which are obtained when these schemes are used for two specific ordinary differential equations:

---

This volume is based on a revised translation of a part of the textbook on dynamic meteorology, written by the first of the present authors, for senior year students of the Department of Meteorology, University of Belgrade. In writing the translated part of that textbook, however, extensive use was made of lecture notes written

oscillation (or frequency) equation, and friction equation. Discussion of the leapfrog scheme includes a more detailed analysis of the computational mode problem.

Chapter III deals with the numerical solution of those forms of the advection equation which describe advection of *one* dependent variable. Schemes are analysed first considering the simplest one-dimensional linear advection equation, with special emphasis given to the problems of phase speed errors and computational dispersion, and group velocity errors. Then a brief account is included of the extension to two space dimensions. Finally, nonlinear advection equation is considered. Aliasing error and nonlinear instability is discussed, and a review is given of methods used to suppress or prevent nonlinear instability in atmospheric numerical models, including a detailed exposition of the principle of the Arakawa method.

In Chapter IV schemes and problems related to the numerical solution of the gravity and gravity-inertia wave equations are considered. First, a discussion is given of the effects of space differencing on the numerical solution of the gravity wave equations. Having now *two* or *three* dependent variables, the problem of the space distribution of variables becomes of interest. Considering gravity-inertia wave equations, five different space distributions are analysed with respect to their effect on the geostrophic adjustment process. Then, a review is given of schemes and methods used to accomplish an economical use of computer time and/or elimination of computational modes in handling the gravity wave terms — the Eliassen grid, economical explicit schemes, the semi-implicit scheme, and the splitting method. Finally, as the gravity waves can generate a false space and/or time noise in the calculations, some techniques available for prevention or suppression of such space (two-grid-interval) and time noise.

---

by A. Arakawa for his course 212A, Numerical Methods in Dynamic Meteorology, that he has been teaching at the Department of Meteorology, University of California at Los Angeles. The revised translation was read and further revised by A. Arakawa and, finally, edited by M. J. P. Cullen of the Meteorological Office.

## RÉSUMÉ

Cette publication passe en revue les méthodes utilisées pour résoudre les équations hydrodynamiques clés dans les modèles numériques de l'atmosphère. On peut constater que le nombre de ces méthodes est étonnamment grand ; en conséquence, après avoir analysé le problème posé et les méthodes mises en œuvre pour étudier les propriétés des divers systèmes, les auteurs ne considèrent que les systèmes les plus couramment utilisés ou ceux dont ils estiment qu'ils le seront à leur tour très prochainement.

Le présent volume ne traite que des méthodes des différences finies aux points de grille et, qui plus est, des problèmes et méthodes utilisés pour la différenciation dans le temps et l'espace horizontal. Un sujet touchant la différenciation spatiale horizontale, qui a été laissé de côté, à savoir la solution numérique de l'équation d'advection avec *deux* variables dépendantes (termes d'advection des équations générales à deux dimensions), sera traité dans le Volume II de la publication.

Dans le chapitre I du présent volume, après une brève introduction historique dans laquelle ils rappellent comment les méthodes numériques ont été mises au point et utilisées dans les modèles de l'atmosphère, les auteurs font un rapide tour d'horizon des diverses méthodes disponibles pour résoudre numériquement les équations différentielles qui régissent l'atmosphère. Ensuite, ils exposent les éléments fondamentaux de la méthode des différences finies pour la résolution de ces équations. Enfin, ils développent le concept de stabilité des équations aux différences finies et les méthodes permettant de vérifier la stabilité de ces équations.

Le chapitre II expose les systèmes de différenciation dans le temps qui sont suffisamment élémentaires pour qu'on puisse les définir au moyen d'une simple équation différentielle ordinaire à *une* variable dépendante. Après avoir défini un certain nombre de ces systèmes, les auteurs étudient le comportement des solutions numériques obtenues lorsqu'on applique ces systèmes pour résoudre deux équations différentielles ordinaires particulières : équation d'oscillation (ou de fréquence) et

---

Ce volume est fondé sur une version révisée de la traduction d'une partie du manuel de météorologie dynamique, rédigé par le premier des auteurs cités à l'intention des étudiants du Département de météorologie de l'Université de Belgrade. Pour la traduction de cette partie dudit manuel, il a toutefois été fait largement usage des notes rédigées par A. Arakawa pour le cours 212A « Méthodes

équation du frottement. Lors de l'étude du système dit « saute-mouton », les auteurs analysent de façon plus détaillée le problème du mode de calcul.

Le chapitre III traite de la résolution numérique des formes de l'équation d'advection qui décrivent l'advection d'*une* variable dépendante. Les auteurs analysent les systèmes en considérant d'abord l'équation d'advection linéaire la plus simple à une dimension et en insistant particulièrement sur les problèmes d'erreur de vitesse de phase et de dispersion du calcul, ainsi que sur les erreurs de vitesse de groupe. Ils examinent ensuite brièvement l'extension à deux dimensions. Finalement, ils considèrent l'équation d'advection non linéaire et analysent les problèmes des erreurs dues aux variantes de traitement et d'instabilité non linéaire. Les auteurs passent en revue les différentes méthodes utilisées pour éliminer ou empêcher l'instabilité non linéaire dans les modèles numériques de l'atmosphère, ce qui les conduit à exposer en détail le principe de la méthode d'Arakawa.

Le chapitre IV traite des systèmes et des problèmes relatifs à la solution numérique des équations des ondes de gravité et de gravité-inertie. Les auteurs exposent d'abord les effets de la différenciation dans l'espace sur la solution numérique des équations des ondes de gravité. Du fait qu'on a maintenant *deux* ou *trois* variables dépendantes, le problème de la distribution spatiale des variables revêt de l'intérêt. En ce qui concerne les équations des ondes de gravité-inertie, les auteurs analysent cinq distributions spatiales différentes quant à l'influence qu'elles exercent sur le processus d'ajustement géostrophique. Ensuite, ils passent en revue les systèmes et les méthodes mis en œuvre pour utiliser rationnellement le temps d'ordinateur ou éliminer certains modes de calcul lors du traitement des termes des ondes de gravité — la grille d'Eliassen, les systèmes explicites économiques, le système implicite et la méthode de fractionnement. Finalement, étant donné que les ondes de gravité peuvent engendrer dans les calculs un bruit spatial et/ou temporel erroné, les auteurs décrivent certaines méthodes qui peuvent être utilisées pour éliminer ou supprimer ce bruit spatial (double pas de grille) ou temporel.

---

numériques appliquées en météorologie dynamique » qu'il donne au Département de météorologie de l'Université de Californie, à Los Angeles. La traduction révisée a été revue par A. Arakawa, puis mise au point définitivement par M. J. P. Cullen du Meteorological Office.

EMS  
 LIB  
 880  
 M47  
 1976  
 v. 1

## TABLE OF CONTENTS

	Page
<b>FOREWORD . . . . .</b>	<b>v</b>
<b>SUMMARY . . . . .</b>	<b>vi</b>
<b>I. INTRODUCTION ; GENERAL REMARKS ABOUT GRID POINT METHODS . . . . .</b>	<b>1</b>
1. Historical introduction . . . . .	1
2. Methods for the numerical solution of the equations of motion . . . . .	1
3. Basic elements of the grid point method . . . . .	2
4. Finite difference schemes . . . . .	3
5. Convergence . . . . .	5
6. Stability . . . . .	6
<b>II. TIME DIFFERENCING SCHEMES . . . . .</b>	<b>9</b>
1. Definitions of some schemes . . . . .	9
2. Properties of schemes applied to the oscillation equation . . . . .	11
3. Properties of schemes applied to the friction equation . . . . .	19
4. A combination of schemes . . . . .	21
<b>III. THE ADVECTION EQUATION . . . . .</b>	<b>22</b>
1. Schemes with centered second-order space differencing . . . . .	22
2. Computational dispersion . . . . .	26
3. Schemes with uncentered space differencing . . . . .	30
4. Schemes with centered fourth-order space differencing . . . . .	33
5. The two-dimensional advection equation . . . . .	34
6. Aliasing error and nonlinear instability . . . . .	35
7. Suppression and prevention of nonlinear instability . . . . .	37
<b>IV. THE GRAVITY AND GRAVITY-INERTIA WAVE EQUATION . . . . .</b>	<b>43</b>
1. One-dimensional gravity waves: centered space differencing . . . . .	43
2. Two-dimensional gravity waves . . . . .	44
3. Gravity-inertia waves and space distribution of variables . . . . .	46
4. Time differencing; the leapfrog scheme and the Eliassen grid . . . . .	50
5. Economical explicit schemes . . . . .	53
6. Implicit and semi-implicit schemes . . . . .	55
7. The splitting or Marchuk method . . . . .	58
8. Two-grid-interval noise . . . . .	59
9. Time noise and time filtering . . . . .	61
10. Dissipation in numerical schemes . . . . .	62

## CHAPTER I

### INTRODUCTION; GENERAL REMARKS ABOUT GRID POINT METHODS

In this chapter, following a short historical introduction on the development and use of numerical methods in atmospheric models, methods available for numerical solution of the differential equations governing the atmosphere will be briefly reviewed. Then, basic elements of the finite difference method for solving these equations will be introduced. Finally, the concept of stability of finite difference equations, and methods for testing the stability of such equations, will be discussed at some length.

#### 1. Historical introduction

It is considered that Wilhelm Bjerknes (1904) was the first to point out that the future state of the atmosphere can in principle be obtained by an integration of differential equations which govern the behaviour of the atmosphere, using as initial values fields describing an observed state of the atmosphere. Such an integration performed using numerical methods is called *numerical weather prediction*. When, however, a numerical integration is performed starting from fictitious initial fields, it is called *numerical simulation*.

A first practical attempt at a numerical weather prediction was made by Richardson. After very tedious and time-consuming computations, carried out mostly during the First World War, Richardson obtained a totally unacceptable result. Despite this, he described his method and results in a book (Richardson, 1922), and this is today one of the most famous in meteorology.

The wrong result obtained by Richardson, and his estimate that 64,000 men are necessary to advance the calculations as fast as the weather itself is advancing, left some doubt as to whether the method would be of practical use. A number of developments that followed, however, improved the situation. Courant, Friedrichs and Lewy (1928) found that space and time increments in integrations of this type have to meet a certain stability criterion. Mainly due to the work of Rossby in the late 1930's, it became understood that even a rather simple equation, that describing the conservation of absolute vorticity following the motion of air particles, suffices for an approximate description of large-scale motions of the atmosphere. Finally, in 1945, the first electronic computer ENIAC (Electronic Numerical Integrator and Computer)

was constructed. The absolute vorticity conservation equation, and this first electronic computer, were used by Charney, Fjørtoft and von Neumann in the late 1940's for the first successful numerical forecast (Charney *et al.*, 1950).

Much faster computers, and improved understanding of computational problems, now also enable long-term integrations of the basic primitive equations. It is generally considered that integration of the primitive equations enables easier incorporation of various physical processes than the integration of modified equations, that is, integration of the divergence and vorticity equations. Thus, it is mostly the primitive equations that are used today for practical numerical forecasting by meteorological services. Charts obtained by numerical forecasting are used by synopticians in these services as the principal basis for decisions on forecasts issued for public use.

A number of research groups have been actively engaged for more than a decade in development of models for the numerical simulation of the general circulation of the atmosphere. In such simulations starting from a fictitious initial state, e.g. an isothermal and motionless atmosphere, is often considered to be an advantage for the experiments. It enables a test of the ability of the computational and physical schemes of the model to simulate an atmosphere with statistical properties similar to those of the real atmosphere, with no, or not much, prior information on these properties.

Numerical models are also very frequently developed for studies of some smaller-scale atmospheric phenomena. Foremost among these are studies of the cumulus convection problem, and simulation of processes within the planetary boundary layer. In this text, however, we shall primarily have in mind the application of numerical methods to prediction and simulation of large-scale atmospheric motions.

#### 2. Methods for the numerical solution of the equations of motion

Numerical solution of the equations of motion today in most cases is performed using the *grid point method*. In this method a set of points is introduced in the region of interest and dependent variables are initially defined

and subsequently computed at these points. This set of points is called the *grid*. The words *mesh* or *lattice* are also used. It is necessary to have the grid points at fixed locations in the horizontal. This means that, according to the Eulerian system of equations, space and time coordinates are chosen as independent variables.

A number of attempts have been made to develop atmospheric models using an approach which is at least partly Lagrangian. Serious difficulties are encountered when a straightforward numerical integration of the Lagrangian system of equations is undertaken. However, it is possible to construct methods with some Lagrangian properties; for example, to have some or all of the computation points moving with the fluid. In hydrodynamics a number of such methods have proved to be very useful, especially for some problems which are not amenable to treatment by a strictly Eulerian technique (e.g. Harlow and Amsden, 1971). However, in meteorology the performance of Lagrangian or semi-Lagrangian models that have so far been developed has not been quite satisfactory. A discussion of one way of constructing a Lagrangian model, and a review of earlier attempts, can be found in a paper by Mesinger (1971).

Another possible approach is to express the spatial dependence of the variables in terms of a series of orthogonal functions, and then substitute this into the governing equations. In this way the equations reduce to a set of ordinary differential equations, so that the coefficients of the series can be computed as functions of time. This is the *spectral method* of solving the governing equations. Until relatively recently it was considered that in efficiency the spectral method could not be competitive with the grid point method. But the use of the fast Fourier transform has completely changed the situation and investigation of spectral methods is now the subject of intensive research.

In the following we shall consider the technique of using the grid point method, and the problems associated with it, using grid of computation points fixed in space. This is the most direct way of solving the equations of motion numerically. Furthermore, knowledge of this method is necessary for the investigation and understanding of the relative merits of other alternatives mentioned in this section.

### 3. Basic elements of the grid point method

With the grid point method, the most common way of solving the governing equations is to find approximate expressions for derivatives appearing in the equations. These approximate expressions are defined using only values of the dependent variables at the grid points, and at discrete time intervals. Thus, they are formed

using differences of dependent variables over finite space and time intervals; for that reason this approach is called the *finite difference method*. The approximations for derivatives are then used to construct a system of algebraic equations that approximates the governing partial differential equations. This algebraic system is considered valid at each of the interior grid points of the computation region. For the initial time and at space boundary points, additional constraints or equations are defined that approximate the initial and boundary conditions as required by the physics of the problem. The set of algebraic equations obtained in this way is then solved, usually using an electronic computer, by a suitable step-wise procedure.

We shall now consider some basic elements of the finite difference method. For simplicity, we start by considering a function of one independent variable

$$u = u(x).$$

The function  $u$  is a solution to a differential equation that we are interested in. We want to find an approximation to this solution in a bounded region  $R$  of the independent variable, having a length  $L$ . The simplest way of introducing a set of grid points is to require that they divide the region  $R$  into an integer number of intervals of equal length  $\Delta x$ . This length  $\Delta x$  is called the *grid interval*, or *grid length*. Let us denote the number of grid intervals by  $J$ . It is convenient to locate the origin of the  $x$  axis at the left-hand end of the region  $R$ . Thus, we are looking for approximations to  $u(x)$  at discrete points  $x = j\Delta x$ , where  $j$  takes integer values  $0, 1, 2, \dots, J$ . These approximate values we shall denote by

$$u_j = u_j(j\Delta x).$$

Thus, we are interested in finding  $J + 1$  values  $u_j$ .

Knowledge of a discrete set of values  $u_j$ , even if the approximations were perfect, offers, obviously, less information than knowledge of the function  $u(x)$ . Let us briefly consider the situation in that respect. We shall very often find it convenient to think of the function  $u(x)$  as being formed by a sum of its Fourier components, that is

$$u(x) = \frac{a_0}{2} + \sum_{n \geq 1} \left( a_n \cos 2\pi n \frac{x}{L} + b_n \sin 2\pi n \frac{x}{L} \right).$$

Now, the available  $J + 1$  values  $u_j$  do not enable the computation of all of the coefficients  $a_n, b_n$ ; rather, they can be used to compute only  $J + 1$  different coefficients. A natural choice is to assume that the  $J + 1$  values  $u_j$  define the near value  $a_0$  and as many as possible of the coefficients of the Fourier components at

the long wave length end of the series, that is, coefficients for  $n = 1, 2, 3, \dots, \frac{J}{2}$ . Of these components, the one with the shortest wavelength will have  $n = J/2$ , with the wave length

$$\frac{L}{n} = \frac{2L}{J} = \frac{2L}{L/\Delta x} = 2\Delta x.$$

Having made that choice, we can say that with values  $u_j$  at discrete points  $x = j\Delta x$  it is not possible to resolve waves with wave length shorter than  $2\Delta x$ .

Now let us consider the differences between values  $u_j$  that will be used to construct approximations to derivatives. These differences are called *finite differences*. They can be calculated over one or more of the intervals  $\Delta x$ . Depending on the relation of the points from which the values are taken to the point where the derivative is required, they can be *centered* or *uncentered*. An uncentered difference is, for example, the *forward difference*

$$\Delta u_j \equiv u_{j+1} - u_j.$$

More often centered (or *central*) differences are used, such as

$$\delta u_{j+\frac{1}{2}} \equiv u_{j+1} - u_j.$$

In a centered difference the difference is between values symmetrical about the point where the difference is being calculated.

One way to construct an approximation to a differential equation is to simply replace the derivatives by appropriate *finite difference quotients*. For example, for the first derivative one can use the approximation

$$\left( \frac{du}{dx} \right)_j \rightarrow \frac{u_{j+1} - u_j}{\Delta x}. \quad (3.1)$$

The finite difference quotient here is, of course, only one of many possible approximations to the first derivative at point  $j$ .

If a finite difference quotient, or a more complex expression, is to be used as an approximation to a derivative, it is required, above all, that this approximation be *consistent*. This means that the approximation should approach the derivative when the grid interval approaches zero. The quotient (3.1), obviously, has that property.

Important information is obtained when the true solution  $u(j\Delta x)$  is substituted into an approximation to the derivative in place of the grid point values  $u_j$ , and  $u(j\Delta x)$  is expanded in a Taylor series about the central point. For the quotient (3.1) this procedure gives

$$\frac{u_{j+1} - u_j}{\Delta x} \rightarrow \left( \frac{du}{dx} \right)_j + \frac{1}{2} \left( \frac{d^2 u}{dx^2} \right)_j \Delta x + \frac{1}{6} \left( \frac{d^3 u}{dx^3} \right)_j (\Delta x)^2 + \dots$$

The difference between this expression and the derivative  $\left( \frac{du}{dx} \right)_j$  being approximated; in this case

$$\varepsilon = \frac{1}{2} \left( \frac{d^2 u}{dx^2} \right)_j \Delta x + \frac{1}{6} \left( \frac{d^3 u}{dx^3} \right)_j (\Delta x)^2 + \dots,$$

is called the *truncation error* of the approximation to the derivative. These are terms that were "truncated off" to form the approximation. The truncation error gives a measure of how accurately the difference quotient approximates the derivative for small values of  $\Delta x$ .

The usual measure of this is the *order of accuracy* of an approximation. This is the lowest power of  $\Delta x$  that appears in the truncation error. Thus, approximation (3.1) is of the first order of accuracy. We can write

$$\varepsilon = O(\Delta x).$$

For an approximation to the derivative to be consistent it must, obviously, be at least first order accurate.

### 4. Finite difference schemes

The algebraic equation obtained when derivatives in a differential equation are replaced by appropriate finite difference approximations is called a *finite difference approximation* to that differential equation, or a *finite difference scheme*. In this section we shall introduce the concepts of consistency, truncation error, and accuracy, for a finite difference scheme.

As an example, we shall use the linear advection equation

$$\frac{\partial u}{\partial t} + c \frac{\partial u}{\partial x} = 0; \quad u = u(x, t), \quad c = \text{a positive const.} \quad (4.1)$$

It describes advection of the variable  $u$  at a constant velocity  $c$  in the direction of the  $x$  axis. The solution to this simple equation can, of course, also be obtained by an analytic method. It will be useful to obtain the analytic solution first, in order to investigate properties of numerical solutions by comparing them against known properties of the true solution.

It is convenient to this end to change from variables  $x, t$  to variables  $\xi, t$  with the substitution  $\xi \equiv x - ct$ . Using the notation

$$u(x, t) = U(\xi, t)$$

we obtain

$$\frac{\partial u}{\partial t} = \frac{\partial U}{\partial \xi} \frac{\partial \xi}{\partial t} + \frac{\partial U}{\partial t} = -c \frac{\partial U}{\partial \xi} + \frac{\partial U}{\partial t},$$

$$\frac{\partial u}{\partial x} = \frac{\partial U}{\partial \xi} \frac{\partial \xi}{\partial x} + \frac{\partial U}{\partial x} = \frac{\partial U}{\partial \xi}.$$

Substitution of these expressions into (4.1) gives

$$\frac{\partial}{\partial t} U(\xi, t) = 0.$$

Thus, it is seen that  $U$  cannot be a function of  $t$ , but can be an arbitrary function of  $\xi$ . A solution of (4.1) is, therefore,

$$u = f(x - ct), \quad (4.2)$$

where  $f$  is an arbitrary function. This, we see, is the general solution of the advection equation (4.1), since it can satisfy an arbitrary initial condition

$$u(x, 0) = F(x). \quad (4.3)$$

Thus,

$$u = F(x - ct), \quad (4.4)$$

is the solution of (4.1) satisfying the initial condition (4.3).

For a physical interpretation, it is often convenient to consider the solution in the  $x, t$  plane. In the present case, we see that the solution takes constant values along the straight lines

$$x - ct = \text{const.}$$

These lines are the *characteristics* of the advection equation; one of them is shown in Fig. 4.1. We can say that the solution propagates along the characteristics.

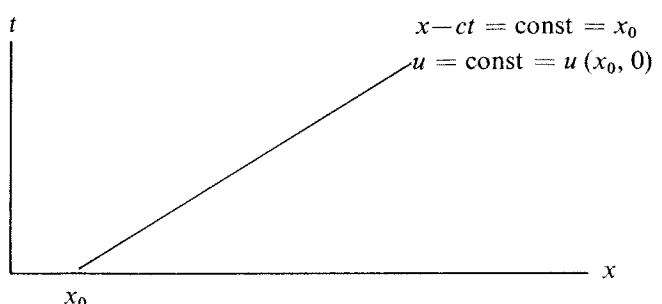


Figure 4.1 One of the characteristics of the linear advection equation (4.1).

Let us now construct a scheme for finding an approximate solution to (4.1) using the grid point method.

We are now looking only for an approximate solution at the discrete points in the  $(x, t)$  plane formed by the grid shown in Fig. 4.2. The approximate solution at a point  $(j\Delta x, n\Delta t)$  is denoted by  $u_j^n$ .

The behaviour of the true solution, which propagates along characteristics in the  $x, t$  plane, suggests constructing the approximate equation by replacing the time derivative

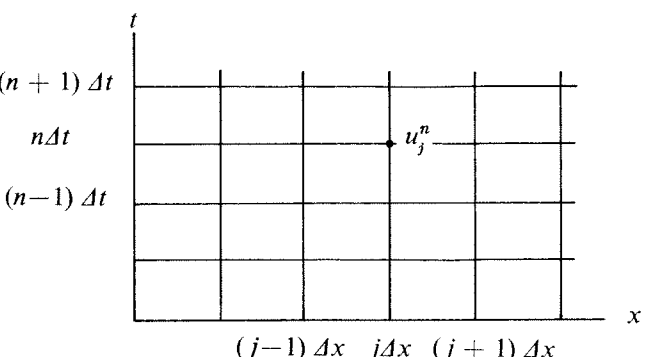


Figure 4.2 A finite difference grid for finding an approximate solution of (4.1).

by a forward difference quotient, and the space derivative by a *backward* difference quotient. In this way we obtain the scheme

$$\frac{u_j^{n+1} - u_j^n}{\Delta t} + c \frac{u_j^n - u_{j-1}^n}{\Delta x} = 0. \quad (4.5)$$

This scheme could be called a *forward and upstream* scheme, the latter word indicating the position of the point  $j-1$  relative to the advection velocity. It is, of course, only one of many possible *consistent* finite difference schemes for the differential equation. There are many schemes which approach the differential equation when the increments  $\Delta x, \Delta t$  approach zero.

Since for small values of  $\Delta x, \Delta t$  a finite difference equation approximates the corresponding differential equation, we can expect that its solution will be an approximation to the solution of that equation. We shall call solutions given by finite difference schemes *numerical* solutions. There are, of course, both approximate and numerical solutions obtained by other methods which will not be considered in this publication. It is most convenient to study the properties of numerical solutions when they can be compared with known solutions of the original differential equation, which we shall refer to as *true* solutions. The difference between the numerical and the true solution

$$u_j^n - u(j\Delta x, n\Delta t) \quad (4.6)$$

is the *error* of the numerical solution.

For obvious reasons, we cannot often expect to know the error of the numerical solution. However, we can always find a measure of the accuracy of the *scheme* by substituting the true solution  $u(j\Delta x, n\Delta t)$  of the equation into the numerical scheme. Since the true solution will not satisfy the numerical equations exactly, we will have to add an additional term to keep the equation valid. Let us denote this term by  $\epsilon$ . For example, in the case of scheme (4.5) this procedure gives

$$\begin{aligned} & \frac{u(j\Delta x, (n+1)\Delta t) - u(j\Delta x, n\Delta t)}{\Delta t} + \\ & + c \frac{u(j\Delta x, n\Delta t) - u((j-1)\Delta x, n\Delta t)}{\Delta x} = \epsilon. \end{aligned} \quad (4.7)$$

The term  $\epsilon$  we shall call the *truncation error* of the finite difference scheme. It shows how closely the true solution satisfies the equation of the scheme, and, thus, gives a measure of the accuracy of the scheme.

We can obtain a more useful form for the expression for the truncation error by performing a Taylor series expansion of the true solution about the central space and time point. Using the original differential equation to eliminate the leading term we obtain the truncation error (4.7) as

$$\begin{aligned} \epsilon = & \frac{1}{2} \frac{\partial^2 u}{\partial t^2} \Delta t + \frac{1}{6} \frac{\partial^3 u}{\partial t^3} (\Delta t)^2 + \dots - \\ & - c \left( \frac{1}{2} \frac{\partial^2 u}{\partial x^2} \Delta x - \frac{1}{6} \frac{\partial^3 u}{\partial x^3} (\Delta x)^2 + \dots \right). \end{aligned} \quad (4.8)$$

As before, these are the terms that were "truncated off" to make the differential equation reduce to our finite difference scheme.

In the same way as for an approximation to the derivative, the *order of accuracy* of a finite difference scheme is the lowest power of  $\Delta x$  and  $\Delta t$  that appears in the truncation error. Thus, scheme (4.5) is first order accurate. We can write

$$\epsilon = 0(\Delta t) + 0(\Delta x),$$

or

$$\epsilon = 0(\Delta x, \Delta t).$$

It is useful to make a distinction between orders of accuracy *in space* and *in time*, especially when the lowest powers of  $\Delta x$  and  $\Delta t$  are not the same. As before, a necessary condition for consistency of a scheme is that it be at least of the first order of accuracy.

## 5. Convergence

The truncation error of a consistent scheme can be made arbitrarily small by a sufficient reduction of the increments  $\Delta x$  and  $\Delta t$ . Unfortunately, we cannot be sure that this will also result in a reduction of the error of the numerical solution. For that reason, we return to consideration of the error  $u_j^n - u(j\Delta x, n\Delta t)$ .

Following Richtmyer and Morton (1967) we ask two questions :

(a) What is the behaviour of the error  $u_j^n - u(j\Delta x, n\Delta t)$  when, for a fixed total time  $n\Delta t$ , the increments  $\Delta x, \Delta t$  approach zero ?

(b) What is the behaviour of the error  $u_j^n - u(j\Delta x, n\Delta t)$  when, for fixed values of  $\Delta x, \Delta t$ , the number of time steps  $n$  increases ?

The answer to the first of these questions depends on the *convergence* of the numerical solution : if the error approaches zero as the grid is refined (as  $\Delta x, \Delta t \rightarrow 0$ ) the solution is called convergent. If a *scheme* gives a convergent solution for any initial conditions, then the scheme also is called convergent.

Consistency of a scheme does not guarantee convergence ; we shall illustrate this by a simple example. We still consider the scheme (4.5) ; its truncation error (4.8) approaches zero as the grid is refined, and, therefore, this is a consistent scheme. But consider the numerical solution, when the grid lines and characteristics are as shown in Fig. 5.1. The characteristic passing through the grid point taken as the origin in this example passes through another grid point,  $A$ , denoted by a square. Thus, the true solution at  $A$ , is equal to the initial value at the origin. However the numerical solution given by (4.5)  $A$  is computed using the values at points denoted by circles. The shaded domain, including all of these points, is called the *domain of dependence* of the numerical scheme. The grid point at the origin is outside that domain, and, thus, cannot affect the numerical solution at  $A$ . Therefore, the error can be arbitrarily great. If the space and time steps were reduced by the same relative amount, say to one half of their values in the figure, the domain of dependence would still remain the same, and this situation would not change. Thus, as long as the ratio of the steps  $\Delta x$  and  $\Delta t$  remains the same, refinement of the grid cannot bring about a reduction in the error of the numerical solution.

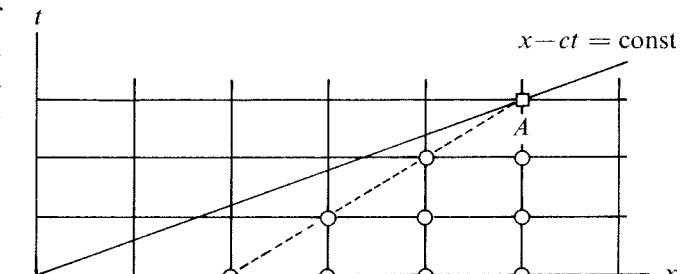


Figure 5.1 A possible relative position of a characteristic and of a domain of dependence.

A necessary condition for convergence of a scheme is, obviously, that the characteristic defining the true solution at a grid point is inside the domain of dependence of the numerical solution at that point. In our example, this will happen when the slope of the characteristics is greater than the slope of the dashed line bounding the domain of dependence, that is, when

$$c\Delta t \leq \Delta x \quad (5.1)$$

Thus, this is a necessary condition for convergence of (4.5).

## 6. Stability

The answer to the second question raised at the beginning of the section 5 depends on the *stability* of the numerical solution. A rigorous definition of stability employs the concepts of functional analysis, and refers to the boundedness of the numerical solution only (e.g. Richtmyer and Morton, 1967). The difficulties in defining stability are caused by the fact that the true solution, in general, does not have to be bounded. However, when we know that the true solution is bounded, as in the equations we are interested in here, we can use a definition referring to the boundedness of the error  $u_j^n - u(j\Delta x, n\Delta t)$ . We say that a solution  $u_j^n$  is stable if this error remains bounded as  $n$  increases, for fixed values of  $\Delta x, \Delta t$ . As before, we say that a finite difference scheme is stable if it gives a stable solution for any initial conditions.

Stability of a scheme is a property of great practical significance. There are consistent schemes, of a high order of accuracy, that still give solutions diverging unacceptably fast from the true solution. Thus, conditions for stability, if any, should be known. There are three methods that can be used to investigate the stability of a scheme, and we shall give an example of each of these methods. We shall do this by considering again the forward and upstream scheme (4.5).

*Direct method.* Since we know that the true solution is bounded, it suffices to test the boundedness of the numerical solution. The scheme (4.5) can be written as

$$u_j^{n+1} = (1-\mu)u_j^n + \mu u_{j-1}^n, \quad (6.1)$$

where

$$\mu \equiv c\Delta t/\Delta x.$$

If  $1-\mu \geq 0$ , which happens to be also the necessary condition for convergence, we will have

$$|u_j^{n+1}| \leq (1-\mu)|u_j^n| + \mu|u_{j-1}^n|. \quad (6.2)$$

We can apply this at the point where at time level  $n+1$   $|u_j^{n+1}|$  is a maximum,  $\text{Max}_{(j)}|u_j^{n+1}|$ . The right side of (6.2) can only be increased by replacing  $|u_j^n|$  and  $|u_{j-1}^n|$  by the maximum value at level  $n$ ,  $\text{Max}_{(j)}|u_j^n|$ . The two terms on the right side can then be added, and we obtain

$$\text{Max}_{(j)}|u_j^{n+1}| \leq \text{Max}_{(j)}|u_j^n|.$$

This proves the boundedness of the numerical solution. Hence,  $1-\mu \geq 0$  is seen to be a sufficient condition for stability of (6.1).

This direct testing of the stability is simple. Unfortunately, as might be anticipated from the argument, it is successful only for a rather limited number of schemes.

*Energy method.* This method is of a much wider applicability, and can be used even for nonlinear equations. If we know that the true solution is bounded, we test whether  $\sum_j (u_j^n)^2$  is also bounded. If it is, then every value  $u_j^n$  must be bounded, and the stability of the scheme has been proved. The method is called the energy method since in physical applications  $u^2$  is often proportional to some form of energy. Of course, there are examples when this is not so.

Squaring (6.1) and summing over  $j$  we obtain

$$\sum_j (u_j^{n+1})^2 = \sum_j [(1-\mu)^2 (u_j^n)^2 + 2\mu(1-\mu)u_j^n u_{j-1}^n + \mu^2 (u_{j-1}^n)^2]. \quad (6.3)$$

We shall assume a *cyclic boundary condition*, for example

$$u_{-1} \equiv u_J,$$

then

$$\sum_j (u_{j-1}^n)^2 = \sum_j (u_j^n)^2. \quad (6.4)$$

Now, using Schwarz's inequality

$$\sum ab < \sqrt{\sum a^2} \sqrt{\sum b^2},$$

and (6.4), we can write

$$\sum_j u_j^n u_{j-1}^n < \sqrt{\sum_j (u_j^n)^2} \sqrt{\sum_j (u_{j-1}^n)^2} = \sum_j (u_j^n)^2. \quad (6.5)$$

Using (6.4) and (6.5) we see that, if  $1-\mu \geq 0$ , (6.3) gives the inequality

$$\sum_j (u_j^{n+1})^2 \leq [(1+\mu)^2 + 2\mu(1-\mu) + \mu^2] \sum_j (u_j^n)^2,$$

or

$$\sum_j (u_j^{n+1})^2 < \sum_j (u_j^n)^2.$$

Thus,  $1-\mu \geq 0$ , coupled with the cyclic boundary condition, is proved to be a sufficient condition for stability of (6.1).

*Von Neumann's method.* Von Neumann's, or the Fourier series method is the most frequently used method.

We will usually not be able to use it to test the stability of nonlinear equations, and will have to resort to the analysis of their linearized versions. A solution to a linear equation, however, can be expressed in form of a Fourier series, where each harmonic component is also a solution. Thus, we can test the stability of a single harmonic solution; stability of all admissible harmonics will then be a necessary condition for stability of the scheme.

For an illustration of this method, it is useful first to obtain an analytic solution of the equation (4.1)

$$\frac{\partial u}{\partial t} + c \frac{\partial u}{\partial x} = 0,$$

in the form of a single harmonic

$$u(x, t) = \text{Re} [U(t) e^{ikx}]. \quad (6.6)$$

Here  $U(t)$  is the wave amplitude, and  $k$  the wave number. Substituting this into the preceding equation we obtain

$$\frac{dU}{dt} + ikcU = 0.$$

Thus, the problem of solving a partial differential equation has been reduced to that of solving this ordinary differential equation. Its solution is

$$U(t) = U(0) e^{-ikct},$$

where  $U(0)$  is the initial value of the amplitude. Hence, the desired harmonic solution is

$$u(x, t) = \text{Re} [U(0) e^{ik(x-ct)}]. \quad (6.7)$$

Each wave component is, thus, advected at a constant velocity  $c$  along the  $x$  axis with no change in amplitude.

Returning to the von Neumann method, we now look for an analogous solution of the finite difference equation (6.1). Into this equation we substitute a solution of the form

$$u_j^n = \text{Re} [U^{(n)} e^{ikj\Delta x}]. \quad (6.8)$$

Here  $U^{(n)}$  is the amplitude at time level  $n$ . This substitution shows that (6.8) is a solution provided that

$$U^{(n+1)} = (1-\mu)U^{(n)} + \mu U^{(n)} e^{-ik\Delta x}. \quad (6.9)$$

An equation of this kind enables analysis of the behaviour of the amplitude  $U^{(n)}$  as  $n$  increases. To this end we define an *amplification factor*  $|\lambda|$  by

$$U^{(n+1)} \equiv \lambda U^{(n)}. \quad (6.10)$$

This gives

$$|U^{(n+1)}| = |\lambda| |U^{(n)}|.$$

For each harmonic solution (6.8) to be stable it is required that

$$|U^{(n)}| = |\lambda| |U^{(0)}| < B,$$

where  $B$  is a finite number. This gives

$$n \ln |\lambda| < \ln(B/|U^{(0)}|) \equiv B',$$

where  $B'$  is a new constant. Since  $n = t/\Delta t$ , the necessary condition for stability becomes

$$\ln |\lambda| < \frac{B'}{t} \Delta t. \quad (6.11)$$

Now, suppose that we require boundedness of the solution for a *finite* time  $t$ . Condition (6.11) can then be written as

$$\ln |\lambda| \leq 0(\Delta t).$$

If we now define

$$|\lambda| \equiv 1 + \delta,$$

we see, in view of the power series expansion of  $\ln(1 + \delta)$ , that the stability condition obtained is equivalent to

$$\delta \leq 0(\Delta t).$$

or

$$|\lambda| \leq 1 + 0(\Delta t). \quad (6.12)$$

This is the *von Neumann necessary condition for stability*.

The von Neumann condition allows an exponential, but no faster, growth of the solution. This, of course, is needed to analyze cases when the true solution grows exponentially. However, when we know that the true solution does not grow, as in our example (6.7), it is customary to replace (6.12) by a sufficient condition

$$|\lambda| \leq 1. \quad (6.13)$$

This condition is much less generous than that required by the original definition of stability. Returning to our example, substitution of (6.10) into (6.9) gives

$$\lambda = 1 - \mu + \mu e^{-ik\Delta x}. \quad (6.14)$$

From this we obtain

$$|\lambda|^2 = 1 - 2\mu(1-\mu)(1 - \cos k\Delta x), \quad (6.15)$$

and, therefore,  $1-\mu \geq 0$  is again found to be a sufficient condition for stability of (6.1).

An equation such as (6.15) gives further information about the behaviour of the numerical solution. This can be obtained by studying the variation of  $|\lambda|$  with  $\mu$  for various fixed values of  $k\Delta x$ . To this end we plot the  $|\lambda|^2$  curves; (6.15) shows that in the present case all of these curves are parabolas. Furthermore, recall that the minimum resolvable wave length is  $2\Delta x$ . Thus, the maximum value that wave number  $k$  can take is  $\pi/\Delta x$ . We thus plot the  $|\lambda|^2$  curves for this maximum value  $k = \pi/\Delta x$  (or wave length  $L = 2\Delta x$ ), and for half this value,  $k = \pi/2\Delta x$  ( $L = 4\Delta x$ ), and a quarter of this value,  $k = \pi/4\Delta x$  ( $L = 8\Delta x$ ). The first derivative

$$\frac{d|\lambda|^2}{d\mu} = -2(1-2\mu)(1-\cos k\Delta x),$$

shows that all the  $|\lambda|^2$  curves have minima at  $\mu = 1/2$ . This information, in addition to calculation of the ordinates of (6.15) at  $\mu = 0, 1/2$  and 1, suffices for sketching

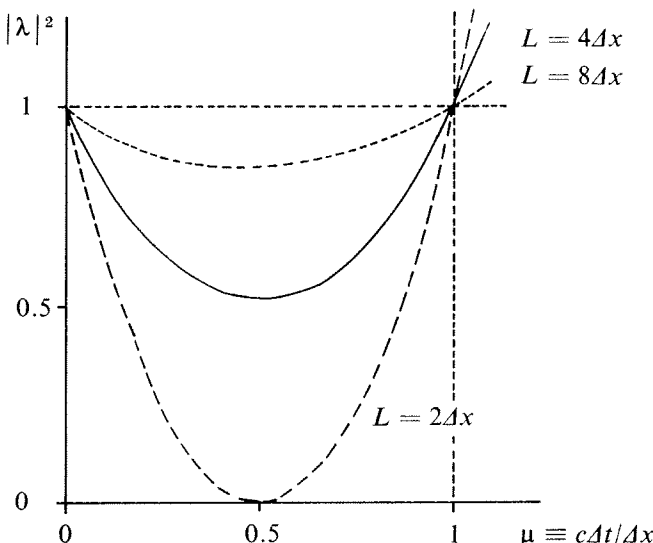


Figure 6.1 Sketches of  $|\lambda|^2$  curves, for the scheme (6.1), and for various values of  $L$ .

the graphs of the  $|\lambda|^2$  curves as shown in Fig. 6.1. In general, as the wave length  $L$  increases, that is, as  $k$  approaches zero, the amplification factor approaches unity for any value of the parameter  $\mu$ .

The figure shows that within the stable region the scheme is damping for all values  $\mu < 1$ . The damping increases as the wave length decreases. Since the true solution has a constant amplitude, this damping reveals an error due to finite differencing. We see that this error increases as the wave length decreases. At the shortest resolvable wave length,  $L = 2\Delta x$ , the error may be very great unless  $\Delta t$  is extremely small. It is even possible for this wave to be completely removed after only a single time step! The dependence of the error on wave length, as seen here, might have been anticipated by considering representation of harmonics of various wave lengths by the finite difference grid. The shortest resolvable wave, with only two data points per wave length, is very poorly represented; as the wave length increases, the representation by a finite difference grid improves, and approaches the continuous representation as the wave length tends to infinity.

There exists a wealth of more precise definitions of stability and convergence, as well as stability criteria. For a further discussion of these subjects, and of the relation between the properties of stability and convergence, the interested reader is referred to the book by Richtmyer and Morton (1967) and to the publication by Kreiss and Oliger (1973). However, for application of numerical methods to atmospheric models, it is more important to discuss other problems than to refine the stability and convergence concepts beyond the outline given here. These numerical problems, such as phase speed errors and computational dispersion, nonlinear instability, effect of the space-time grid on the properties of the numerical solution, and, also the ideas behind and properties of the great variety of schemes that are currently being used in atmospheric models, will be discussed in the remaining chapters of this publication.

## CHAPTER II

### TIME DIFFERENCING SCHEMES

In this chapter we consider ordinary differential equations with *one* dependent and *one* independent variable. Although atmospheric models are essentially always models for solving a complex set of partial differential equations, in some formulations the numerical solution of ordinary differential equations forms an important part of the computational procedure. For instance in spectral models the governing partial differential equations reduce to a set of ordinary differential equations for the expansion coefficients as dependent variables. A set of ordinary differential equations will also be obtained if a Lagrangian method is used, in which the computational points move with the fluid. But, most of all, schemes for solving *ordinary* differential equations are of interest here since they are often used without modification to construct approximations to the time derivative terms in the governing *partial* differential equations. Knowledge of the properties of schemes for solving ordinary differential equations will then be used in investigating the properties of more complex schemes for solving the partial differential equations.

With that in mind, we shall here first define some of the schemes that will be interesting to analyze. Then we shall investigate the behaviour of numerical solutions obtained when these schemes are used for two specific ordinary differential equations: the oscillation (or frequency) equation, and the friction equation. These equations will serve as prototypes for later extension of the results to advection, gravity-inertia wave, and diffusion processes within the atmospheric primitive equations.

#### 1. Definitions of some schemes

Schemes used for the time derivative terms within the primitive equations are relatively simple, usually of the second and sometimes even only of the first order of accuracy. There are several reasons for this. First, it is a general experience that schemes constructed so as to have a high order of accuracy are mostly not very successful when solving partial differential equations. This is in contrast to the experience with ordinary differential equations, where very accurate schemes, such as the Runge-Kutta method, are extremely rewarding. There is a basic reason for this difference. With

an ordinary differential equation, the equation and a single initial condition is all that is required for an exact solution. Thus, the error of the numerical solution is entirely due to the inadequacy of the scheme. With a partial differential equation, the error of the numerical solution is brought about both by the inadequacy of the scheme and by insufficient information about the initial conditions, since they are known only at discrete space points. Thus, an increase in the accuracy of the scheme improves only one of these two components, and the results are not too impressive.

Another reason for not requiring a scheme of high accuracy for approximations to the time derivative terms is that, in order to meet a stability requirement of the type discussed in the preceding chapter, it is usually necessary to choose a time step significantly smaller than that required for adequate accuracy. With the time step usually chosen, other errors, for example in the space differencing, are much greater than those due to the time differencing. Thus, computational effort is better spent in reducing these other errors, and not in increasing the accuracy of the time differencing. This, of course, does not mean that it is not necessary to consider carefully the properties of various possible time differencing schemes. Accuracy is only one important consideration in choosing a scheme.

To define some schemes, we consider the equation

$$\frac{dU}{dt} = f(U, t); \quad U = U(t). \quad (1.1)$$

The independent variable  $t$  is here called time. We divide the time axis into segments of equal length  $\Delta t$ . We shall denote by  $U^{(n)}$  the approximate value of  $U$  at time  $n\Delta t$ . We assume that we know at least the first of the values  $U^{(n)}, U^{(n-1)}, \dots$  and we want to construct a scheme for computation of an approximate value  $U^{(n+1)}$ . There are many possibilities.

*A. Two level schemes.* These are schemes that relate values of the dependent variable at two time levels:  $n$  and  $n + 1$ . Only a two level scheme can be used to advance an integration over the first time step, when just a single initial condition is available. With such a scheme we want to approximate the exact formula

$$U^{(n+1)} = U^{(n)} + \int_{n\Delta t}^{(n+1)\Delta t} f(U, t) dt. \quad (1.2)$$

We shall first list several schemes which do not use an iterative procedure.

A1. Euler (or forward) scheme. This is the scheme

$$U^{(n+1)} = U^{(n)} + \Delta t \cdot f^{(n)}, \quad (1.3)$$

where

$$f^{(n)} \equiv f(U^{(n)}, n\Delta t).$$

The truncation error of this scheme is  $O(\Delta t)$ . Thus, this is a first order accurate scheme. For the integrand in (1.2) we have here taken a constant value equal to that at the lower boundary of the time interval. Thus,  $f$  in (1.3) is not centered in time, and the scheme is said to be *uncentered*. In general, uncentered schemes will be found to be of the first order of accuracy, and simple centered schemes to be of the second order of accuracy.

A2. Backward scheme. We can also take a constant value of  $f$  equal to that at the upper boundary of the time interval. We then obtain

$$U^{(n+1)} = U^{(n)} + \Delta t \cdot f^{(n+1)}. \quad (1.4)$$

If, as here, a value of  $f$  depending on  $U^{(n+1)}$  appears in the difference equation, the scheme is called *implicit*. For an ordinary differential equation, it may be simple to solve such a difference equation for the desired value  $U^{(n+1)}$ . But, for partial differential equations, this will require solving a set of simultaneous equations, with one equation for each of the grid points of the computation region. If a value of  $f$  depending on  $U^{(n+1)}$  does not appear in the difference equation the scheme is called *explicit*.

The truncation error of (1.4) is also  $O(\Delta t)$ .

A3. Trapezoidal scheme. If we approximate  $f$  in (1.2) by an average of the values at the beginning and the end of the time interval, we obtain the trapezoidal scheme

$$U^{(n+1)} = U^{(n)} + \frac{1}{2}\Delta t (f^{(n)} + f^{(n+1)}). \quad (1.5)$$

This is also an implicit scheme. Its truncation error, however, is  $O[(\Delta t)^2]$ .

To increase the accuracy or for other reasons we can also construct iterative schemes. Two schemes that we will now define are constructed in the same way as (1.4) and (1.5), except that an iterative procedure is used to make them explicit.

A4. Matsuno (or Euler-backward) scheme. With this scheme a step is made first using the Euler scheme;

the value of  $U$  obtained for time level  $n+1$  is then used for an approximation to  $f^{(n+1)}$ , and this approximate value  $f^{(n+1)*}$  is used to make a backward step. Thus,

$$\begin{aligned} U^{(n+1)*} &= U^{(n)} + \Delta t \cdot f^{(n)}, \\ U^{(n+1)} &= U^{(n)} + \Delta t \cdot f^{(n+1)*}, \end{aligned} \quad (1.6)$$

where

$$f^{(n+1)*} \equiv f(U^{(n+1)*}, (n+1)\Delta t).$$

This is an explicit scheme, of the first order of accuracy.

A5. Heun scheme. Here, in much the same way, an approximation is constructed to the trapezoidal scheme. Thus,

$$\begin{aligned} U^{(n+1)*} &= U^{(n)} + \Delta t \cdot f^{(n)}, \\ U^{(n+1)} &= U^{(n)} + \frac{1}{2}\Delta t (f^{(n)} + f^{(n+1)*}). \end{aligned} \quad (1.7)$$

Thus, this is also an explicit scheme. It is of the second order of accuracy.

B. Three level schemes. Except at the first step, one can store the value  $U^{(n-1)}$ , and construct schemes taking advantage of this additional information. These are three level schemes. They may approximate the formula

$$U^{(n+1)} = U^{(n-1)} + \int_{(n-1)\Delta t}^{(n+1)\Delta t} f(U, t) dt, \quad (1.8)$$

or, they can use the additional value  $U^{(n-1)}$  to make a better approximation to  $f$  in (1.2).

B1. Leapfrog scheme. The simplest way of making a centered evaluation of the integral in (1.8) is to take for  $f$  a constant value equal to that at the middle of the interval  $2\Delta t$ . This gives the leapfrog scheme

$$U^{(n+1)} = U^{(n-1)} + 2\Delta t \cdot f^{(n)}. \quad (1.9)$$

Its truncation error is  $O[(\Delta t)^2]$ . This is probably the scheme most widely used at present in atmospheric models. It has also been called the "mid-point rule", or "step-over" scheme.

B2. Adams-Basforth scheme. The scheme that is usually called the Adams-Basforth scheme in the atmospheric sciences is, in fact, a simplified version of the original Adams-Basforth scheme, which is of the fourth order of accuracy. The simplified version is obtained when  $f$  in (1.2) is approximated by a value obtained at the centre of the interval  $\Delta t$  by a linear extrapolation using values  $f^{(n-1)}$  and  $f^{(n)}$ . This gives

$$U^{(n+1)} = U^{(n)} + \Delta t \left( \frac{3}{2}f^{(n)} - \frac{1}{2}f^{(n-1)} \right). \quad (1.10)$$

This also is a second order accurate scheme.

There are many other rather obvious possibilities. For example, one can approximate the integral in (1.8) using Simpson's rule, that is, by fitting a parabola to the values  $f^{(n-1)}$ ,  $f^{(n)}$  and  $f^{(n+1)}$ . The implicit scheme obtained in this way is called the Milne-Simpson scheme. To illustrate the wealth of possible alternatives we note that in a paper by Young (1968) properties of 13 different schemes have been studied. Furthermore, when we are solving a more complicated partial differential equation, or a system of such equations, time (or space-time) differencing schemes can be constructed which are more complex than those which can be defined using the simple equation (1.1). Such schemes are widely used in atmospheric models, and some of them will be described in later chapters of this publication.

## 2. Properties of schemes applied to the oscillation equation

The stability and other important properties of the time differencing schemes defined in section (1) depend on the form of the function  $f(U, t)$ . Thus, in order to discuss these properties we have to prescribe this function. For applications in atmospheric models it is of particular interest to consider the case

$$f \equiv i\omega U,$$

that is, the equation

$$\frac{dU}{dt} = i\omega U, \quad U = U(t). \quad (2.1)$$

Equation (2.1) we shall call the *oscillation equation*. The word *frequency* equation is also used. We allow  $U$  to be complex; then (2.1) can be thought of as representing a system of two equations. The parameter  $\omega$  is real, and is called the *frequency*.

It is easy to give some justification for our interest in the equation (2.1). As an example, recall that the harmonic component

$$u(x, t) = \operatorname{Re}[U(t) e^{ikx}],$$

is a solution of the linear wave equation

$$\frac{\partial u}{\partial t} + c \frac{\partial u}{\partial x} = 0, \quad c = \text{const.},$$

provided that

$$\frac{dU}{dt} + ikcU = 0.$$

This ordinary differential equation reduces to (2.1) if we substitute  $\omega = -kc$ .

As another simple example we can consider the acceleration and Coriolis terms of the horizontal component of the equation of motion of the atmosphere, that is

$$\frac{du}{dt} = fv, \quad \frac{dv}{dt} = -fu.$$

If we define

$$U \equiv u + iv,$$

we can write these two equations as

$$\frac{dU}{dt} = -ifU.$$

This again reduces to (2.1), this time if we substitute  $\omega = -f$ .

Since there are many more important types of wave motion, we can hope that results obtained by a study of (2.1) will be much more general. It can, indeed, be shown (e.g. Young, 1968) that the equation (2.1) can be obtained from a rather general linearized system of governing equations, describing a number of types of wave motion in the atmosphere.

The general solution of (2.1) is

$$U(t) = U(0) e^{i\omega t},$$

or, for discrete values  $t = n\Delta t$ ,

$$U(n\Delta t) = U(0) e^{in\omega\Delta t} \quad (2.2)$$

Thus, considering the solution in a complex plane, its argument rotates by  $\omega\Delta t$  in each time step  $\Delta t$ , and there is no change in amplitude.

The properties of various schemes when applied to (2.1) are conveniently analyzed using the von Neumann method. This method, as we have seen, involves defining a variable  $\lambda$  by

$$U^{(n+1)} \equiv \lambda U^{(n)} \quad (2.3)$$

We also write

$$\lambda \equiv |\lambda| e^{i\theta} \quad (2.4)$$

Thus, the numerical solution can formally be written as

$$U^{(n)} = |\lambda|^n U^{(0)} e^{in\theta}. \quad (2.5)$$

We see that  $\theta$  represents the change in argument (or phase change) of the numerical solution in each time step.

Since we know that the amplitude of the true solution does not change, we shall require  $|\lambda| \leq 1$  for stability.

In accordance with this and (2.5), we shall say that a scheme is

unstable	$>$
neutral	if $ \lambda  = 1$ .
damping	$<$
(or dissipative)	

It will also be instructive to compare the phase change of the numerical solution per time step,  $\theta$ , with that of the true solution,  $\omega\Delta t$ . The ratio of these changes,  $\theta/\omega\Delta t$ , is the *relative phase change* of the numerical solution. Obviously, we can say that a scheme is

accelerating of no effect on phase speed	$\theta >$
decelerating	$\frac{\theta}{\omega\Delta t} < 1$ .

For accuracy, therefore, it is desirable to have both the amplification factor and the relative phase speed close to unity. Exceptions to this are so-called "computational modes", which, as we shall see later, can appear as false solutions superposed on the physical solution. These are solutions that do not approach the true solution as the space and time steps approach zero. If such solutions exist they will each have their own value of the amplification factor. Since they are not an approximation to the true solution, it is desirable to have their amplitudes as small as possible, that is, to have their amplification factors less than unity.

We shall now discuss the properties of the schemes that have been defined in the preceding section.

*Two level schemes.* The three *non-iterative* two level schemes can be described by a single finite difference equation

$$U^{(n+1)} = U^{(n)} + \Delta t (\alpha f^{(n)} + \beta f^{(n+1)}), \quad (2.6)$$

with a consistency requirement

$$\alpha + \beta = 1.$$

Obviously,  $\alpha = 1$ ,  $\beta = 0$  for the Euler scheme,  $\alpha = 0$ ,  $\beta = 1$  for the backward scheme, and  $\alpha = 1/2$ ,  $\beta = 1/2$  for the trapezoidal scheme.

Applied to the oscillation equation (2.6) gives

$$U^{(n+1)} = U^{(n)} + i\omega\Delta t (\alpha U^{(n)} + \beta U^{(n+1)}). \quad (2.7)$$

In order to evaluate  $\lambda$  we must solve this equation for  $U^{(n+1)}$ . Denoting, for brevity,

$$p \equiv \omega\Delta t, \quad (2.8)$$

we obtain

$$U^{(n+1)} = \frac{1+i\alpha p}{1-i\beta p} U^{(n)}. \quad (2.9)$$

Therefore,

$$\lambda = \frac{1+i\alpha p}{1-i\beta p}, \quad (2.10)$$

or,

$$\lambda = \frac{1}{1+\beta^2 p^2} (1-\alpha\beta p^2 + ip).$$

Substituting for  $\alpha$  and  $\beta$  allows us to investigate the effect of particular schemes. For the Euler scheme we have

$$\lambda = 1 + ip, \quad (2.11)$$

for the backward scheme

$$\lambda = \frac{1}{1+p^2} (1+ip), \quad (2.12)$$

and, for the trapezoidal scheme,

$$\lambda = \frac{1}{1+\frac{1}{4}p^2} \left( 1 - \frac{1}{4}p^2 + ip \right). \quad (2.13)$$

To test for stability we need to know  $|\lambda|$ . Since the modulus of a ratio of two complex numbers is equal to the ratio of their moduli, we can obtain the values of  $|\lambda|$  directly from (2.10). For the Euler scheme we have

$$|\lambda| = (1+p^2)^{1/2}. \quad (2.14)$$

The Euler scheme is, thus, always unstable. It is interesting to note that, if  $\Delta t$  is chosen so as to make  $p$  relatively small, we have

$$|\lambda| = 1 + \frac{1}{2}p^2 + \dots. \quad (2.15)$$

This shows that  $|\lambda| = 1 + O[(\Delta t)^2]$ , that is,  $|\lambda| - 1$  is an order of magnitude less than the maximum allowed by the von Neumann necessary condition for stability. However, experience shows that an indiscriminate use of the Euler scheme for solution of the atmospheric equations leads to amplification at a quite unacceptable rate.

For the backward scheme we obtain

$$|\lambda| = (1+p^2)^{-1/2}. \quad (2.16)$$

The backward scheme is, thus, stable no matter what value of  $\Delta t$  is chosen. Thus, it is an *unconditionally stable* scheme. We can, furthermore, notice that it is damping, and that the amount of damping increases as the frequency  $\omega$  increases. This is often considered to

be a desirable property of a scheme. For instance, we can think of a system in which a number of frequencies are present at the same time; for example, solving a system of equations of the type (2.1). This situation is similar to that existing in the real atmosphere. It would appear to be necessary to maintain the amplitudes of motions of different frequencies in the correct ratio. However, in numerical integrations, high frequency motions are often excited to unrealistically large amplitudes through errors in the initial data. It may then be desirable to reduce the amplitudes of high frequency motions by a selective damping in the time differencing scheme. In other words, a scheme with frequency dependent damping properties can be used to *filter out* undesirable high frequency motions.

For the trapezoidal scheme we find

$$|\lambda| = 1. \quad (2.17)$$

The trapezoidal scheme is, thus, always neutral. The amplitude of the numerical solution remains constant, just as does that of the true solution. It is useful to note that both the implicit schemes considered here were stable no matter how large a value of  $\Delta t$  was chosen.

The *iterative* two level schemes can also be described by a single equation in the same way as (2.6). Thus, we write

$$\begin{aligned} U^{(n+1)*} &= U^{(n)} + \Delta t \cdot f^{(n)}, \\ U^{(n+1)} &= U^{(n)} + \Delta t (\alpha f^{(n)} + \beta f^{(n+1)*}), \\ \alpha + \beta &= 1. \end{aligned} \quad (2.18)$$

Now  $\alpha = 0$ ,  $\beta = 1$  for the Matsuno scheme, and  $\alpha = 1/2$ ,  $\beta = 1/2$  for the Heun scheme.

Applied to the oscillation equation (2.18) gives

$$\begin{aligned} U^{(n+1)*} &= U^{(n)} + i\omega\Delta t U^{(n)}, \\ U^{(n+1)} &= U^{(n)} + i\omega\Delta t (\alpha U^{(n)} + \beta U^{(n+1)*}). \end{aligned} \quad (2.19)$$

Eliminating  $U^{(n+1)*}$  we obtain, again using (2.8),

$$U^{(n+1)} = (1-\beta p^2 + ip) U^{(n)}.$$

Thus,

$$\lambda = 1 - \beta p^2 + ip \quad (2.20)$$

Substituting the appropriate values of  $\beta$  we now obtain the values of  $\lambda$  for the two schemes. Hence, for the Matsuno scheme

$$\lambda = 1 - p^2 + ip, \quad (2.21)$$

and for the Heun scheme

$$\lambda = 1 - \frac{1}{2}p^2 + ip. \quad (2.22)$$

To test for stability we evaluate  $|\lambda|$ . For the Matsuno scheme we obtain

$$|\lambda| = (1-p^2 + p^4)^{1/2}. \quad (2.23)$$

Thus, the Matsuno scheme is stable if

$$|p| \leq 1.$$

In other words, to achieve stability we have to choose  $\Delta t$  sufficiently small so that

$$\Delta t \leq 1/|\omega|. \quad (2.24)$$

The Matsuno scheme, thus, is *conditionally stable*. The higher the frequency, the more restrictive is the stability condition.

Differentiating (2.23) we find that

$$\frac{d|\lambda|}{dp} = \frac{p}{(1-p^2+p^4)^{3/2}} (1-2p^2).$$

Hence, the amplification factor of the Matsuno scheme has a minimum for  $p = 1/\sqrt{2}$ . Therefore, as pointed out by Matsuno (1966a) when dealing with a system with a number of frequencies we can choose a time step so as to have  $0 < p < 1/\sqrt{2}$  for all the frequencies present, and then, in the same way as backward implicit scheme, this scheme will reduce the relative amplitudes of high frequencies. This technique has recently become very popular for initialization of atmospheric models, where it is used to damp the spurious high frequency noise generated by the assimilation of the observed data. As shown by Matsuno (1966b) higher order accuracy schemes with similar filtering characteristics can be constructed.

For the Heun scheme (2.22) gives

$$|\lambda| = \left( 1 + \frac{1}{4}p^4 \right)^{1/2} \quad (2.25)$$

This is always greater than unity. Thus, the Heun scheme is always unstable, like the Euler scheme. However, instead of (2.15), for small  $p$  we now have

$$|\lambda| = 1 + \frac{1}{8}p^4 + \dots, \quad (2.26)$$

that is,  $|\lambda| = 1 + 0 [(\Delta t)^4]$ . This instability is quite weak. Experience shows that it can be tolerated when we can choose a relatively small value of  $\Delta t$ . (Note that, whenever the amplification rate is less than that allowed by the von Neumann necessary condition, the total amplification in a given time is reduced as the time step is reduced.)

Fig. 2.1 summarizes the results obtained for the five schemes considered so far. For all of these schemes the amplification factors were found to be even functions of  $p$ , so the amplification factor curves are shown only for  $p \geq 0$ .

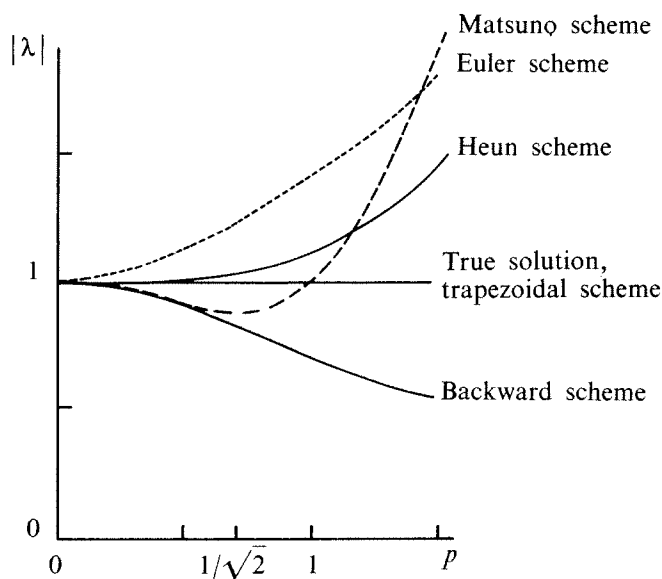


Figure 2.1 The amplification factor as a function of  $p \equiv \omega \Delta t$  for five two level schemes and for the true solution.

It is also of interest to consider the phase change per time step,  $\theta$ , and the relative phase change per time step,  $\theta/p$ . Using the notation

$$\lambda \equiv \lambda_{re} + i\lambda_{im}, \quad (2.27)$$

we have, using (2.4),

$$\theta = \arctan \frac{\lambda_{im}}{\lambda_{re}}, \quad (2.28)$$

or

$$\frac{\theta}{p} = \frac{1}{p} \arctan \frac{\lambda_{im}}{\lambda_{re}}. \quad (2.29)$$

For the Euler and the backward schemes, using (2.11) and (2.12) we obtain

$$\frac{\theta}{p} = \frac{1}{p} \arctan p. \quad (2.30)$$

Since the right-hand side is always less than unity, we can see that these two schemes are decelerating. For  $p = 1$  we have  $\theta/p = \pi/4$ .

In other cases the effect may not be so obvious. For the Matsuno scheme, for example, (2.21) gives

$$\frac{\theta}{p} = \frac{1}{p} \arctan \frac{p}{1-p^2}. \quad (2.31)$$

It is not obvious whether the right-hand side here is greater or less than unity. However, the behaviour of (2.31) for all  $p$  is of no practical interest, since we already know that  $p$  must be chosen less than unity in order to ensure stability, and rather small for frequencies for which we want the integration errors to be small. Thus, we need only consider (2.31) for small  $p$ ; we obtain

$$\frac{\theta}{p} = 1 + \frac{2}{3} p^2 + \dots$$

The Matsuno scheme, therefore, is seen to be accelerating. For the special value  $p = 1$  this can be seen directly from (2.13), since then  $\theta/p = \pi/2$ .

Analysis of phase errors of schemes applied to the oscillation equation is not so important as analysis of the amplification factor. Phase errors do not affect stability; and when these schemes are used to solve the partial differential equations of motion additional phase errors due to space differencing will appear. We will then be interested only in the total phase error, and it will be found that the error due to space differencing is usually dominant.

*Three level schemes and computational modes.* We consider first the leapfrog scheme (1.9). Applied to the oscillation equation it gives

$$U^{(n+1)} = U^{(n-1)} + i2\omega\Delta t U^{(n)}. \quad (2.32)$$

A problem with all three or more level schemes including this is that they require more than one initial condition to start the computation. From a physical standpoint a single initial condition  $U^{(0)}$  should have been sufficient. However, in addition to the *physical initial condition*, three level schemes require a *computational initial condition*  $U^{(1)}$ . This value cannot be calculated by a three level scheme, and, therefore, it will usually have to be obtained using one of the two level schemes.

According to (2.3) we also have

$$U^{(n)} = \lambda U^{(n-1)}, \quad U^{(n+1)} = \lambda^2 U^{(n-1)}. \quad (2.33)$$

When these relations are substituted into (2.32) we obtain

$$\lambda^2 - i2p\lambda - 1 = 0,$$

a second degree equation for  $\lambda$ . It has solutions

$$\begin{aligned} \lambda_1 &= \sqrt{1-p^2} + ip, \\ \lambda_2 &= -\sqrt{1-p^2} + ip. \end{aligned} \quad (2.34)$$

Thus, there are two solutions of the form  $U^{(n+1)} = \lambda U^{(n)}$ . This necessarily follows from the fact that we are considering a three level scheme; substitution of (2.33) into the difference equation given by these schemes will always give a second degree equation for  $\lambda$ . In general, an  $m$  level scheme will give  $m-1$  solutions of the form  $U^{(n+1)} = \lambda U^{(n)}$ . A solution of this type corresponding to a single value of  $\lambda$  is called a *mode*.

Consider now the two values that have been obtained for  $\lambda$ . If a solution of the form  $U^{(n+1)} = \lambda U^{(n)}$  is to represent an approximation to the true solution, then we must have  $\lambda \rightarrow 1$  as  $\Delta t \rightarrow 0$ . For the values (2.34), as  $p \equiv \omega \Delta t \rightarrow 0$  we do have  $\lambda_1 \rightarrow 1$ , however at the same time  $\lambda_2 \rightarrow -1$ . Solutions like that associated with  $\lambda_1$  are usually called *physical modes* because we are always solving equations describing physical processes. Solutions like that associated with  $\lambda_2$  are not approximations to the true solution, and are called *computational modes*.

To clarify this situation we consider the simple case  $\omega = 0$ , that is, the equation

$$\frac{dU}{dt} = 0, \quad (2.35)$$

with the true solution

$$U = \text{const.} \quad (2.36)$$

The leapfrog scheme, applied to (2.35), gives

$$U^{(n+1)} = U^{(n-1)}. \quad (2.37)$$

For a given physical initial condition  $U^{(0)}$ , we consider two special choices of  $U^{(1)}$ .

A. Suppose calculating of  $U^{(1)}$  happened to give the true value  $U^{(0)}$ . (2.37) then gives, for all  $n$ ,

$$U^{(n+1)} = U^{(n)},$$

or, since  $p = 0$ ,

$$U^{(n+1)} = \lambda_1 U^{(n)}.$$

Thus, we obtain a numerical solution that is equal to the true solution (2.36), and consists of the physical mode only.

B. Suppose calculating  $U^{(1)}$  gives  $U^{(1)} = -U^{(0)}$ . Then we obtain, for all  $n$ ,

$$U^{(n+1)} = -U^{(n)},$$

$$\text{or} \quad U^{(n+1)} = \lambda_2 U^{(n)}.$$

The numerical solution now consists entirely of the computational mode. Hence, it would appear that a good choice of the computational initial condition is of vital importance for obtaining a satisfactory numerical solution.

In general, since (2.31) is a linear equation, its solution will be a linear combination of the two solutions

$$U_1^{(n)} = \lambda_1^n U_1^{(0)},$$

$$U_2^{(n)} = \lambda_2^n U_2^{(0)}.$$

Therefore, we can write

$$U^{(n)} = a\lambda_1^n U_1^{(0)} + b\lambda_2^n U_2^{(0)}, \quad (2.38)$$

where  $a$  and  $b$  are constants. Now this has to satisfy the *physical* and the *computational* initial condition; we obtain

$$U^{(0)} = a U_1^{(0)} + b U_2^{(0)},$$

$$U^{(1)} = a\lambda_1 U_1^{(0)} + b\lambda_2 U_2^{(0)}.$$

These equations can be solved for  $a U_1^{(0)}$  and  $b U_2^{(0)}$ , and the results substituted into (2.38). In this way we find

$$\begin{aligned} U^{(n)} &= \frac{1}{\lambda_1 - \lambda_2} \left[ \lambda_1^n \left( U^{(1)} - \lambda_2 U^{(0)} \right) - \right. \\ &\quad \left. - \lambda_2^n \left( U^{(1)} - \lambda_1 U^{(0)} \right) \right]. \end{aligned} \quad (2.39)$$

Therefore, the amplitudes of the physical and of the computational modes are seen to be proportional to, respectively,

$$|U^{(1)} - \lambda_2 U^{(0)}| \quad \text{and} \quad |U^{(1)} - \lambda_1 U^{(0)}|.$$

These are seen to depend on  $U^{(1)}$ . If, for example, we are able to choose  $U^{(1)} = \lambda_1 U^{(0)}$ , the numerical solution will consist of the physical mode only. If, on the other hand, the choice of  $U^{(1)}$  is so unsuccessful as to have  $U^{(1)} = \lambda_2 U^{(0)}$ , the solution will consist entirely of the computational mode.

While this analysis illustrates the importance of a careful choice of  $U^{(1)}$ , it is not always possible to calculate

$U^{(1)} = \lambda_1 U^{(0)}$  so as to eliminate the computational mode. Numerical methods are used in practice to solve equations that cannot be solved by analytical methods, and are more complex than the simple oscillation equation (2.1). In these cases we will not know the exact values of  $\lambda_1$  and  $\lambda_2$ . Thus,  $U^{(1)}$  is usually computed using one of the two level schemes. The simplest method is to use the Euler scheme, or, a more refined procedure could be used, for example the Heun scheme. Using (2.39) it can be shown that the latter alternative will give a smaller amplitude of the computational mode.

We also note that even if we did know the exact value of  $\lambda_1$ , this would still not allow the computational mode to be eliminated in a practical numerical calculation. The numerical solution which we calculate is not an exact solution of the finite difference equations, since the arithmetical operations are performed in practice only to a finite number of significant digits. The error produced in this way is called *round off error*, though in electronic computers results of arithmetic operations are sometimes truncated to a given number of digits, instead of being rounded off. With round off errors present, permanent elimination of the computational mode is not possible in principle, since the computational mode would appear in the course of integration in any case even if it were absent initially. However, it is usually found that round off errors are of little importance in atmospheric models, and in solving partial differential equations in general.

Proceeding now to the stability analysis, in view of (2.38) and our inability to eliminate the computational mode completely, we will have to require for stability that neither of the two amplification factors is greater than unity. It is convenient to consider three special cases.

I.  $|p| < 1$ . In (2.34)  $1-p^2$  is positive, and we obtain

$$|\lambda_1| = |\lambda_2| = 1. \quad (2.40)$$

Thus, in this case both modes are stable and neutral. For the phase change, using (2.28)

$$\begin{aligned} \theta_1 &= \arctan(p/\sqrt{1-p^2}), \\ \theta_2 &= \arctan(-p/\sqrt{1-p^2}). \end{aligned} \quad (2.41)$$

It is instructive to consider the behaviour of  $\theta$ , as a function of  $p$ , especially as  $p \rightarrow 0$ . We consider first the case  $p > 0$ . Since for both modes  $\lambda_{im} = |\lambda| \sin \theta = p$  we have  $0 < \theta < \pi$ . Considering the signs of  $\lambda_{re}$  we find that  $0 < \theta_1 < \pi/2$ , and  $\pi/2 < \theta_2 < \pi$ . To illustrate these results, the phase changes (2.41) are plotted in Fig. 2.2. We see that, for all  $p$ ,

$$\theta_2 = \pi - \theta_1.$$

Specifically, as  $p \rightarrow 0$ ,  $\theta_1 \rightarrow p$ , while  $\theta_2 \rightarrow \pi - p$ . Thus, for small  $\Delta t$  the physical mode is seen to approximate the true solution, while the behaviour of the computational mode is quite different. For the case  $p < 0$ , we obtain in the same way

$$\theta_2 = -\pi - \theta_1.$$

Thus, for  $p \geq 0$ ,

$$\theta_2 = \pm \pi - \theta_1. \quad (2.42)$$

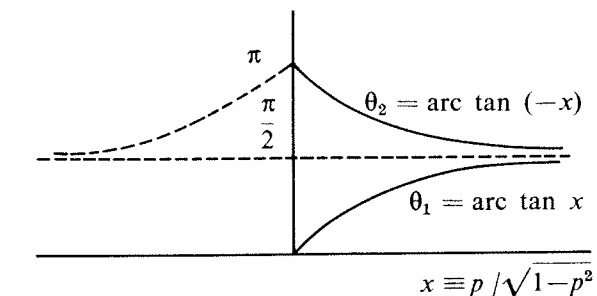


Figure 2.2 Phase change of the physical and of the computational mode for the leapfrog scheme.

For accuracy of the physical mode,  $\theta_1$  should closely approximate the phase change of the true solution,  $p$ . For small  $p$  (2.41)<sub>1</sub> gives

$$\theta_1 = p + \frac{1}{6} p^3 + \dots$$

Thus, the leapfrog scheme is accelerating; the acceleration, though, is four times less than that of the Matsuno scheme. It is instructive to note that schemes of different orders of accuracy can still have the same order of leading term in power series expansions of either the amplification factors or the phase changes.

Differentiating (2.41)<sub>1</sub> we find

$$\frac{d\theta_1}{dp} = \frac{1}{\sqrt{1-p^2}}.$$

The phase error, thus, is seen to increase sharply as  $p \rightarrow 1$ , when  $\theta_1/p \rightarrow \pi/2$ .

It may be useful to illustrate the behaviour of the two modes obtained

$$U_1^{(n)} = U_1^{(0)} e^{in\theta_1}, \quad U_2^{(n)} = U_2^{(0)} e^{in(\pm\pi-\theta_1)}, \quad (2.43)$$

in the complex plane. For simplicity, we consider the case  $\theta_1 = \pi/8$  and assume that the imaginary part of

the solution is equal to zero at the initial moment. The physical mode, as seen in (2.43), rotates in the positive sense by an angle  $\theta_1$  in each time step  $\Delta t$ , while at the same time the computational mode, in the case  $p > 0$ , rotates by an angle  $\pi - \theta_1$ . Therefore, the two modes can be represented graphically as in Fig. 2.3.

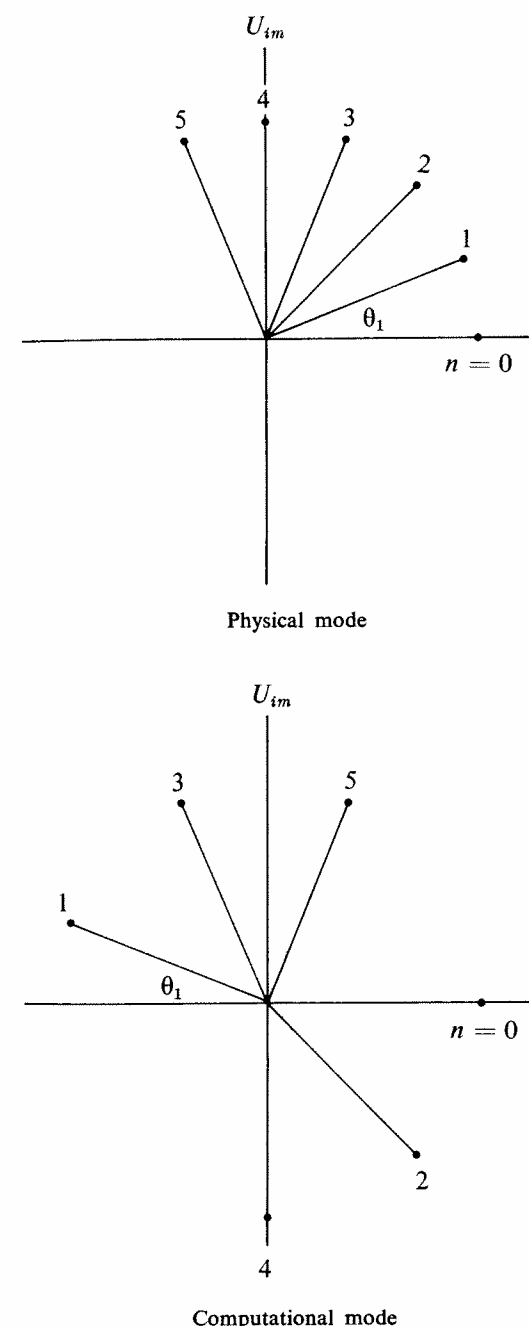


Figure 2.3 The physical and computational modes, for the leapfrog scheme, when  $\theta_1 = \pi/8$  and when the imaginary parts are zero at the initial moment, for a number of values of  $n$ .

A detailed knowledge of the behaviour of the computational mode may be helpful in recognizing its excessive presence in an integration. Thus, we plot the real and imaginary parts of the computational mode as functions of time. This can be done by using an alternative form of (2.43)<sub>2</sub>

$$U_2^{(n)} = (-1)^n U_2^{(0)} (\cos n\theta_1 - i \sin n\theta_1),$$

or directly from Fig. 2.3. We obtain diagrams as shown in Fig. 2.4. Because of the factor  $(-1)^n$ , both real and imaginary parts oscillate between time steps.

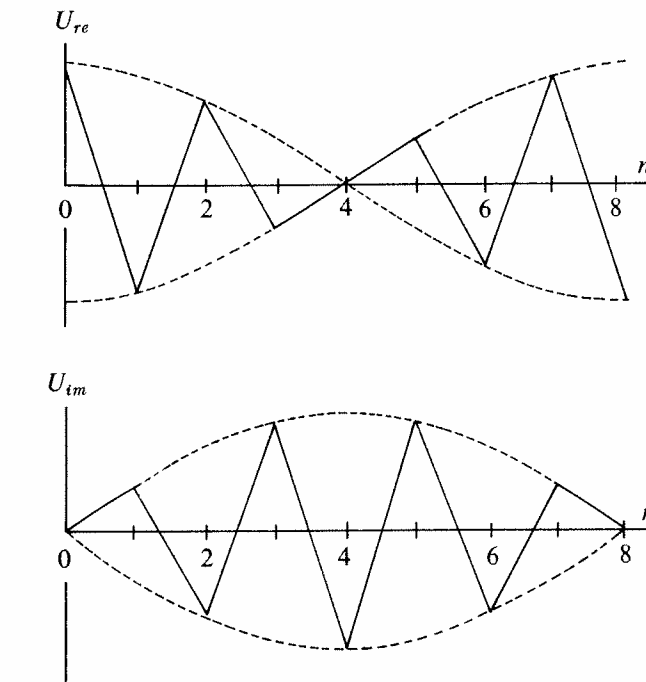


Figure 2.4 Real and imaginary parts of the computational mode, for the leapfrog scheme, for the same case as shown in the preceding figure, as functions of time.

II.  $|p| = 1$ . This is a limiting case of the solutions considered for  $|p| < 1$ . (2.34) shows that the values of  $\lambda$  are now equal,

$$\lambda_1 = \lambda_2 = ip.$$

Therefore

$$|\lambda_1| = |\lambda_2| = 1. \quad (2.44)$$

Thus, both modes are still neutral. Since neither of them has a real part, we obtain, for  $p = \pm 1$ ,

$$\theta_1 = \theta_2 = \pm \frac{\pi}{2}. \quad (2.45)$$

Therefore, the two modes can be written in the form

$$U^{(n)} = U^{(0)} e^{\pm i n \frac{\pi}{2}}. \quad (2.46)$$

In a complex plane, they rotate by an angle of  $\pm \pi/2$  in each time step, while the true solution rotates by an angle of  $\pm 1$  only. The phase error, thus, is large.

III.  $|p| > 1$ . Both values of  $\lambda$  in (2.34) still have imaginary parts only, so that

$$\begin{aligned} \lambda_1 &= i(p + \sqrt{p^2 - 1}), \\ \lambda_2 &= i(p - \sqrt{p^2 - 1}), \end{aligned}$$

where the expressions in parentheses are real. Therefore,

$$\begin{aligned} |\lambda_1| &= |p + \sqrt{p^2 - 1}|, \\ |\lambda_2| &= |p - \sqrt{p^2 - 1}|. \end{aligned} \quad (2.47)$$

Thus, for  $p > 1$  we have  $|\lambda_1| > 1$ , and for  $p < -1$   $|\lambda_2| > 1$ . Therefore, for  $|p| > 1$  the leapfrog scheme is unstable. The instability increases sharply as  $|p|$  increases beyond 1; we can see this, for example for  $p > 1$ , because

$$\frac{d|\lambda_1|}{dp} = 1 + \frac{p}{\sqrt{p^2 - 1}}$$

which is unbounded as  $p \rightarrow 1$ .

Since the two values of  $\lambda$  still have no real parts, we again have

$$\theta_1 = \theta_2 = \pm \frac{\pi}{2}. \quad (2.48)$$

The two modes for  $p \geq 1$ , can thus be written as

$$\begin{aligned} U_1^{(n)} &= |p + \sqrt{p^2 - 1}|^n U_1^{(0)} e^{\pm i n \frac{\pi}{2}}, \\ U_2^{(n)} &= |p - \sqrt{p^2 - 1}|^n U_2^{(0)} e^{\pm i n \frac{\pi}{2}}. \end{aligned} \quad (2.49)$$

In the complex plane, both modes again rotate by an angle of  $\pm \pi/2$  in each time step. However, this time the amplitude of one of the modes increases, and that of the other decreases with time. The real part of the unstable mode can, for instance, be represented as a function of time by a graph like that in Fig. 2.5. Because of (2.48) the period of the unstable oscillation is always  $4\Delta t$ . This can be used to diagnose the instability: if the results appear unsatisfactory, it is a good idea to

check for the presence of growing oscillations of that period.

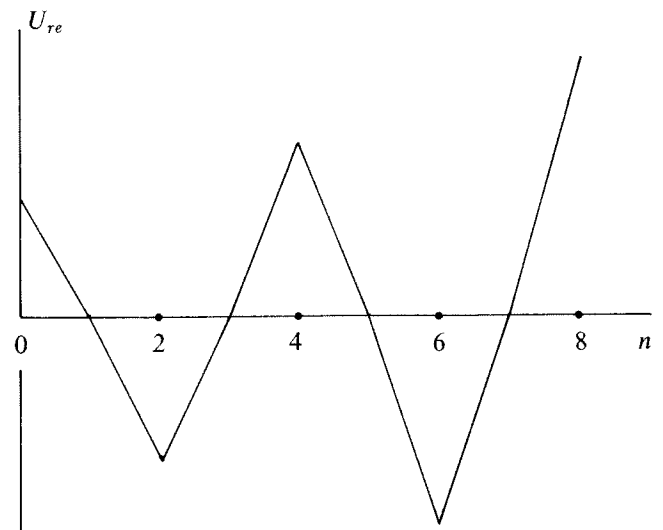


Figure 2.5 The real part of the unstable mode, for the leapfrog scheme, in case when  $|\lambda| = 1.1$  and when the imaginary part is zero at the initial moment, as a function of time.

To sum up, advantages of the leapfrog scheme are that it is a very simple scheme, of second order accuracy, and neutral within the stability range  $|\omega\Delta t| \leq 1$ . A disadvantage of the leapfrog scheme is the presence of a neutral computational mode. With nonlinear equations there is a tendency for a slow amplification of the computational mode. An example of this growth can be seen, for example, in one figure of a paper by Lilly (1965). The usual method used for suppressing this instability is the occasional insertion of a step made by a two level scheme, which eliminates the computational mode. A multi-level scheme that damps the computational mode could also be used for this purpose.

When solving the system of gravity wave equations, as will be shown in Chapter IV, it is possible to construct grids and/or finite difference schemes which have essentially the same properties as the leapfrog scheme, but in which the computational mode is absent. These methods calculate the physical mode only, and at the same time require only one half of the computation time needed for the regular leapfrog scheme as described here.

We consider, finally, stability and other properties of the Adams-Basforth scheme (1.10). Applied to the oscillation equation it gives

$$U^{(n+1)} = U^{(n)} + i\omega\Delta t \left( \frac{3}{2} U^{(n)} - \frac{1}{2} U^{(n-1)} \right). \quad (2.50)$$

Substituting the relations (2.33) we find

$$\lambda^2 - \left( 1 + i \frac{3}{2} p \right) \lambda + i \frac{1}{2} p = 0.$$

We have, of course, again obtained a second degree equation for  $\lambda$ . It has the solutions

$$\begin{aligned} \lambda_1 &= \frac{1}{2} \left( 1 + i \frac{3}{2} p + \sqrt{1 - \frac{9}{4} p^2 + ip} \right), \\ \lambda_2 &= \frac{1}{2} \left( 1 + i \frac{3}{2} p - \sqrt{1 - \frac{9}{4} p^2 + ip} \right). \end{aligned} \quad (2.51)$$

Thus, as  $p \rightarrow 0$   $\lambda_1 \rightarrow 1$ , while  $\lambda_2 \rightarrow 0$ . We see that the solution associated with  $\lambda_1$  again represents a physical mode, and that associated with  $\lambda_2$  a computational mode. However, while for the leapfrog scheme the computational mode was found to be neutral, here it is seen to be damped. This is a very useful property of the Adams-Basforth scheme as the computational mode cannot cause inconveniences.

The exact analysis of the amplification factors here is more difficult because of the presence of square roots in (2.51). However, since for reasons of accuracy we have to choose a relatively small value of  $p$  in any case, it will suffice to consider amplification factors for small values of  $p$  only. The power series expansion of (2.51) then gives

$$\begin{aligned} \lambda_1 &= 1 + ip - \frac{1}{2} p^2 + i \frac{1}{4} p^3 - \frac{1}{8} p^4 + \dots, \\ \lambda_2 &= i \frac{1}{2} p + \frac{1}{2} p^2 - i \frac{1}{4} p^3 + \frac{1}{8} p^4 - \dots. \end{aligned}$$

Now, after rearranging the terms these series can be written as

$$\begin{aligned} \lambda_1 &= \left( 1 - \frac{1}{2} p^2 - \frac{1}{8} p^4 - \dots \right) + i \left( p + \frac{1}{4} p^3 + \dots \right), \\ \lambda_2 &= \left( \frac{1}{2} p^2 + \frac{1}{8} p^4 + \dots \right) + i \left( \frac{1}{2} p - \frac{1}{4} p^3 - \dots \right), \end{aligned}$$

which can be used to obtain the amplification factors

$$\begin{aligned} |\lambda_1| &= \left( 1 + \frac{1}{2} p^4 + \dots \right)^{\frac{1}{2}}, \\ |\lambda_2| &= \left( \frac{1}{4} p^2 + \dots \right)^{\frac{1}{2}}. \end{aligned} \quad (2.52)$$

The higher order terms have been omitted. A final expansion gives

$$\begin{aligned} |\lambda_1| &= 1 + \frac{1}{4} p^4 + \dots, \\ |\lambda_2| &= \frac{1}{2} p + \dots. \end{aligned} \quad (2.53)$$

Expressions (2.52) and/or (2.53) show that the physical mode of the Adams-Basforth scheme is always unstable. However, as for the Heun scheme, the amplification is only by a fourth order term, and it can be tolerated when a sufficiently small value of  $\Delta t$  is chosen. Note that the amplification given by (2.53)<sub>1</sub> is twice that given by (2.26) for the Heun scheme. Since the amplification is proportional to  $(\Delta t)^4$ , however, a small reduction in time step would compensate for that difference. Thus, the Adams-Basforth scheme, with only one evaluation of the right hand side per time step, can still be considered much more economical. It has been fairly frequently used in meteorological numerical studies. For example, it is being used by Deardorff in his numerical simulations of the planetary boundary layer (e.g. Deardorff, 1974).

Analyses of the properties of some other schemes, applied to the oscillation equation, can be found in papers by Lilly (1965), Kurihara (1965) and Young (1968). In practice the choice of a scheme will depend not only on the properties considered here, but also on some practical considerations. For example, we might expect that the three level schemes, since they use more information, would generally give better results than the two level schemes. Our findings agree with that conjecture; for example, for second order accuracy the explicit three level schemes required only one evaluation of the right hand side per time step, while the two level schemes required two evaluations. As another example, if we want to damp high frequency motions with three level schemes we can linearly extrapolate the derivative beyond the centre of the interval  $(n\Delta t, (n+1)\Delta t)$ , and thus obtain a scheme that will perform such a damping in a more selective and more economical way than the Matsuno scheme (Mesinger, 1971). However, three level schemes generally require more core storage space in the computer than two level schemes and this may affect our decision.

### 3. Properties of schemes applied to the friction equation

We shall now consider the properties of schemes when applied to the equation

$$\frac{dU}{dt} = -\kappa U, \quad U = U(t), \quad \kappa > 0. \quad (3.1)$$

We shall call this equation the *friction equation*.

Again it is easy to justify our interest in this equation. For example, if we define  $U \equiv u + iv$ , it describes the

effect of friction proportional to the velocity vector, as is often assumed for motions near the ground. As another example, note that when seeking a solution of the heat transfer, or Fick's diffusion equation

$$\frac{\partial u}{\partial t} = \sigma \frac{\partial^2 u}{\partial x^2}; \quad \sigma > 0,$$

in the form of a single harmonic component

$$u(x, t) = \operatorname{Re}[(U(t) e^{ikx})],$$

we obtain

$$\frac{dU}{dt} = -\sigma k^2 U.$$

This is equivalent to (3.1) if we substitute  $x = \sigma k^2 t$ .

The general solution of (3.1) is

$$U(t) = U(0) e^{-\kappa t}. \quad (3.2)$$

Thus, both the real and the imaginary part decrease exponentially with time.

The properties of schemes applied to (3.1) will again be analyzed using the von Neumann method. As in the previous section, we consider first the non-iterative two level scheme (2.6). Applied to the friction equation, (2.6) gives

$$U^{(n+1)} = U^n - \kappa \Delta t (\alpha U^{(n)} + \beta U^{(n+1)}). \quad (3.3)$$

Writing

$$K \equiv \kappa \Delta t, \quad (3.4)$$

we obtain, rearranging the terms in (3.3),

$$U^{(n+1)} = \frac{1 - \alpha K}{1 + \beta K} U^{(n)}. \quad (3.5)$$

For the Euler scheme  $\alpha = 1$  and  $\beta = 0$ ; thus, (3.5) shows that the Euler scheme is now stable if  $|1 - K| \leq 1$ , that is, if

$$0 < K \leq 2. \quad (3.6)$$

Thus we see that the stability criteria of particular schemes do not have to be the same when they are applied to different equations. In the case of (3.6), one will normally be more demanding in the choice of  $\Delta t$ . For example, we will want  $K \leq 1$ , to prevent the solution (3.5) oscillating from time step to time step.

For the backward scheme  $\alpha = 0$  and  $\beta = 1$ ; it is always stable if  $K > 0$ . The solution does not oscillate in sign.

For the trapezoidal scheme  $\alpha = 1/2$  and  $\beta = 1/2$ ; the scheme is again always stable for  $K > 0$ . The solution does not oscillate if  $K < 2$ .

Considering the iterative two level scheme (2.18) we obtain

$$U^{(n+1)} = (1 - K + \beta K^2) U^{(n)}. \quad (3.7)$$

Therefore, both the Matsuno and the Heun scheme are stable for sufficiently small values of  $K$ .

It is instructive to consider in some detail the behaviour of the numerical solution obtained using the leapfrog scheme. Applied to (3.1) it gives

$$U^{(n+1)} = U^{(n-1)} - 2 \times \Delta t \cdot U^{(n)} \quad (3.8)$$

The equation for the amplification factor is

$$\lambda^2 + 2K\lambda - 1 = 0,$$

giving the solutions

$$\begin{aligned} \lambda_1 &= -K + \sqrt{1 + K^2}, \\ \lambda_2 &= -K - \sqrt{1 + K^2}. \end{aligned} \quad (3.9)$$

As  $K \rightarrow 0$   $\lambda_1 \rightarrow 1$ , while  $\lambda_2 \rightarrow -1$ ; thus, the solution associated with  $\lambda_1$  again represents the physical mode, and that associated with  $\lambda_2$  the computational mode. For  $K > 0$ , that is, for the normal case of a forward integration in time, we have  $\lambda_2 < -1$ ; hence, the computational mode is always unstable. It changes sign from time step to time step, and its magnitude increases. As before, we cannot hope to eliminate the computational mode completely. This amplification is not negligible, and the leapfrog scheme is therefore not suitable for numerical integration of the friction equation.

A simple example can be given to illustrate the instability of the leapfrog scheme. Let  $U$  have only a real part, and suppose we have set  $U^{(1)} = U^{(0)}$ , as shown in Fig. 3.1. Furthermore, let the dashed curve in the figure represent the true solution satisfying the given initial condition  $U^{(0)}$ . Knowing  $U^{(0)}$ ,  $U^{(1)}$  and the true solution it is possible to construct a graph of the numerical solution, using the fact that  $dU/dt = -\kappa U$  is equal to the slope of the line tangent to the true solution at the appropriate value of  $U$ . In this way we obtain the numerical solution shown by the full line. In this method, the derivative is calculated as a function of the current value of  $U^{(n)}$ , and the increment due to this derivative is added to the preceding value. This is seen to result in an unbounded growth of the difference between consecutive values of  $U^{(n)}$ , even when this difference is equal to zero initially.

#### 4. A combination of schemes

A natural question to ask at this point is what can we do if, for example, the equation contains both the oscillation and the friction term, that is

$$\frac{dU}{dt} = i\omega U - \kappa U. \quad (4.1)$$

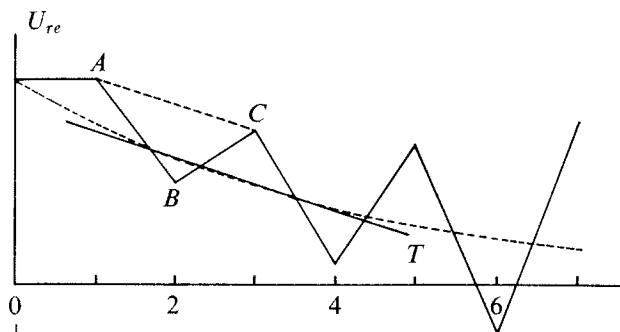


Figure 3.1 An example illustrating the instability of the leapfrog scheme applied to the friction equation.  $AC$  is constructed to be parallel to the tangent  $T$ .

Finally, for the Adams-Basforth scheme we obtain

$$\lambda = \frac{1}{2} \left( 1 - \frac{3}{2} K \pm \sqrt{1 - K + \frac{9}{4} K^2} \right). \quad (3.10)$$

The Adams-Basforth scheme, thus, is stable for sufficiently small values of  $K$ . The computational mode is damped.

Here we might like to use the leapfrog scheme because of the oscillation term  $i\omega U$ , but we know that it cannot be used for the friction term  $-\kappa U$ . In this and similar situations we can use different schemes for the different terms; for example, we might use the leapfrog scheme for the oscillation term and the forward scheme for the friction term. We then obtain

$$U^{(n+1)} = U^{(n-1)} + 2\Delta t (i\omega U^{(n)} - \kappa U^{(n-1)}).$$

Other combinations, of course, are also possible.

### CHAPTER III THE ADVECTION EQUATION

We now consider differential equations with one dependent and *two or three* independent variables, that is, partial differential equations. More specifically, we shall consider various simplified forms of the *advection equation*, describing advection of a dependent variable. This is considered in practice to be the most important part of the atmospheric governing equations.

We have already discussed the one-dimensional linear advection equation to some extent in the introductory chapter. We shall organize the analysis here so as first to continue considering problems associated with the simplest one-dimensional linear form of the advection equation, and then to proceed to problems introduced by more complex forms of the advection equation.

#### 1. Schemes with centered second-order space differencing

We shall first consider the equation

$$\frac{\partial u}{\partial t} + c \frac{\partial u}{\partial x} = 0; \quad c = \text{const.} \quad (1.1)$$

Here  $u = u(x, t)$  is a function of *two* independent variables : the independent variable  $x$  will represent a space variable, and, thus, (1.1) will be called the *one-dimensional* linear advection equation. As seen earlier, its general solution is

$$u = f(x - ct), \quad (1.2)$$

where  $f$  is an arbitrary function. The name "advection equation" was suggested by Phillips (1960).

One of the finite difference schemes for (1.1) is the forward and upstream scheme, which has been shown excessively damping in Chapter I.

If the space derivative in (1.1) is approximated by a centered finite difference quotient using values at the two nearest points, we obtain for the time derivative

$$\frac{\partial u_j}{\partial t} = -c \frac{u_{j+1} - u_{j-1}}{2\Delta x}. \quad (1.3)$$

The subscript here, as before, denotes the distance from the origin in space increments ; that is,  $x = j\Delta x$ . A number of schemes for the numerical solution of (1.1) can now be constructed because we can approximate the time derivative in (1.3) by one of the methods studied

in the preceding chapter. For example, when the time derivative is approximated using the leapfrog scheme, we obtain

$$\frac{u_j^{n+1} - u_j^n}{\Delta t} = -c \frac{u_{j+1}^n - u_{j-1}^n}{2\Delta x}, \quad (1.4)$$

as one of many possible consistent schemes for the numerical solution of (1.1).

The properties of schemes constructed in this way can be inferred from the known properties of time differencing schemes applied to the oscillation equation. To see this, we substitute into (1.3) a tentative solution in form of the single harmonic component

$$u_j = \text{Re} [U(t) e^{ikj\Delta x}]. \quad (1.5)$$

After some rearrangement, this gives

$$\frac{dU}{dt} = i \left( -\frac{c}{\Delta x} \sin k\Delta x \right) U. \quad (1.6)$$

If we denote

$$\omega \equiv -\frac{c}{\Delta x} \sin k\Delta x, \quad (1.7)$$

this is equivalent to the oscillation equation of the previous chapter. Now, if we approximate (1.6) using one of the time differencing schemes studied in that chapter, the same finite difference equation is obtained as when we apply that scheme to (1.3) and then substitute the wave solution (1.5). Hence, properties of finite difference schemes derived from (1.3) can be inferred from the results of Section 2 of Chapter II, where the frequency  $\omega$  is given by (1.7).

As an example, if (1.6) is approximated using the *leapfrog* scheme, we obtain

$$U^{(n+1)} = U^{(n-1)} + 2i \left( -c \frac{\Delta t}{\Delta x} \sin k\Delta x \right) U^{(n)}. \quad (1.8)$$

Using the notation of chapter II, we write

$$p \equiv -c \frac{\Delta t}{\Delta x} \sin k\Delta x. \quad (1.9)$$

We obtain the same finite difference equation (1.8) by first applying the leapfrog scheme to (1.3) giving (1.4) and then substituting (1.5) into (1.4). Thus, properties of (1.4) can be inferred from (1.7) and from the known properties of the leapfrog scheme applied to the oscillation equation.

Let us look at some of conclusions obtained in this way. For stability of the leapfrog scheme it was required that the condition  $|p| \leq 1$  be satisfied for all values of  $\omega$  occurring. Thus, we have to satisfy

$$\left| c \frac{\Delta t}{\Delta x} \sin k\Delta x \right| \leq 1$$

for any admissible  $k$ . Since  $|\sin k\Delta x|$  does reach the maximum value of unity in the admissible range of  $k$ , we obtain the stability condition

$$\left| c \right| \frac{\Delta t}{\Delta x} \leq 1. \quad (1.10)$$

This criterion, obtained already in Chapter I, shows that stability cannot simply be achieved by reduction of the time and space increments. Rather, it is necessary to reduce the ratio of these increments  $\Delta t/\Delta x$  to obtain stability. The condition (1.10) was first found by Courant, Friedrichs and Lewy (1928), and, therefore, is usually referred to as the Courant-Friedrichs-Lowy, or CFL, stability criterion.

It is instructive to note that the maximum value of  $|p|$ , that is, the minimum stability, is associated with the wave with  $k\Delta x = \pi/2$ . This is the component with wave length  $4\Delta x$ , twice the shortest resolvable wave length  $2\Delta x$ .

We can also use other results of the previous analysis. There are two solutions for  $U^{(n)}$ , the physical and the computational mode

$$U_1^{(n)} = \lambda_1^n U_1^{(0)}, \quad U_2^{(n)} = \lambda_2^n U_2^{(0)}. \quad (1.11)$$

$\lambda_1$  and  $\lambda_2$  are given here by Eqs. (2.34) of Chapter II. In the stable case, we have, for  $p \leq 0$ ,

$$\lambda_1 = e^{i\theta}, \quad \theta = \arctan(p/\sqrt{1-p^2}); \quad (1.12)$$

$$\lambda_2 = e^{i(\pm\pi-\theta)} = -e^{-i\theta}.$$

Using (1.5), it is seen that the approximation  $u_j^n$  also has a physical and a computational mode. For the physical mode

$$u_j^n = \text{Re} \left[ U_1^{(0)} e^{ik(j\Delta x + \frac{\theta}{k\Delta t} n\Delta t)} \right]. \quad (1.13)$$

For the computational mode, on the other hand, we obtain

$$u_j^n = \text{Re} \left[ (-1)^n U_2^{(0)} e^{ik(j\Delta x - \frac{\theta}{k\Delta t} n\Delta t)} \right]. \quad (1.14)$$

These expressions can be compared with the true solution of (1.1) in the form of a single harmonic component, as given in chapter I,

$$u(x, t) = \text{Re} [U(0) e^{ik(x-ct)}]. \quad (1.15)$$

We find that the phase speed of the physical mode,  $c_1$ , is equal to  $-\theta/k\Delta t$ , and the phase speed of the computational mode,  $c_2$ , considering the even time steps only, is equal to  $\theta/k\Delta t$ . Eq. (1.12)<sub>2</sub> shows that as  $\Delta t \rightarrow 0$   $\theta \rightarrow p$ , and (1.9) shows that as  $\Delta x \rightarrow 0$   $p \rightarrow -ck\Delta t$ . Thus, as  $\Delta x, \Delta t \rightarrow 0$   $c_1 \rightarrow c$ , that is, the phase speed of the physical mode approaches the phase speed of the true solution, while at the same time  $c_2 \rightarrow -c$ . In addition, the computational mode changes sign at all grid points from time step to time step, because of the factor  $(-1)^n$  in (1.14).

Now let us use another scheme from chapter II to approximate the time derivative in (1.3), the *Matsuno* scheme. First the approximate values  $u_j^{(n+1)*}$  are computed using the forward scheme, that is,

$$\frac{u_j^{(n+1)*} - u_j^n}{\Delta t} = -c \frac{u_{j+1}^n - u_{j-1}^n}{2\Delta x}. \quad (1.16)$$

Then, these approximate values are used in the backward scheme, that is

$$\frac{u_j^{n+1} - u_j^n}{\Delta t} = -c \frac{u_{j+1}^{(n+1)*} - u_{j-1}^{(n+1)*}}{2\Delta x}. \quad (1.17)$$

It is instructive to eliminate the approximate values  $u_j^{(n+1)*}$  from this equation, by substituting values given by (1.16), with the subscript  $j$  replaced by  $j+1$ , and then by  $j-1$ . In this way we obtain

$$\begin{aligned} \frac{u_j^{n+1} - u_j^n}{\Delta t} &= -c \frac{u_{j+1}^n - u_{j-1}^n}{2\Delta x} + \\ &+ c^2 \Delta t \frac{u_{j+2}^n - 2u_j^n + u_{j-2}^n}{(2\Delta x)^2}. \end{aligned} \quad (1.18)$$

Without the last term, this represents the finite difference equation obtained when the forward scheme is used for the time derivative in (1.3). The third term approaches zero as  $\Delta x, \Delta t \rightarrow 0$ , and (1.18) is therefore also a consistent scheme for the advection equation. On the other hand, for a fixed  $\Delta t$  this term approaches  $c^2 \Delta t (\partial^2 u / \partial x^2)$  as  $\Delta x \rightarrow 0$ . It is therefore of the same form as a finite difference approximation to a Fick's diffusion term,

and it has a damping effect. This damping effect, however, is dependent on the wave length. As the third term is calculated over an interval of  $4\Delta x$ , the maximum damping occurs for a wave with wave length of  $4\Delta x$ . There is no damping of the shortest resolvable wave with wave length  $2\Delta x$ . Even if a damping effect were desirable when solving the advection equation, we would not want this particular dependence on wave length. Thus, the Matsuno scheme does not appear suitable for solving the advection equation.

It is convenient to include here one more example of the use of the *energy method* for testing stability. In addition to being applicable also to nonlinear equations, it can be used to study the effect of boundary conditions on stability. We will use the energy method here to test the stability of a group of schemes that can be used for solving (1.3).

A fairly wide class of schemes for solving (1.3) can be written as

$$u_j^{n+1} - u_j^n = -\frac{1}{2}\mu(u_{j+1}^* - u_{j-1}^*), \quad (1.19)$$

$$\text{where } \mu \equiv c\Delta t/\Delta x, \quad (1.20)$$

and  $u_j^*$  is a linear function of a number of values  $u_j^n$ . For example, to obtain the non-iterative two level schemes we write

$$u_j^* = \alpha u_j^n + \beta u_j^{n+1}. \quad (1.21)$$

For the iterative two level schemes write

$$u_j^* = u_j^n - \frac{\beta}{2}\mu(u_{j+1}^n - u_{j-1}^n). \quad (1.22)$$

Finally, for the Adams-Basforth scheme

$$u_j^* = \frac{3}{2}u_j^n - \frac{1}{2}u_j^{n-1}. \quad (1.23)$$

Here we shall analyze the stability of the non-iterative two level schemes. It is convenient first to multiply (1.19) by  $u_j^*$  and sum for all  $j$ ; we obtain

$$\sum_j u_j^*(u_j^{n+1} - u_j^n) = -\frac{1}{2}\mu \sum_j u_j^*(u_{j+1}^* - u_{j-1}^*).$$

The right hand side vanishes if cyclic boundary conditions are assumed; we then have

$$\sum_j u_j^*(u_j^{n+1} - u_j^n) = 0.$$

Adding this to the relation gives

$$\sum_j \frac{1}{2}[(u_j^{n+1})^2 - (u_j^n)^2] = \sum_j \frac{1}{2}(u_j^{n+1} + u_j^n)(u_j^{n+1} - u_j^n)$$

Substituting (1.21), and eliminating  $\beta$  using  $\beta = 1-\alpha$ , we obtain, after some rearrangement

$$\sum_j \frac{1}{2}[(u_j^{n+1})^2 - (u_j^n)^2] = \left(\alpha - \frac{1}{2}\right) \sum_j (u_j^{n+1} - u_j^n)^2. \quad (1.24)$$

Thus, if  $\alpha > 1/2$  we have an unstable scheme; if  $\alpha = 1/2$  a stable and neutral scheme, and, if  $\alpha < 1/2$  a stable and damping scheme, which makes the total "energy"

$\sum_j \frac{1}{2}(u_j^n)^2$  monotonically decrease with time.

Finally in this section, we shall analyze a scheme that was proposed by Lax and Wendroff (1960) and is thus called the *Lax-Wendroff* scheme, or, more specifically, the *two-step Lax-Wendroff* scheme. In contrast with the schemes discussed so far, the Lax-Wendroff scheme cannot be constructed by an independent choice of finite difference approximations to the space and to the time derivative of the advection equation. To describe the procedure, we use the stencil shown in Fig. 1.1. First,

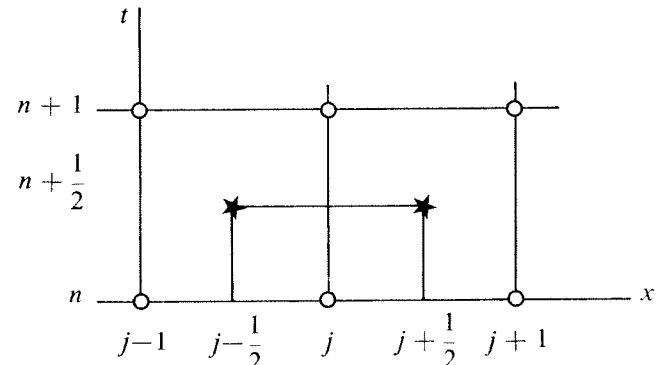


Figure 1.1 The space-time stencil used for the construction of the Lax-Wendroff scheme.

provisional values are calculated at the centres of the two rectangular meshes of this stencil, for points denoted by  $x$  signs. This is done using centered space and forward time differencing, taking for  $u_{j+1/2}^n$  and  $u_{j-1/2}^n$  arithmetic averages of the values  $u_j^n$  at the two nearest grid points. Therefore,

$$\frac{u_{j+1/2}^{n+1/2} - \frac{1}{2}(u_{j+1}^n + u_j^n)}{\frac{1}{2}\Delta t} = -c \frac{u_{j+1}^n - u_j^n}{\Delta x}, \quad (1.25)$$

$$\frac{u_{j-1/2}^{n+1/2} - \frac{1}{2}(u_j^n - u_{j-1}^n)}{\frac{1}{2}\Delta t} = -c \frac{u_j^n - u_{j-1}^n}{\Delta x}.$$

Using these provisional values another step is made, centered in both space and time; thus

$$\frac{u_j^{n+1} - u_j^n}{\Delta t} = -c \frac{u_{j+1/2}^{n+1/2} - u_{j-1/2}^{n+1/2}}{\Delta x}. \quad (1.26)$$

Substitution of the provisional values from (1.25) into this equation gives

$$\begin{aligned} \frac{u_j^{n+1} - u_j^n}{\Delta t} &= -c \frac{u_{j+1}^n - u_{j-1}^n}{2\Delta x} + \\ &+ \frac{1}{2}c^2\Delta t \frac{u_{j+1}^n - 2u_j^n + u_{j-1}^n}{(\Delta x)^2}. \end{aligned} \quad (1.27)$$

It is interesting to note that this finite difference equation is very similar to (1.18), that is, to the scheme obtained using simple centered space differencing and the Matsuno time differencing. The only difference is in the last term. This again approaches zero as  $\Delta x, \Delta t \rightarrow 0$ . However, if  $\Delta x \rightarrow 0$  with  $\Delta t$  fixed, it now approaches  $\frac{1}{2}c^2\Delta t(\partial^2 u / \partial x^2)$ . Thus, we see that it is again equivalent in form to a finite difference approximation to the Fickian diffusion term, but with a coefficient of half the size given by (1.18). Furthermore, this term is now calculated over an interval of  $2\Delta x$ , and its damping effect will be a maximum at that wave length. This sort of dependence on wave length is often considered desirable for damping in a finite difference scheme. This is because, as we will see later, there are serious problems with finite difference calculations for small wave lengths, especially around  $2\Delta x$ . It is often possible to alleviate these problems by using a dissipative scheme, which damps the two-grid-interval waves preferentially.

While (1.18) was of the first order of accuracy in time, (1.27) has truncation error  $O[(\Delta x)^2] + O[(\Delta t)^2]$ ; thus, it is of second order accuracy in both space and time.

To test the stability of the Lax-Wendroff scheme, we substitute

$$u_j^n = \operatorname{Re}[U^{(n)} e^{ikj\Delta x}] \quad (1.28)$$

into (1.27). This gives

$$U^{(n+1)} = [1 + \mu^2(\cos k\Delta x - 1) - i\mu \sin k\Delta x] U^{(n)}. \quad (1.29)$$

Therefore

$$\lambda = 1 + \mu^2(\cos k\Delta x - 1) - i\mu \sin k\Delta x. \quad (1.30)$$

Since

$$\cos k\Delta x - 1 = -2 \sin^2 \frac{k\Delta x}{2},$$

$$\sin k\Delta x = 2 \sin \frac{k\Delta x}{2} \cos \frac{k\Delta x}{2},$$

we finally obtain

$$|\lambda| = \left[ 1 - 4\mu^2(1 - \mu^2) \sin^4 \frac{k\Delta x}{2} \right]^{1/2}. \quad (1.31)$$

The expression within the bracket is a sum of two squares and never negative. Thus, the Lax-Wendroff scheme is stable for  $1 - \mu^2 \geq 0$ , or, for

$$|c| \frac{\Delta t}{\Delta x} \leq 1.$$

This is again the Courant-Friedrichs-Lowy stability criterion (1.10). The scheme is damping for  $|c| \Delta t / \Delta x < 1$ .

It is instructive to analyze in some detail the dependence of the damping wave length and on  $\mu$ . For the shortest resolvable wave length of  $2\Delta x$  we have  $k\Delta x = \pi$ , and, therefore,

$$|\lambda| = (1 - 4\mu^2 + 4\mu^4)^{1/2} = |1 - 2\mu^2|. \quad (1.32)$$

For waves of twice the wave length,  $4\Delta x$ ,  $k\Delta x = \pi/2$ , and

$$|\lambda| = (1 - \mu^2 + \mu^4)^{1/2}. \quad (1.33)$$

In general, since

$$\frac{d|\lambda|}{d\mu} = -\frac{4\mu(1 - 2\mu^2)\sin^4 \frac{k\Delta x}{2}}{\left[1 - 4\mu^2(1 - \mu^2)\sin^4 \frac{k\Delta x}{2}\right]^{1/2}},$$

all the  $|\lambda|$  curves have minima at  $\mu = 1/\sqrt{2}$ . Substituting this value of  $\mu$  into (1.31) we find that these minimum values of the amplification factor are equal to

$$\left(1 - \sin^4 \frac{k\Delta x}{2}\right)^{1/2} \quad (1.34)$$

Thus, as the wave length increases from the minimum value of  $2\Delta x$  this minimum value of  $|\lambda|$  monotonically increases from zero and approaches unity as the wave length leads to infinity.

The amplification factors for wave lengths of  $2\Delta x$  and  $4\Delta x$ , as calculated in (1.32) and (1.33), are shown in Fig. 1.2. The amount of damping is seen to be generally quite large for shorter wave lengths, especially for the wave length  $2\Delta x$ . The amount of damping also depends on the time step and the advection velocity. This is a disadvantage of the Lax-Wendroff scheme because there is no reason why the amount of damping should depend on these quantities and it is either impractical or impossible to control the damping by changing them. For example, for small values of  $\mu$  expansion of (1.31) gives

$$|\lambda| = 1 - 2\mu^2 \sin^4 \frac{k\Delta x}{2} + \dots,$$

showing that for a given amount of time (a fixed value of  $n\Delta t$ ) the total damping will be approximately proportional to  $\Delta t$ . However, we wish to choose  $\Delta t$  to give the best accuracy and stability properties, not to give the optimal amount of damping.

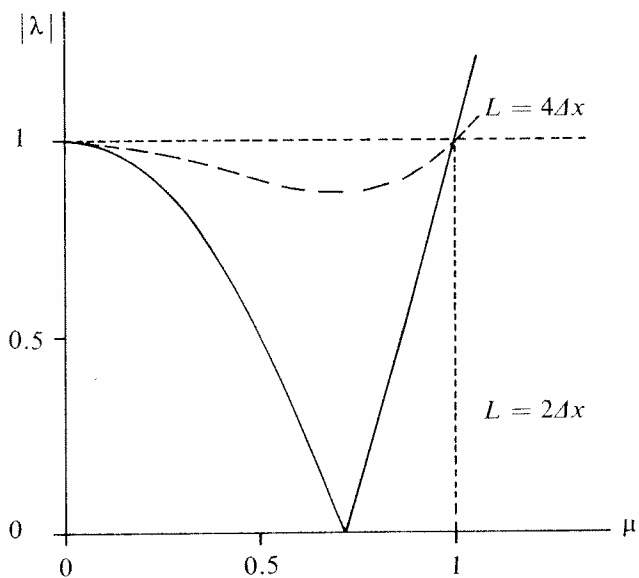


Figure 1.2 Amplification factor of the Lax-Wendroff scheme, as a function of  $\mu = c\Delta t/\Delta x$ , for the wave lengths  $2\Delta x$  and  $4\Delta x$ .

The Lax-Wendroff scheme has been fairly widely used in atmospheric models, due to a recommendation by Richtmyer (1963), and its reasonably good behaviour. It is second order accurate, explicit, not unconditionally unstable, and since it is a two levels scheme there is no computational mode. None of the schemes obtained by combining centered space differencing with one of the seven time differencing schemes studied in chapter II has all of these advantages. The dissipation of the Lax-Wendroff scheme will not be harmful if its total effect is

negligible compared with the physical dissipation, and it can also be useful for controlling the shortest waves. If the physical dissipation is very small or non-existent, it is better to use a neutral scheme.

One should point out here that we can change the time differencing scheme intermittently during an integration, so as to get the required amount of a particular effect. For example, in the general circulation model developed at the National Center for Atmospheric Research, Boulder, Colo., the Lax-Wendroff scheme is used because of its damping effect on the shortest waves. However, to keep the amount of damping small, it is used only once in every hundred steps, the rest are made using a neutral leapfrog scheme (Kasahara, 1969). On the other hand, in the British operational model (e.g. Gadd, 1974b) the Lax-Wendroff scheme is used every time step, with the authors of the model making no mention of any excessive damping due to the scheme for the purposes of that model.

## 2. Computational dispersion

As we have seen, the linear advection equation

$$\frac{\partial u}{\partial t} + c \frac{\partial u}{\partial x} = 0, \quad c = \text{const}, \quad (2.1)$$

has a solution in the form of a single harmonic component

$$u(x, t) = \text{Re}[U(t) e^{ikx}], \quad (2.2)$$

provided that

$$\frac{dU}{dt} + ikcU = 0. \quad (2.3)$$

In this oscillation equation  $kc$  is equal to the frequency  $\nu$ , and  $c = \nu/k$  is the phase speed of the waves. It is seen that waves of all wave lengths are propagated with the same phase speed, that is, the function  $u(x, t)$  is advected with no change in shape at a constant velocity  $c$  along the  $x$  axis. There is no dispersion.

Now consider the equation

$$\frac{\partial u_j}{\partial t} + c \frac{u_{j+1} - u_{j-1}}{2\Delta x} = 0. \quad (2.4)$$

that is obtained by approximating the space derivative in (2.1) by a centered difference quotient. The equation (2.4) is neither a differential nor a difference equation, but a hybrid of these two. An equation of this type can be called a *differential-difference equation*, or a *semi-*

*discrete* equation. The finite difference equations obtained when the time derivative in (2.4) is approximated using a consistent time differencing scheme will approach (2.4) as the time step approaches zero. Thus, for small  $\Delta t$  (2.4) represents an approximation to these finite difference equations. Since the time derivative has retained its differential form, any error in (2.4) is due to the space differencing.

For this reason, equations of this type are used to study the effect of particular space difference approximations on the properties of the numerical solution.

Recall that (2.4) has a solution in the form of a single harmonic component

$$u_j(t) = \text{Re}[U(t) e^{ikj\Delta x}], \quad (2.5)$$

provided that

$$\frac{dU}{dt} + ik \left( c \frac{\sin k\Delta x}{k\Delta x} \right) U = 0. \quad (2.6)$$

We have now written this so that it can conveniently be compared with (2.3). Instead of the constant phase speed  $c$ , we see that waves now propagate with the phase speed

$$c^* = c \frac{\sin k\Delta x}{k\Delta x}. \quad (2.7)$$

This phase speed is a function of the wave number  $k$ . Thus, the finite differencing in space causes a dispersion of the waves; we shall call this effect *computational dispersion*. As  $k\Delta x$  increases from zero, the phase speed  $c^*$  monotonically decreases from  $c$ , and becomes zero for the shortest resolvable wave length  $2\Delta x$ , when  $k\Delta x = \pi$ . Thus, all waves propagate at a speed that is less than the true phase speed  $c$ , with this decelerating effect increasing as the wave length decreases. The two-grid-interval wave is stationary.

The reason for the two-grid-interval wave being stationary is obvious when we look at the plot of that wave, shown in Fig. 2.1. For this wave  $u_{j+1} = u_{j-1}$  at all grid points, and (2.4) gives a zero value for  $\frac{\partial u_j}{\partial t}$ .

We have encountered two effects here. Firstly, the advection speed is less than the true advection speed. The consequence of this error is a general retardation of the advection process. Secondly, the advection speed changes with wave number; this false dispersion is particularly serious for the shortest waves.

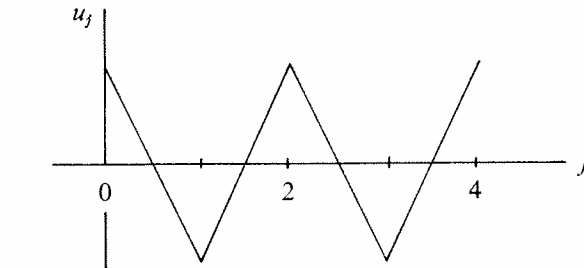


Figure 2.1 A plot of the "two-grid-interval" wave, with a wave length of  $2\Delta x$ .

If the pattern that is being advected represents a superposition of more than one wave, this false dispersion will result in a deformation of that pattern. It is especially small-scale patterns in the atmosphere, e.g. fronts, shear lines, etc., that represent a superposition of many waves, including a significant proportion of the shortest waves. For this reason, in numerical forecasting, such patterns, if present in the initial fields, are fairly rapidly deformed, until they acquire a form which is less sharp than in the beginning. Since such small-scale features are of particular importance in weather processes, the effect of computational dispersion deserves very careful consideration.

We now turn our attention to the group velocity. In the case of the linear equation (2.1) we obtain for the group velocity  $c_g$

$$\tau_c = \frac{d(kc)}{dk} = c. \quad (2.8)$$

Thus, the group velocity is constant and equal to the phase speed  $c$ . With the differential-difference equation (2.4), however, (2.7) gives for the group velocity  $c_g^*$

$$c_g^* = \frac{d(kc^*)}{dk} = c \cos k\Delta x. \quad (2.9)$$

Thus, as  $k\Delta x$  increases from zero, the group velocity  $c_g^*$  decreases monotonically from  $c_g$ , and becomes equal to  $-c_g$  for the shortest resolvable wave length of  $2\Delta x$ .

These results are summarized in Fig. 2.2. For the exact advection equation (2.1) both individual waves and wave packets, that is, places where superposition of waves results in a maximum amplitude of a group of neighbouring wave numbers, propagate at the same constant velocity  $c = c_g$ . Introduction of the centered space finite difference quotient in (2.4) both makes the phase speed and the group velocity decrease as the wave number increases. The error is particularly great for the shortest resolvable wave lengths; waves with wave lengths less

Phase  
or  
group  
velocity

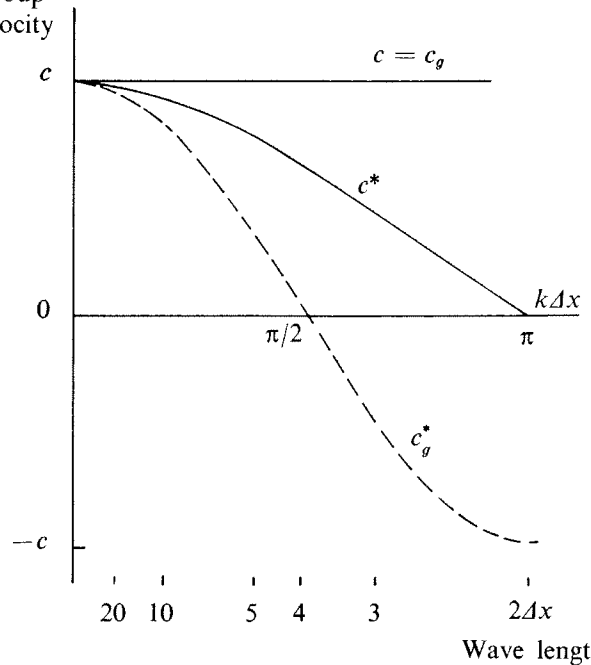


Figure 2.2 Phase speed and group velocity, in the case of the linear advection equation,  $c$  and  $c_g$ , and in the case of the corresponding differential-difference equation with second-order centered space differencing,  $c^*$  and  $c_g^*$  (Matsuno, 1966c).

than  $4\Delta x$  even have a negative group velocity. This means that wave packets made up of these waves propagate in the direction opposite to the advection velocity and opposite to the direction of propagation of individual waves.

It is possible to obtain an analytic solution of (2.4), which can be used to analyze its behaviour for some given initial conditions of interest. To this end it is convenient to define a non-dimensional time variable

$$\tau \equiv ct/\Delta x, \quad (2.11)$$

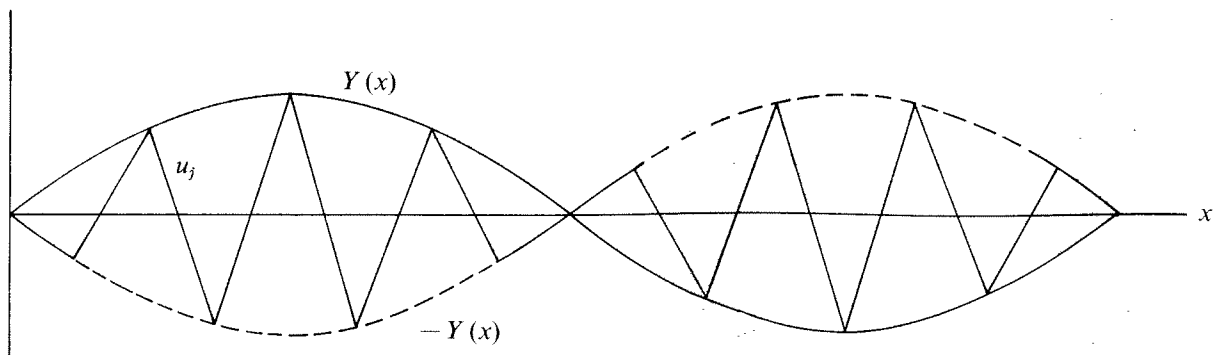


Figure 2.3 Functions  $u_j$  and  $\pm Y(x)$ , illustrating propagation of an envelope of short waves when their advection is calculated using second-order centered space differencing.

This situation can be illustrated by a simple example. Let us define  $Y(x)$  as a function that is slowly varying in space; for example, it can be a sine function of a large wave length. Furthermore, we define

$$u_j \equiv (-1)^j Y_j, \quad (2.10)$$

as shown in Fig. 2.3. Thus, the function  $\pm Y(x)$  is the envelope of the function  $u_j$ . Suppose that we calculate the advection of  $u_j$  using (2.4), then substituting (2.10) into (2.4) we obtain

$$\frac{\partial Y_j}{\partial t} - c \frac{Y_{j+1} - Y_{j-1}}{2\Delta x} = 0.$$

Thus, the advection of  $Y_j$  is governed by the same equation as the advection of  $u_j$ , except that the advection velocity appears with an opposite sign! Therefore, as the individual short waves of the function  $u_j$  slowly propagate in the direction of the positive  $x$  axis, the envelope  $\pm Y(x)$ , which has a long wave length, propagates relatively fast in the opposite direction. When it is a sine function, so that it consists of a single harmonic, it propagates with no change in shape. Because of (2.10),  $u_j$  must also be advected with no change in shape; from this we conclude that  $u_j$  also consists of a single harmonic component. If, on the other hand, the function  $Y(x)$  consisted of a number of harmonic components, the shapes of both  $Y(x)$  and  $u_j$  would change during the advection process, as a result of the computational dispersion of these components.

and, after dividing equation (2.4) by  $c/2\Delta x$ , to write it in the form

$$2 \frac{d}{d\tau} u_j(\tau) = u_{j-1}(\tau) - u_{j+1}(\tau). \quad (2.12)$$

This can be recognized as the recurrence formula of the Bessel function of the first kind of order  $j$ ,  $J_j(\tau)$ , (e.g. Courant and Hilbert, 1953, p. 488). In other words,

$$u_j(\tau) = J_j(\tau) \quad (2.13)$$

is a solution of (2.12). Several of these functions, of the lowest order, are shown in Fig. 2.4. The figure illustrates more of these functions than indicated, since, for any  $j$ ,

$$J_{-j} = (-1)^j J_j.$$

Note, furthermore, that in (2.12) the subscript  $j$  can take any integer value, since the location of the grid point for which we choose  $j = 0$  is arbitrary. Thus, a solution that is more general than (2.13) is

$$u_j(\tau) = J_{j-p}(\tau),$$

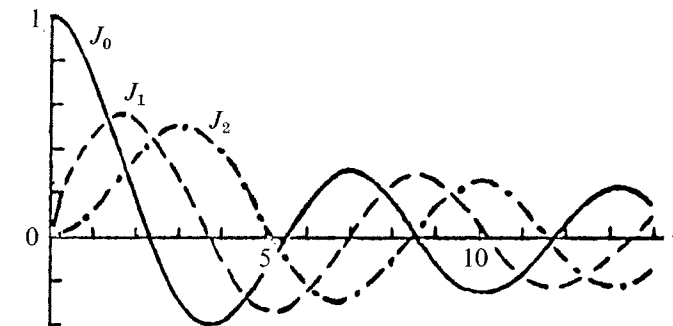


Figure 2.4 The Bessel functions  $J_0(\tau)$ ,  $J_1(\tau)$  and  $J_2(\tau)$ .

where  $p$  is an arbitrary integer. Since we are solving a linear equation, a still more general solution is a linear combination of all these solutions, that is

$$u_j(\tau) = \sum_{p=-\infty}^{\infty} a_p J_{j-p}(\tau), \quad (2.14)$$

where  $a_p$  are arbitrary constants. Now, for  $\tau = 0$  all of the functions  $J_k$  are equal to zero, except  $J_0$ , for which  $J_0(0) = 1$ . Hence, substituting  $\tau = 0$  into (2.14) we obtain

$$u_j(0) = a_j, \quad (2.15)$$

Therefore the constants in (2.14) can be chosen so as to satisfy arbitrary initial conditions  $u_j = u_j(0)$ . Since it can satisfy arbitrary initial conditions, (2.14) is seen to represent the general solution of (2.12), or (2.4).

It is instructive to look in some detail at the solution satisfying the initial conditions

$$u_j(0) = \begin{cases} 1 & \text{for } j=0 \\ 0 & \text{for } j \neq 0, \end{cases} \quad (2.16)$$

the simplest solution of the form (2.13), for different values of the non-dimensional time. At the initial moment the function  $u_j$  consists of a single pulse-like disturbance, centered at the point  $j = 0$ , as shown in the upper diagram of Fig. 2.5. We note that, because of (2.12),  $du_j/d\tau$  is then equal to zero at all points except at  $j = -1$  and  $j = 1$ , where it is equal to  $-1/2$  and  $1/2$ , respectively.

Thus, at the initial moment the disturbance propagates at the same rate in the directions of both the positive and the negative  $x$  axis. Further propagation of the disturbance according to (2.13) can be followed using Fig. 2.4, or, more accurately, using some tables of Bessel functions. Solutions obtained in this way for  $\tau = 5$  and  $\tau = 10$  are shown in the middle and lower diagrams of Fig. 2.5, respectively.

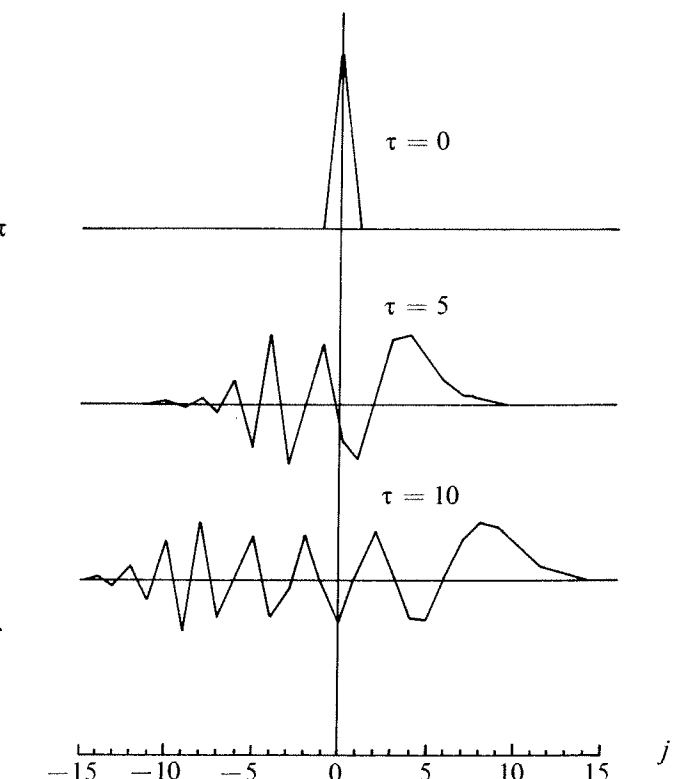


Figure 2.5 The analytic solution of (2.4), for the initial conditions shown in the uppermost of the three diagrams, for two subsequent values of the non-dimensional time  $\tau$  (Matsuno, 1966c).

The three diagrams present an example of the computational dispersion of the second-order centered space differencing. We note that if we expand a single pulse-like disturbance as a cosine Fourier integral

$$u(x) = \int_0^\infty a(k) \cos kx dk,$$

$$a(k) = \frac{2}{\pi} \int_0^\infty u(x) \cos kx dx,$$

and  $a(k)$  is calculated numerically using the grid point values only, we obtain a constant value

$$a(k) = \frac{2}{\pi} \Delta x.$$

Therefore, all the harmonic components have equal amplitude. By analogy with the light spectrum, such a function is called *white noise* if it does not appear for physical reasons. Its Fourier components are advected with different phase speeds, as summarized in Fig. 2.2, bringing about a dispersion of the disturbance. With the non-dimensional time chosen here we see from (2.12) that the physical advection velocity should keep the pulse located at the point  $j = \tau$ . Because of the space difference approximation, however, all the phase speeds are less than the physical advection velocity. The main disturbance, as seen in Fig. 2.5, is advected at a speed only slightly less than the physical one; obviously it mostly consists of the longer wave components, which have an advection speed not much different from the physical advection velocity. However, it is seen to be diffusing away with time, which is again a result of the dispersion. We also observe propagation of a group of short waves in the direction opposite to that of the physical advection. Since the appearance of these waves contradicts the physical properties of the advection equation, such waves are called *parasitic waves*.

The solution of the differential-difference equation is, obviously, quite unsatisfactory as an approximation to the true solution. However, this example, with the initial disturbance located at one point only, is completely unsuitable for a good solution by a difference approximation. This is exactly the reason why it provides an instructive illustration of the difficulties involved.

Analytic solutions for a more general case, when a centered difference approximation is made to the time derivative also have been considered by Egger (1971).

### 3. Schemes with uncentered space differencing

The space derivative in (2.1) can also be approximated using uncentered differencing. Still using values at two points for this approximation it is attractive for

physical reasons to have one of these points as the central point and the second located on the side from which the fluid is being advected toward the centre. Therefore we approximate (2.1) by

$$\frac{\partial u_j}{\partial t} + c \frac{u_j - u_{j-1}}{\Delta x} = 0, \quad \text{for } c > 0, \quad (3.1a)$$

$$\frac{\partial u_j}{\partial t} + c \frac{u_{j+1} - u_j}{\Delta x} = 0, \quad \text{for } c < 0. \quad (3.1b)$$

These equations are again differential-difference equations. (3.1a) employs the backward and (3.1b) the forward difference quotient for the approximation to the space derivative. However, in both cases the differences are calculated on the side from which the advection velocity reaches the centre; hence, these differences are called *upstream differences*. Calculated on the opposite side the differences would be called *downstream differences*.

Eqs. (3.1) can be used to construct schemes for the advection equation, by approximating the time derivative by one of the many possible consistent methods. The resulting schemes will only be of the first order of accuracy. However, they have a particular advantage over centered schemes in space when applied to the advection of a disturbance similar to the one considered in the preceding section. This is that, with upstream differences, a disturbance cannot propagate in the direction opposite to the physical advection. Thus, no parasitic waves will contaminate the numerical solution.

If, specifically, a forward difference is used for the time derivative in (3.1), we obtain, for  $c > 0$ ,

$$\frac{u_j^{n+1} - u_j^n}{\Delta t} + c \frac{u_j^n - u_{j-1}^n}{\Delta x} = 0. \quad (3.2a)$$

This is the scheme that was used for the examples of the introductory chapter. It was found that this scheme was damping, with the amount of damping depending on the wave length, with a maximum for the shortest resolvable wave length of  $2\Delta x$ . The analytic solution of the difference equation (3.2a) has been discussed by Wurtele (1961).

### 3. Schemes with uncentered space differencing

The space derivative in (2.1) can also be approximated using uncentered differencing. Still using values at two points for this approximation it is attractive for

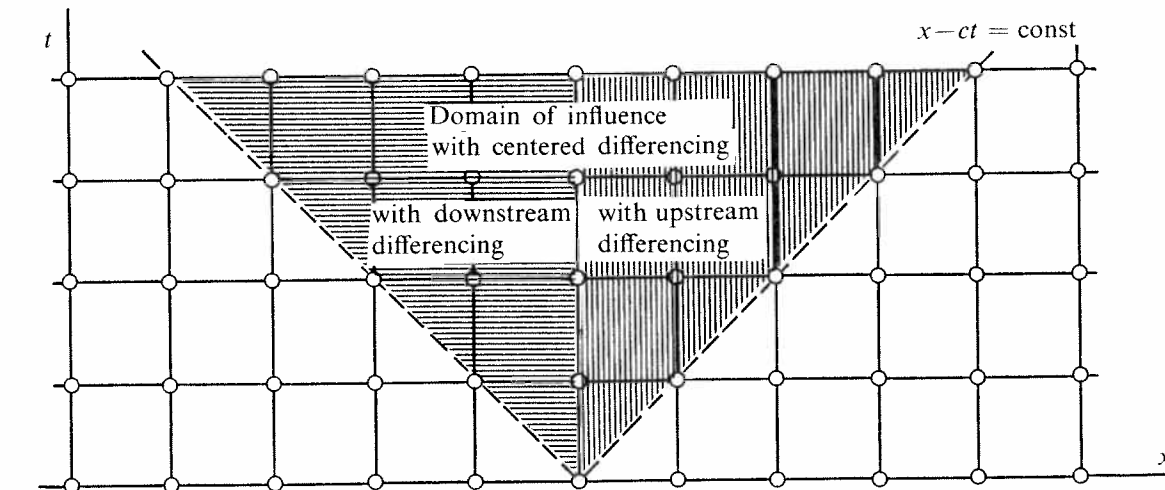


Figure 3.1 Domains of influence of a grid point, for the scheme (3.2a) with upstream differencing, for corresponding schemes with centered and intersect downstream differencing, and for the true solution.

In the true solution, a grid point value can be said to propagate along the characteristic  $x - ct = \text{const}$ . Fig. 3.1 shows a grid point marked by a circle with the associated characteristic passing through it. With upstream differencing as in (3.2a), the value at that grid point will influence the values at points within the domain shaded by vertical lines. The figure also shows the domains of influence with centred and downstream differencing. Of the three domains of influence, that given by upstream differencing is clearly the best approximation to the characteristic line representing the domain of influence in the true solution.

This discussion suggests constructing a scheme for (2.1) by tracing a characteristic back from the point  $(j\Delta x, (n+1)\Delta t)$  to intersect the previous time level  $t = n\Delta t$  and calculating the value  $u^*$  at the point of intersection by interpolation. We then set  $u_j^{n+1} = u^*$ . Choosing a linear interpolation procedure, that employs values at two neighbouring points at the time  $n\Delta t$ , we obtain

$$u_j^{n+1} = u_{j-1}^n + \frac{u_j^n - u_{j-1}^n}{\Delta x} (c\Delta t).$$

This can be identical to the scheme (3.2a), with upstream differencing. If, on the other hand, a quadratic interpolation procedure is chosen, using three neighbouring points, one obtains the Lax-Wendroff scheme, as the reader can readily verify.

For further insight into the properties of schemes that can be obtained from (3.1a) we consider the analytic solution of this differential-difference equation. For small values of  $\Delta t$  this will approximate the solution obtained

from the difference schemes. As in Section 2 we introduce the non-dimensional time  $\tau = ct/\Delta x$ . Eq. (3.1a) can then be written as

$$\frac{d}{d\tau} u_j(\tau) + u_j(\tau) - u_{j-1}(\tau) = 0. \quad (3.3)$$

A solution of this equation is the Poisson frequency function

$$u_j(\tau) = \begin{cases} \frac{e^{-\tau} \tau^{j-p}}{(j-p)!} & \text{for } j \geq p, \\ 0 & \text{for } j < p. \end{cases} \quad (3.4)$$

as can easily be checked by substitution. Here  $p$  is again an arbitrary integer, that is, we have already taken into account the fact that the location of the point  $j = 0$  is

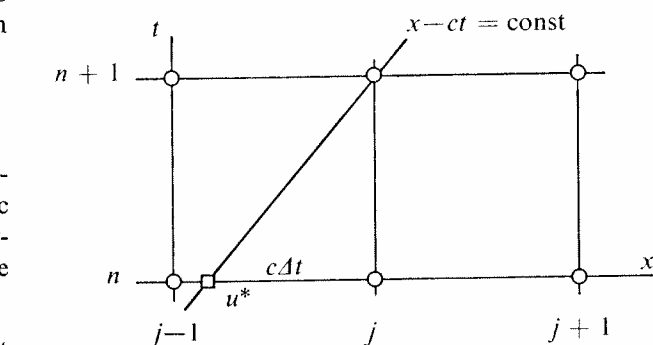


Figure 3.2 Sketch for construction of schemes by calculation of a previous value on a characteristic passing through the point  $(j\Delta x, (n+1)\Delta t)$ .

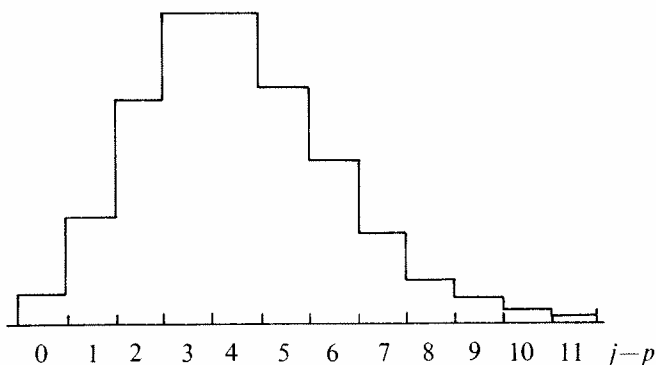


Figure 3.3 The Poisson frequency function (3.4), for the case  $\tau = 4$ .

arbitrary. An example of the Poisson frequency function is shown in Fig. 3.3; the graph in the figure represents the shape of this function for  $\tau = 4$ . There is no need to include a vertical scale, since the area enclosed by the graph of a frequency function has to be equal to unity, so

$$\sum_{j-p=0}^{\infty} \frac{e^{-\tau} \tau^{j-p}}{(j-p)!} = 1. \quad (3.5)$$

Thus, for  $\tau = 0$ , when, as shown by (3.4), the histogram consists of a single rectangle, its ordinate is equal to unity.

Consider now the change in shape of the histogram (3.4) as the non-dimensional time  $\tau$  increases from zero. The initial shape of this histogram, that of a parallelogram having a base  $\Delta x$  and erected at a single grid point, is, of course, equivalent to the shape of the pulse-like disturbance (2.16) used for the example of the previous section. As  $\tau$  increases beyond zero (3.4) transforms into a skewed bell-shaped histogram of the type as shown in the figure, with its mean position on the  $x$  axis

$$\sum_{j-p=0}^{\infty} (j-p) \frac{e^{-\tau} \tau^{j-p}}{(j-p)!} = \tau,$$

moving at a constant speed. Thus, the mean position propagates with a speed equal to the physical advection velocity. The maximum point of the histogram, however, lags behind as is shown by the skewed shape of the histogram. Physically unjustified negative values of  $u_j$  never occur and no parasitic waves appear on the opposite side of zero from the direction of the physical advection. Furthermore, as follows from (3.5), the total amount of the advected quantity is exactly conserved. However, the disturbance is damped out during the advection process at quite a high rate.

As in section 2 we can form a solution more general than (3.4), as a linear combination of all possible solutions (3.4), that is

$$u_j(\tau) = \sum_{p=-\infty}^j a_p \frac{e^{-\tau} \tau^{j-p}}{(j-p)!}, \quad (3.6)$$

where  $a_p$  are arbitrary constants. Substituting  $\tau = 0$  into (3.6) we obtain

$$u_j(0) = a_j. \quad (3.7)$$

Thus, the constants  $a_p$  can again be chosen so as to satisfy arbitrary initial conditions  $u_j = u_j(0)$ , and so (3.6) represents the general solution of (3.3), or (3.1a). Considering the behaviour of the simple solution (3.4), and the summation limits in (3.6), we see that in general the value  $u_j(\tau)$  at a point  $j$  can be considered as a result of superposition of the effect of the initial values at that point and of the initial values at all the points located upstream of it.

An example of the solutions (2.14), for centered differencing, and (3.6), for upstream differencing, for an initial disturbance of a somewhat larger space scale

$$u_j(0) = \begin{cases} 1 & \text{for } j = -1, 0, 1 \\ 0 & \text{for } j \neq -1, 0, 1 \end{cases}$$

is shown in Fig. 3.4. If the grid distance is of the order of 300 km, and  $c$  is about 15 msec<sup>-1</sup> we can see that

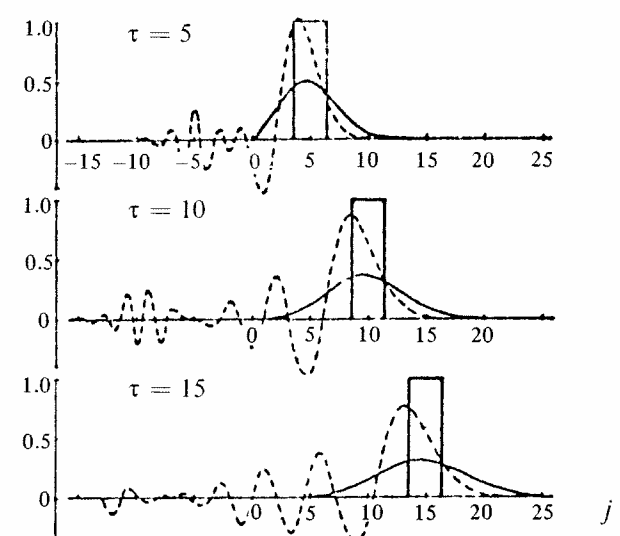


Figure 3.4 Analytic solutions of the exact advection equation (heavy solid line), of the equation using centered differencing (dashed line), and of the equation using upstream differencing (thin solid line), for three different values of the non-dimensional time  $\tau$  (Wurtele, 1961).

5 units of non-dimensional time approximately correspond to the physical time of one day. Thus, the damping effect of the upstream differencing is seen to be quite severe. The figure also illustrates the properties of the two methods described, but to a lesser extent than the examples with the initial disturbance limited to a single grid point only. Thus we can hardly claim that the use of upstream differencing instead of centered second-order differencing has, generally speaking, improved the solution.

$\Delta x$  away from the centre. A simple calculation shows that the approximation (4.3) is obtained by extrapolation for the value  $d = 2\Delta x/3$ . Of course, there is no reason to expect that the accuracy of such an approximation should decrease monotonically as  $d$  decreases.

We now want to look at the effect on the phase speed of using the approximation (4.3) for the space derivative in the advection equation. Replacing the space derivative in (2.1) by (4.3) we obtain the differential-difference equation

$$\frac{\partial u_j}{\partial t} + c \left( \frac{4}{3} \frac{u_{j+1} - u_{j-1}}{2\Delta x} - \frac{1}{3} \frac{u_{j+2} - u_{j-2}}{4\Delta x} \right) = 0. \quad (4.4)$$

As in Section 2, we investigate the behaviour of a tentative solution in form of a harmonic component

$$u_j(t) = Re [U(t) e^{ikj\Delta x}].$$

With second-order space differencing, we obtain the phase speed

$$c^* = c \frac{\sin k\Delta x}{k\Delta x},$$

Now, in the same way, with fourth-order differencing we find the phase speed

$$c^{**} = c \left( \frac{4}{3} \frac{\sin k\Delta x}{k\Delta x} - \frac{1}{3} \frac{\sin 2k\Delta x}{2k\Delta x} \right). \quad (4.5)$$

We shall compare these two results. For second order differencing, we obtain by series expansion for small values of  $k$

$$c^* = c \left( 1 - \frac{1}{3!} (k\Delta x)^2 + \dots \right).$$

On the other hand, with fourth order differencing we have

$$c^{**} = c \left( 1 - \frac{4}{5!} (k\Delta x)^4 + \dots \right).$$

Thus, even though the decelerating effect is still present, the phase speed error has been much reduced for small values of  $k$ .

These phase speeds are shown in Fig. 4.1 as functions of  $k\Delta x$ , for all admissible values of  $k$ . The figure illustrates the very significant increase in accuracy of the phase speed for large-scale and medium-scale waves. However, as the wave length approaches its minimum value of  $2\Delta x$ , the increase in phase speed obtained by fourth order differencing diminishes, until, finally, the wave with wave length  $2\Delta x$  is again stationary.

We can also think of the approximation (4.3) as representing a linear extrapolation of the quotients (4.2) and (4.1) so as to simulate an approximation corresponding to differences taken between points at a distance  $d$  less than

Phase speed

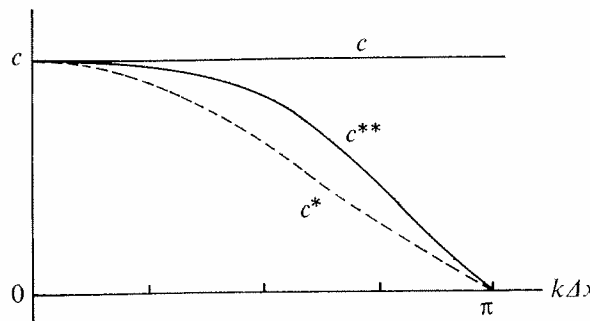


Figure 4.1 Phase speed for the linear advection equation,  $c$ , and for the corresponding differential-difference equations with second order ( $c^*$ ) and with fourth order ( $c^{**}$ ) centered space differencing.

Moreover, for short waves the slope of the phase speed curve is greater than with second order differencing, and, therefore, the computational dispersion of these waves is greater. Thus, although a short wave-length disturbance will now be advected at a somewhat greater speed its false deformation, due to computational dispersion, will be faster.

Because of the decrease in the phase speed error of the longer waves, the use of fourth order schemes for advection has brought about significant improvements in operational numerical forecasting in both the U.S.A. and Japan, in barotropic and quasi-geostrophic baroclinic models. With primitive equation models, now in use in all advanced forecasting centres, fourth order advection schemes are not yet quite so widespread. Still, it is generally believed that fourth-order advection schemes should be used in operational forecasting. However, the use of advection schemes of a high-order of accuracy in general circulation models may not be so important. The choice is between increasing the accuracy of space differencing or spending an equivalent amount of extra computation time in reducing the grid size of the model. A straightforward calculation (e.g. Thompson, 1961, p. 157) shows that the first alternative should be advantageous.

The use of the additional grid points needed for higher order differencing does create some side difficulties. In much the same way as using more than two levels for time differencing resulted in the appearance of computational modes in time, so the use of additional grid points for space differencing results in the appearance of computational modes in space. Furthermore, formulation of boundary conditions becomes more complicated. Simply formulated boundary conditions may be a source of serious problems.

For small scale disturbances, of a scale close to two grid intervals in space, no finite difference method is really satisfactory. Additional ways of constructing difference schemes for the advection equation are discussed in the paper by Anderson and Fattahi (1974) where further references are given. If it is felt that, in a particular situation, the improvement of the advection of scales close to two grid intervals is necessary, the obvious method is to find a way of making the computation with a reduced grid size. As can be inferred from Fig. 4.1., halving the grid size with simple second-order differencing makes the stationary two-grid-interval wave move at a speed of almost  $2/3$  of its physical advection speed. But this, of course, is not easily attainable: in two-dimensional problems, halving the grid size increases the computational time requirements by a factor of four, and, with the usual time difference schemes by an additional factor of two in order to maintain computational stability. Still, a steady increase in the capabilities of commercially available computers enables constant improvements of this kind, so that it is expected that in a few years the resolution of atmospheric models may be such that advection errors will not be a major problem. At present it is estimated that the horizontal truncation errors in the advection terms are the largest single source of errors in short range numerical forecasting, accounting for almost 40 per cent of the total error (Robert, 1974).

Another way of improving the advection of small scale systems may be to develop a computational method more in spirit of the Lagrangian system of equations. As yet, such methods have not been very much explored in meteorology.

## 5. The two-dimensional advection equation

We now consider the two-dimensional linear advection equation

$$\frac{\partial u}{\partial t} + c_x \frac{\partial u}{\partial x} + c_y \frac{\partial u}{\partial y} = 0, \quad c_x, c_y = \text{const} \quad (5.1)$$

where  $u = u(x, y, t)$  is a function of two space variables, and  $c_x, c_y$  are the components of the advection velocity. Thus, the advection speed is given by

$$c = \sqrt{c_x^2 + c_y^2}. \quad (5.2)$$

We shall test the stability of schemes for the numerical solution of (5.1) by the procedure of Section 1. Thus, space derivatives are approximated by standard second-order difference quotients, giving

$$\frac{\partial}{\partial t} u_{i,j} = -c_x \frac{u_{i+1,j} - u_{i-1,j}}{2\Delta x} - c_y \frac{u_{i,j+1} - u_{i,j-1}}{2\Delta y}. \quad (5.3)$$

Here, as is usual for two-dimensional problems, we have changed the choice of subscript denoting the grid points along  $x$  axis, so that the coordinates of the grid points are now  $x = i\Delta x$ ,  $y = j\Delta y$ , and approximate values  $u(i\Delta x, j\Delta y)$  are denoted by  $u_{i,j}$ . As a tentative solution of (5.3) we substitute

$$u_{i,j} = Re [U(t) e^{i(kx+l y)}], \quad (5.4)$$

giving the oscillation equation

$$\frac{dU}{dt} = i \left( -\frac{c_x}{\Delta x} \sin k\Delta x - \frac{c_y}{\Delta y} \sin l\Delta y \right) U. \quad (5.5)$$

If the leapfrog scheme is used for the time derivative, we obtain as the stability criterion

$$\left| \left( \frac{c_x}{\Delta x} \sin k\Delta x + \frac{c_y}{\Delta y} \sin l\Delta y \right) \Delta t \right| < 1. \quad (5.6)$$

This has to be satisfied for all admissible values of the wave numbers  $k, l$ .

For simplicity, we shall consider only the cases where  $\Delta x = \Delta y$ ; we denote this grid size by  $d^*$ . In the *wave number plane*, that is, a diagram with co-ordinates  $k, l$ , the admissible wave numbers are contained within the square region shown in Fig. 5.1. Inside that region the maximum value of the left-hand side of (5.6) is obtained at the centre of the square, marked by a circle. The wave represented by that point has wave lengths  $4d^*$  in both the  $x$  and  $y$  directions so that  $\sin k\Delta x = \sin l\Delta y = 1$ .

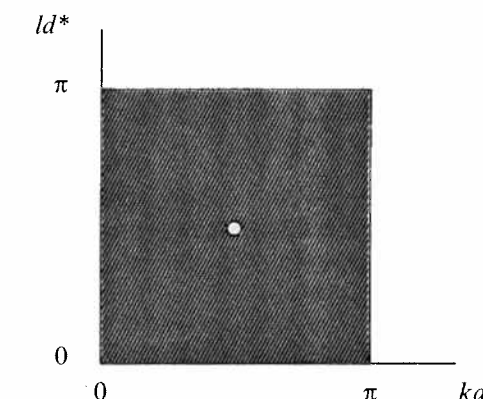


Figure 5.1 Admissible region of wave numbers for a square two-dimensional grid, with grid length  $\Delta x = \Delta y = d^*$ .

For a given value of the advection speed the left-hand side of (5.6) has a maximum value at this point if the advection velocity makes an angle of  $\pi/4$  with the  $x$  axis, in this case  $c_x = c_y = \frac{\sqrt{2}}{2} c$ . Thus we obtain the stability criterion

$$\sqrt{2} c \frac{\Delta t}{\Delta x} \leq 1. \quad (5.7)$$

Therefore, in the two-dimensional case we have to choose a time step that is  $\sqrt{2}$  times less than that permitted in the one-dimensional case.

We note that the minimum stability is associated with wave lengths in both the  $x$  and  $y$  directions twice as long as the shortest resolvable wave length of  $2d^*$ , exactly as in the one-dimensional case. The two-dimensional wave number of this wave

$$\sqrt{k^2 + l^2},$$

is, however, greater by a factor of  $\sqrt{2}$  than wave numbers along the axes, and its wave length is therefore shorter by the same factor. This applies to all waves with  $k = l$ .

## 6. Aliasing error and nonlinear instability

Another generalization of the simple one-dimensional linear advection equation is to consider the *nonlinear* advection equation

$$\frac{\partial u}{\partial t} + u \frac{\partial u}{\partial x} = 0, \quad (6.1)$$

We have returned to dimension, so that  $u = u(x, t)$ .

Shuman (1974) calls (6.1) the *shock equation*. Its general solution (e.g. Platzman, 1964) is

$$u = f(x - ut),$$

as can readily be verified. Here  $f$  is an arbitrary function.

Here we consider only the effect of the multiplication in (6.1). When performed in finite differences, it results in an error related to the inability of the discrete grid to resolve wave lengths shorter than  $2\Delta x$ , that is, wave numbers greater than  $k_{\max} = \pi/\Delta x$ . Thus, consider a function  $u(x)$  which can be represented by values at grid points, for example

$$u = \sin kx, \quad (6.2)$$

where  $k < k_{\max}$ . However, substituting (6.2) into the nonlinear term of (6.1) gives

$$u \frac{\partial u}{\partial x} = k \sin kx \cos kx = \frac{1}{2} k \sin 2kx.$$

Hence, if the wave number in (6.2) is in the interval  $\frac{1}{2}k_{\max} < k \leq k_{\max}$ , the nonlinear term will give a wave

number that is beyond the range that can be resolved by the grid. It cannot, therefore, be properly reproduced in a finite difference calculation.

To gain some insight into what happens in such a situation, consider a wave for which  $k > k_{\max}$ . For example, let  $L = 4\Delta x/3$ . A wave of that wave length is shown by the full line in Fig. 6.1. Knowing only the values at grid points we will not be able to distinguish this wave from the one shown by the dashed line. Thus, with the convention adopted earlier which assumes that the longest waves are present, we will make an error. This is called *aliasing error*.

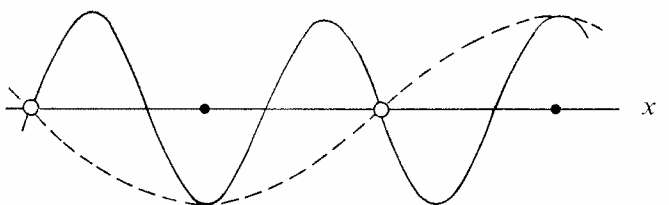


Figure 6.1 A wave of wave length  $4\Delta x/3$ , misrepresented by the finite difference grid as a wave of wave length  $4\Delta x$ .

In a more general case, suppose that the function  $u$  consists of a number of harmonic components

$$u = \sum_n u_n.$$

The nonlinear term will then contain products of harmonics of different wave lengths, such as

$$\sin k_1 x \sin k_2 x.$$

However,

$$\sin k_1 x \sin k_2 x = \frac{1}{2} [\cos (k_1 - k_2)x - \cos (k_1 + k_2)x].$$

Thus, even if a finite difference calculation is started with waves which all have  $k \leq k_{\max}$ , very soon through this process of nonlinear interaction waves will be formed with  $k > k_{\max}$ , and a misrepresentation of waves will occur.

In general we can write

$$\sin kx = \sin [2k_{\max} - (2k_{\max} - k)]x.$$

Substituting here  $k_{\max} = \pi/\Delta x$  and using the formula for the sine of a difference, we obtain

$$\begin{aligned} \sin kx &= \sin \frac{2\pi}{\Delta x} x \cos \left( \frac{2\pi}{\Delta x} - k \right) x - \\ &\quad - \cos \frac{2\pi}{\Delta x} x \sin \left( \frac{2\pi}{\Delta x} - k \right) x. \end{aligned}$$

However, at the grid points  $x = j\Delta x$ , and

$$\sin \frac{2\pi}{\Delta x} j\Delta x = 0, \quad \cos \frac{2\pi}{\Delta x} j\Delta x = 1.$$

Therefore, we find

$$\sin k j\Delta x = -\sin (2k_{\max} - k) j\Delta x. \quad (6.3)$$

In this way, we see that, knowing only the grid point values, we cannot distinguish the wave numbers  $k$  from  $2k_{\max} - k$ . Thus, if  $k > k_{\max}$ , using the convention mentioned earlier, we can say that the wave number  $k$  is misrepresented as the wave number

$$k^* = 2k_{\max} - k. \quad (6.4)$$

Hence, as shown in Fig. 6.2, the resulting wave has a wave number  $k^*$  which is less than  $k_{\max}$  by an amount equal to that by which  $-k$  was greater than  $k_{\max}$ . We can think of the wave number  $k^*$  as being an image obtained by the reflection of  $k$  across the value  $k_{\max}$  into the admissible range of wave numbers.

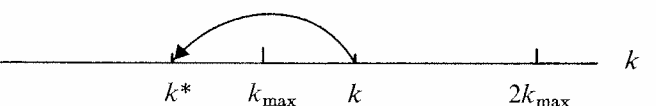


Figure 6.2 Misrepresentation of a wave number  $k > k_{\max}$ , in accordance with (6.4).

As an example consider the case  $L = 4\Delta x/3$ , illustrated in Fig. 6.1. Then  $k = 3\pi/2\Delta x$ , and (6.4) gives  $k^* = \pi/2\Delta x$  as the wave number "seen" by the finite difference grid. This, of course, is the same wave, of wave length  $4\Delta x$ , as the one found graphically and shown by the dashed line.

Now consider the consequences of aliasing errors in a numerical integration. An atmospheric variable, as a function of space co-ordinates, can be thought of as consisting of a series of harmonic components. It is useful to consider the "energy" of these components, that is, their contribution to the mean square value of the variable considered as a function of wave number.

This is the *spectrum* of the "energy". For example, if the variables are velocity components, this function is the *kinetic energy spectrum*. This spectrum describes

the relative importance of features of different scales in the field of the variable. Now, experience shows that the spectrum of atmospheric variables does not change much with time. On synoptic maps we do not have situations where small scale features are dominant on one day, and absent on the next. Accordingly, spectra of atmospheric variables also do not change much in their general shape. The energy of a particular component can, of course, change, but the characteristic shape of the spectrum as a whole is fairly constant. For example, a zonal spectrum of the eastward velocity component in middle latitudes typically has a maximum for wave numbers 4 to 7, that is, 4 to 7 wave lengths along a latitude circle, with the energy tapering off rather rapidly as the wave number increases beyond about 10. Thus, there is very little energy in wave numbers of the order of the maximum wave numbers that can be resolved by finite difference grids used in atmospheric models.

In a finite difference integration, in addition to these relatively small physical changes, the shape of a spectrum is subject to changes due to aliasing errors. If we have a spectrum of the shape just described, and consider the representation of various combinations  $k_1 + k_2$  that are greater than  $k_{\max}$ , we see that most of the energy of such combinations will belong to components with wave numbers not much greater than  $k_{\max}$ . Thus, due to aliasing errors a spurious energy inflow is expected at wave numbers that are not much less than  $k_{\max}$ , and, in time, the energy of these components can be expected to grow beyond physically acceptable limits. Experience shows that, if no precautionary measures are taken, this can indeed happen, and even cause a catastrophic end to the integration. The phenomenon is due to the nonlinear terms of the equations, and, therefore, is called the *nonlinear instability*. Nonlinear instability was first encountered by Norman Phillips (1956) in his famous work that laid the foundation for the numerical modelling of the atmospheric general circulation. Starting from an atmosphere at rest, he integrated the vorticity equation for a simulated time of the order of 30 days. The calculation then came to an end due to an explosive increase in the total energy of the system, associated with an appearance of elongated shapes in the vorticity field. Phillips initially believed that the breakdown was due to excessive truncation errors, and he later repeated the experiment using space and time steps both reduced to about half of their previous values. This must have greatly reduced the truncation errors, but the catastrophic increase in total energy still happened at about the same time.

In a later paper Phillips (1959) gave the interpretation of nonlinear instability similar to what has been presented here, but for the nondivergent vorticity equation. For a test of this explanation Phillips again repeated his

experiment, but after every two hours of simulated time he performed a harmonic analysis of the vorticity fields, and eliminated all components with  $k > \frac{1}{2}k_{\max}$ . If there are no components with  $k > \frac{1}{2}k_{\max}$  the advection term cannot produce waves with  $k > k_{\max}$ . We expect that it will be some time before the amplitudes of the eliminated waves are built up again to an appreciable extent. This filtering procedure eliminated the appearance of the spurious increase in energy, thereby confirming this explanation of the instability.

## 7. Suppression and prevention of nonlinear instability

If an integration is to be performed for an extended period of time, it is necessary to suppress or prevent nonlinear instability. For short range integrations it is not necessary to do this, though such a procedure might still have a beneficial effect on the model.

It has been pointed out by Orszag (1971) that to eliminate aliasing errors it is not necessary to filter the top half of the admissible wave numbers. It is sufficient to eliminate the top one-third, because, if waves with  $k > \frac{2}{3}k_{\max}$  are filtered out, all the aliases satisfy  $k > \frac{2}{3}k_{\max}$  and will thus be eliminated.

If, however, we consider that such a suppression of the shortest waves is a satisfactory method of dealing with the problem, it would be simpler to use a differencing scheme that has a built-in damping of the shortest waves. This idea is due to Richtmyer (1963), who suggested use of the Lax-Wendroff scheme for this purpose. It was found by experience that such a practice does suppress the nonlinear instability, and that to do this it is sufficient to use an intermittent Lax-Wendroff step at quite long intervals (Kasahara, 1969). Kreiss and Oliker (1973), on the other hand, recommend adding a dissipative term to a scheme which is not dissipative, so that the amount of dissipation can be controlled in a more practical way.

Another way of avoiding nonlinear instability is to use a Lagrangian formulation of the advection terms instead of an Eulerian formulation. We calculate the position of the parcel that should be advected to the grid point considered in step  $\Delta t$ . A value of the dependent variable can be found corresponding to that position by interpolation in space. The change due to advection is set equal to the difference between the value obtained by interpolation and that at the grid point. In some cases, these schemes turn out to be identical to schemes obtained using the Eulerian formulation, but other schemes can also be obtained. A procedure of this type was first used by Leith (1965); an example of its use more recently is given in the paper by Krishnamurti *et al.* (1973).

A conceptually elegant approach for dealing with the nonlinear instability problem has been suggested and developed by Arakawa (1966, 1972). His idea is that it is better, if possible, to use schemes for the advection terms that are not only free of the nonlinear computational instability but also free of the spurious inflow of energy to these short waves, instead of artificially suppressing their amplitudes. The amplitudes of the shortest waves in atmospheric models are small initially, and they will remain small if a false generation of these short waves is avoided. Arakawa has shown that it is possible to construct such schemes, and that they are obtained when care is taken to conserve in the finite difference form some integral properties of the original differential equations.

When the Arakawa conservation schemes are used there is no need for an artificial dissipation in the advection process. This enables the statistical properties of the schemes to be maintained under advection, a feature especially useful in general circulation studies.

It has sometimes been argued that, because the phase error of the short waves is very large, they should be eliminated before they erroneously affect the longer waves through nonlinear interactions. This argument does not take account of several factors. If the phase speeds of the short waves are wrong, the situation will not necessarily improve if their amplitudes are also made wrong. They may still be performing a useful function of a statistical nature. Also damping or elimination of the shortest waves will also remove some energy from the longer waves that we are interested in. If we wish to dissipate energy, it is obviously better to do so for physical and not for computational reasons.

We shall introduce the procedure of Arakawa by considering the vorticity equation

$$\frac{\partial \zeta}{\partial t} + \mathbf{v} \cdot \nabla \zeta = 0; \quad \zeta = \nabla^2 \psi, \quad (7.1)$$

where the velocity  $\mathbf{v}$  is assumed to be nondivergent, that is

$$\mathbf{v} = \mathbf{k} \times \nabla \psi. \quad (7.2)$$

Substituting this into (7.1) we obtain

$$\frac{\partial}{\partial t} \nabla^2 \psi = J(\nabla^2 \psi, \psi). \quad (7.3)$$

This equation gives the local change in vorticity as a result of advection by a two-dimensional nondivergent velocity. It is also a nonlinear advection equation. However, in contrast with the one-dimensional equation (6.1), (7.3) gives a good approximate description of

large scale atmospheric processes. Thus, for more than a decade it has been used as a basic prognostic equation for the numerical weather prediction, eventually supplemented by some additional terms of a smaller order of magnitude.

To illustrate the Arakawa procedure for the vorticity equation (7.3), we need some knowledge of its integral properties in wave number space. We want to study the energy exchanges between different harmonics that are permitted by that equation.

Consider first the kinetic energy spectrum when the velocity is two-dimensional and nondivergent, so that it can be given by (7.2). We can almost always assume that in the region considered A, the stream function can be expressed as a series of orthogonal functions

$$\psi = \sum_n \psi_n, \quad (\text{e.g. Courant and Hilbert, 1953, p. 369}) \quad (7.4)$$

where the functions  $\psi_n$  are eigenfunctions of the Helmholtz equation

$$\nabla^2 \psi_n + \lambda_n^2 \psi_n = 0. \quad (7.5)$$

The parameters  $\lambda_n$  are known as the *generalized wave numbers* of the components  $\psi_n$ .

As an example, let A be a rectangular region with sides  $L_x, L_y$ . For boundary conditions assume that the stream function is periodic in  $x$  with period  $L_x$  and is zero along the lower and upper boundary. Then we can write the stream function

$$\begin{aligned} \psi = & \sum_{n_1, n_2} \left( a_{n_1, n_2} \cos \frac{2\pi n_1}{L_x} x + \right. \\ & \left. + b_{n_1, n_2} \sin \frac{2\pi n_1}{L_x} x \right) \sin \frac{\pi n_2}{L_y} y. \end{aligned} \quad (7.6)$$

Differentiating this we obtain

$$\nabla^2 \psi_n = - \left[ \left( \frac{2\pi n_1}{L_x} \right)^2 + \left( \frac{\pi n_2}{L_y} \right)^2 \right] \psi_n,$$

that is,

$$\lambda_n^2 = \left( \frac{2\pi n_1}{L_x} \right)^2 + \left( \frac{\pi n_2}{L_y} \right)^2.$$

If the region A had different geometry, another set of orthogonal functions would satisfy (7.5) and the boundary conditions, and could be used for the expansion (7.4). These functions will be solutions of the Helmholtz equation (7.5).

Define the average of a variable  $\alpha$  by

$$\bar{\alpha} = \frac{1}{A} \int_A \alpha dA.$$

We are interested in the average value of the kinetic energy per unit mass

$$\bar{K} = \frac{1}{2} \overline{(\mathbf{u}^2 + \mathbf{v}^2)} = \frac{1}{2} \overline{\nabla \psi \cdot \nabla \psi}. \quad (7.7)$$

Substituting (7.4), and assuming that this series can be differentiated and integrated term by term, we obtain

$$\begin{aligned} \bar{K} &= \frac{1}{2} \overline{\nabla \sum_n \psi_n \cdot \nabla \sum_m \psi_m} = \frac{1}{2} \sum_n \overline{\nabla \psi_n \cdot \sum_m \nabla \psi_m} = \\ &= \frac{1}{2} \sum_m \sum_n \overline{\nabla \psi_m \cdot \nabla \psi_n}. \end{aligned}$$

We note that

$$\nabla \psi_m \cdot \nabla \psi_n = \nabla \cdot (\psi_m \nabla \psi_n) - \psi_m \nabla^2 \psi_n,$$

Assume that no mass transport occurs through the boundaries of A, that is,

$$\nabla \cdot (\psi_m \nabla \psi_n) = 0.$$

Using (7.5), we then obtain

$$\bar{K} = -\frac{1}{2} \sum_m \sum_n \overline{\psi_m \nabla^2 \psi_n} = \frac{1}{2} \sum_m \sum_n \lambda_n^2 \overline{\psi_m \psi_n}.$$

Since the functions  $\psi_n$  are orthogonal, that is,

$$\psi_m \psi_n = 0 \quad \text{for } m \neq n,$$

the double sum reduces to a sum over only a single subscript, namely,

$$\bar{K} = \frac{1}{2} \sum_n \lambda_n^2 \overline{\psi_n^2}.$$

We have therefore expressed the average kinetic energy in the region A as a sum of contributions of different harmonics

$$\bar{K} = \sum_n K_n, \quad (7.8)$$

where

$$K_n \equiv \frac{1}{2} \lambda_n^2 \overline{\psi_n^2}. \quad (7.9)$$

The contributions  $K_n$ , considered as a function of  $n$ , represent the kinetic energy spectrum. As seen from (7.9), they are never negative. When the stream function  $\psi$  is known, the functions  $\psi_n$  can be computed by standard series expansion methods. In fact, we calculate

the coefficients of these components; in (7.4), these coefficients have been absorbed into the functions  $\psi_n$ . Since the values of  $\lambda_n$  are already known, for commonly used geometries, we can calculate the kinetic energy spectra using (7.9). Such a calculation, as well as the calculation of the spectra of other variables, has been used for numerous studies of the behaviour and structure of both the observed and numerically simulated fields of atmospheric variables.

The mean square vorticity

$$\bar{\zeta}^2 = \overline{(\nabla^2 \psi)^2}$$

can be expressed as a sum of contributions of different harmonics in a similar way. Substituting (7.4), using (7.5), and the orthogonality of the functions  $\psi_n$ , we obtain

$$\bar{\zeta}^2 = \sum_n \lambda_n^4 \overline{\psi_n^2}. \quad (7.10)$$

Substituting the expression (7.9) for the kinetic energy of a component  $\psi_n$ ; we find for the average value of the enstrophy half the vorticity squared,

$$\frac{1}{2} \bar{\zeta}^2 = \sum_n \lambda_n^2 K_n. \quad (7.11)$$

Comparing this with (7.8) we see that the average wave number is related to average values of enstrophy and kinetic energy. Define the average wave number as

$$\lambda = \sqrt{\sum_n \lambda_n^2 K_n / \sum_n K_n}. \quad (7.12)$$

Substituting (7.11) and (7.8) we find

$$\lambda = \sqrt{\frac{1}{2} \bar{\zeta}^2 / \bar{K}}. \quad (7.13)$$

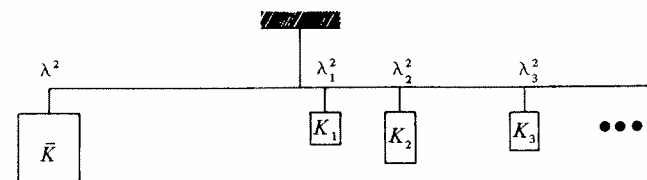
Thus, when the velocity is two-dimensional and nondivergent, the average wave number is determined by the ratio of the average values of enstrophy and kinetic energy.

We originally wished to study the time dependence of the energy of spectral components permitted by the vorticity equation (7.3). It will suffice to look at the time dependence of (7.13). (7.3) gives

$$\frac{\partial}{\partial t} \frac{1}{2} \bar{\zeta}^2 = \bar{\zeta} \frac{\partial}{\partial t} \bar{\zeta} = \overline{\zeta J(\zeta, \psi)}. \quad (7.14)$$

Again assuming no mass transport through the boundaries of A, we find

$$\begin{aligned}\frac{\partial}{\partial t} \bar{K} &= \frac{\partial}{\partial t} \frac{1}{2} (\nabla \psi)^2 = \nabla \psi \cdot \frac{\partial}{\partial t} \nabla \psi = \\ &= -\psi \frac{\partial}{\partial t} \nabla^2 \psi = -\psi J(\zeta, \psi).\end{aligned}\quad (7.15)$$



However, for any two scalar quantities  $p, q$ , we have

$$J(p, q) = k \cdot \nabla \times (p \nabla q) = -k \cdot \nabla \times (q \nabla p),$$

Using Stokes' theorem, we see that

$$\overline{J(p, q)} = 0, \quad (7.16)$$

if either  $p$  or  $q$  is constant along the boundary of  $A$ . Under the same conditions, we have

$$\overline{pJ(p, q)} = 0, \quad \overline{qJ(p, q)} = 0. \quad (7.17)$$

Therefore, if we assume that  $\psi$  is constant along the boundary of  $A$ , (7.14) and (7.15) give

$$\frac{1}{2} \overline{\zeta^2} = \text{const}, \quad \text{and} \quad \overline{K} = \text{const}. \quad (7.18)$$

In this way, we find that *the average wave number does not change with time* with two-dimensional nondivergent flow. In other words, *a systematic energy cascade toward higher wave numbers is not possible*. Furthermore, since to obtain the enstrophy the contributions  $K_n$  are multiplied by the wave number squared, *the fraction of the energy that can flow to high wave numbers is clearly limited, and the higher the wave number, the more it is limited* (Fjørtoft, 1953).

As pointed out by Charney (1966) this situation can be illustrated by a simple mechanical analogy. The foregoing relations show that

$$K \lambda^2 = \sum_n K_n \lambda_n^2 = \text{const},$$

On the left hand side here each of the two factors is constant, as the first one is equal to the average energy. Thus, as shown in Fig. 7.1, we can imagine a semi-infinite weightless rod on which a weight  $K$  is suspended at a distance  $\lambda^2$  to the left of the point at which the rod itself is suspended, and weights  $K_1, K_2, \dots$  are suspended at distances  $\lambda_1^2, \lambda_2^2, \dots$  right of that point. The rod, as defined, would be in mechanical equilibrium. Its left side, moreover, cannot change, while on the right hand side an interchange of mass between weights is permitted, but only so as not to disturb the equilibrium, that is, the total moment of forces. Thus, at least three components must always take part in an energy transfer. In particular very little energy can be expected to accumulate at the highest wave numbers through a cascade of energy from the lower wave numbers.

Figure 7.1 A mechanical analogy of the interchange of energy between harmonic components.

We now return to the numerical solution of (7.3) and the associated nonlinear instability problem. Obviously, if a finite difference scheme could be constructed so as to conserve the average values of enstrophy and the kinetic energy, the average wave number would not change, and, therefore, a systematic transport of energy toward the highest wave numbers would not be possible. Arakawa has pointed this out, and showed that finite difference approximations can be constructed that, indeed, maintain the properties (7.17) of the analytic Jacobian. Therefore, average enstrophy and kinetic energy are conserved within the advection terms, and so is the average wave number. Nonlinear instability is therefore prevented. His approximations, in addition, maintain the property (7.16), and thus also conserve the average vorticity. Thus the gross characteristics of the frequency distribution of the vorticity field are also conserved. The true nondivergent vorticity equation conserves all moments of the frequency distribution of the vorticity since the area and the vorticity of individual fluid parcels are both conserved. Maintaining properties (7.16) and (7.17)<sub>1</sub> in a finite difference calculation will guarantee the conservation of the first two moments of this distribution.

We illustrate Arakawa's method by considering how to satisfy (7.17)<sub>1</sub>. In our finite difference calculation it takes the form

$$\overline{\zeta_{ij} J_{ij}(\zeta, \psi)} = \frac{1}{N} \sum_{i,j} \zeta_{ij} J_{ij}(\zeta, \psi) = 0, \quad (7.19)$$

where  $J$  denotes a finite difference approximation to the Jacobian, and  $N$  the total number of grid points.

There are many ways of constructing finite difference approximations to the Jacobian. We can use any of the three equivalent analytic expressions

$$\begin{aligned}J(p, q) &= \frac{\partial p}{\partial x} \frac{\partial q}{\partial y} - \frac{\partial p}{\partial y} \frac{\partial q}{\partial x} = \\ &= \frac{\partial}{\partial y} \left( q \frac{\partial p}{\partial x} \right) - \frac{\partial}{\partial x} \left( q \frac{\partial p}{\partial y} \right) = \\ &= \frac{\partial}{\partial x} \left( p \frac{\partial q}{\partial y} \right) - \frac{\partial}{\partial y} \left( p \frac{\partial q}{\partial x} \right).\end{aligned}\quad (7.20)$$

We shall consider only approximations of the second order of accuracy. With the simplest centered space differencing, we require values of  $p, q$  from a box of nine adjacent grid points to evaluate (7.20), as shown in Fig. 7.2. Write  $d$  for the grid size, and  $p_k, q_k$  for the values of  $p, q$  at the point denoted by  $k$ . We then obtain the following approximations to the expressions (7.20)

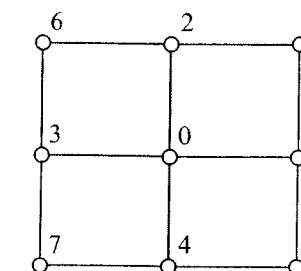


Figure 7.2 Stencil used to define approximations to Jacobian.

$$\begin{aligned}J^{++}(p, q) &= \frac{1}{4d^2} \left[ (p_1 - p_3)(q_2 - q_4) - \right. \\ &\quad \left. -(p_2 - p_4)(q_1 - q_3) \right],\end{aligned}\quad (7.21a)$$

$$\begin{aligned}J^{\times+}(p, q) &= \frac{1}{4d^2} \times \left[ q_2 (p_5 - p_6) - \right. \\ &\quad \left. - q_4 (p_8 - p_7) - q_1 (p_5 - p_8) + q_3 (p_6 - p_7) \right],\end{aligned}\quad (7.21b)$$

$$\begin{aligned}J^{+\times}(p, q) &= \frac{1}{4d^2} \times \left[ p_1 (q_5 - q_8) - \right. \\ &\quad \left. - p_3 (q_6 - q_7) - p_2 (q_5 - q_6) + p_4 (q_8 - q_7) \right].\end{aligned}\quad (7.21c)$$

The superscripts + and  $\times$  denote the positions of the points from which values of  $p$  and  $q$ , respectively, are used to form the approximation. Each of the approximations (7.2) is consistent and of the second order of accuracy. A more general approximation can now be formed as a linear combination of these three, that is

$$J(p, q) = \alpha J^{++} + \beta J^{\times+} + \gamma J^{+\times}, \quad (7.22)$$

with the consistency requirement

$$\alpha + \beta + \gamma = 1.$$

This approximation is also of the second order of accuracy.

When evaluating the sum in (7.19) using (7.22) we obtain 24 terms from each grid point in the computational region. All of these terms will be of the form  $\text{const} \cdot \zeta_k \zeta_l \psi_m$ . By choosing the constants  $d, \beta, \gamma$  appropriately we can make all of these terms cancel out in the summation process, thereby fulfilling (7.19). For example, the point 0 will contribute terms to (7.19) of the form

$$\zeta_0 J_0(\zeta, \psi) = \frac{1}{4d^2} (\alpha \zeta_0 \zeta_1 \psi_2 + 23 \text{ more terms}).$$

A term containing  $\zeta_0 \zeta_1 \psi_2$  will also appear in the expression for  $\zeta_1 J_1(\zeta, \psi)$ . Because of the form of the Jacobian approximations (7.21) it will have to come from the product  $p_3 q_6$ . Thus, one contribution from the point 1 will be

$$\alpha = \beta = \gamma = \frac{1}{3}.$$

These two terms will cancel if  $\alpha = \beta$ . Arakawa has shown that, when

$$\zeta_1 J_1(\zeta, \psi) = \frac{1}{4d^2} (\cdots - \beta \zeta_1 \zeta_0 \psi_2 + \cdots).$$

not only do all the terms in the sum (7.19) cancel, but also all the terms in the expression for the conservation of the average kinetic energy, and the average vorticity (Arakawa, 1966; Lilly, 1965). Thus, the approximation

$$J_A \equiv \frac{1}{3} (J^{++} + J^{\times+} + J^{+\times}), \quad (7.23)$$

will conserve average vorticity, enstrophy and kinetic energy when used for the numerical solution of (7.3). This is more than sufficient for the prevention of nonlinear instability. The approximation (7.23) is usually called the *Arakawa Jacobian*. Arakawa has also shown how to construct an approximation of fourth order accuracy to the Jacobian, conserving these three quantities.

It has recently been demonstrated (Jespersen, 1974) that the Arakawa Jacobian can be derived as a special case of the so called "finite element method", a relatively new and promising development in the field of the numerical solution of partial differential equations. Instead of approximating the space derivatives by finite differences, the finite element method consists of using an interpolation procedure to convert a set of values given at grid points into a field given everywhere. This is done using a variational formulation, minimizing the error of the approximation (e.g. Cullen, 1974).

Arakawa has constructed an analogue of the scheme (7.23) for the vorticity equation to approximate the advection terms in the primitive equations in the case when the wind is nondivergent. This scheme is then generalized to allow for divergence (Arakawa, 1972; Arakawa and Lamb, 1976).

In conclusion, we stress that the essence of the Arakawa method is to control the computational energy cascade, by conservation of the average wave number within the advection terms due to the nondivergent part of the flow.

Thus, it is *not* only a conservation of energy, as has sometimes incorrectly been implied. For example, an approximation can easily be constructed for the nonlinear term of the one-dimensional advection equation (6.1) which would conserve the kinetic energy. Using such an approximation, however, would not prevent nonlinear instability in the way that the Arakawa scheme does. The Arakawa procedure does not have a one-dimensional analogue, as the nondivergent vorticity equation (7.3) is not nonlinear when applied to a one-dimensional problem.

## CHAPTER IV

### THE GRAVITY AND GRAVITY-INERTIA WAVE EQUATIONS

In this chapter we consider the equations describing the horizontal propagation of gravity and gravity-inertia waves. Mathematically, this means that we will be dealing with a system of two or three partial differential equations of the first order. Thus, we will now have *two* or *three* dependent variables. The system of equations will always be equivalent to a single differential equation of a higher order. This equation can be obtained from the system by elimination of dependent variables.

We first put this problem in perspective. Arakawa, (Arakawa, 1970), has stated that there are two main problems in finite difference integrations of the atmospheric governing equations. One is a proper simulation of the geostrophic adjustment process. Through this process the atmosphere establishes a characteristic quasi-nondivergent state, mostly as a result of the dispersion of the gravity-inertia waves. The associated computational considerations will be discussed in this chapter. The second problem is the prediction or simulation of the large-scale quasi-nondivergent flow after it has been established. Here the horizontal advection is the dominating mechanism. The associated computational considerations were discussed in the preceding chapter.

Extensive study of the problems in integrations of the gravity-inertia wave equations began in atmospheric modelling much later than studies of the advection problem. After Richardson's (1922) first unsuccessful numerical integration of the complete primitive equations, the successful result of Charney, Fjørtoft and von Neumann (1950) was largely due to the exclusion of gravity-inertia waves from their equations by using the geostrophic approximation in the vorticity equation. The governing equations with the gravity-inertia waves excluded, are customarily called the *filtered equations*. They bypass the geostrophic adjustment problem. The filtered equations were used almost exclusively in the first decade of numerical forecasting research.

Efforts to improve the performance of numerical models led to a desire to include the non-geostrophic effects. This is very difficult to do within the modified system of equations. Thus, starting with the first successful experiments by Hinkelmann (1959), modellers came back to using the primitive equations. Except for special purposes, the primitive equations are used almost

exclusively in atmospheric models today. They are generally considered superior for both research and operational applications (e.g. Sawyer, 1972). The speed of propagation of the gravity and gravity-inertia waves, and their sensitivity to various numerical errors mean that their treatment requires especially careful consideration.

#### 1. One-dimensional gravity waves: centered space differencing

We shall first consider the simplest case of gravity waves where the dependent variables are functions of one space variable. They are governed by the linearized equations

$$\frac{\partial u}{\partial t} = -g \frac{\partial h}{\partial x}, \quad \frac{\partial h}{\partial t} = -H \frac{\partial u}{\partial x}, \quad g, H = \text{const.} \quad (1.1)$$

Thus, we have a system with two dependent and two independent variables.

We seek wave solutions of (1.1) in the form

$$u(x, t) = Re[\hat{u} e^{i(kx - vt)}], \quad h(x, t) = Re[\hat{h} e^{i(kx - vt)}], \quad (1.2)$$

and obtain the homogeneous system

$$\hat{v}\hat{u} = gk\hat{h}, \quad \hat{v}\hat{h} = H\hat{k}\hat{u},$$

giving the frequency equation

$$v^2 = gHk^2. \quad (1.3)$$

Thus,

$$c = \frac{v}{k} = \pm \sqrt{gH}, \quad (1.4)$$

showing that the gravity waves can propagate along the *x* axis in both directions at a speed  $\sqrt{gH}$ . This speed is not a function of wave number so that there is no dispersion of the waves.

Consider now the differential-difference equations

$$\frac{\partial u_j}{\partial t} = -g \frac{h_{j+1} - h_{j-1}}{2\Delta x}, \quad \frac{\partial h_j}{\partial t} = -H \frac{u_{j+1} - u_{j-1}}{2\Delta x}, \quad (1.5)$$

that we obtain when the space derivatives in (1.1) are approximated by centered finite difference quotients using values at the two nearest points. The solutions (1.2) now take the form

$$u_j(t) = \operatorname{Re}[\hat{u} e^{i(kj\Delta x - vt)}], \quad h_j(t) = \operatorname{Re}[\hat{h} e^{i(kj\Delta x - vt)}]. \quad (1.6)$$

Substitution of these solutions into (1.5) leads to

$$v\hat{u} = g \frac{\sin k\Delta x}{\Delta x} \hat{h}, \quad v\hat{h} = H \frac{\sin k\Delta x}{\Delta x} \hat{u},$$

giving the frequency equation

$$v^2 = gH \left( \frac{\sin k\Delta x}{\Delta x} \right)^2. \quad (1.7)$$

Thus, instead of a constant phase speed, the gravity waves now propagate with the phase speed

$$c^* = \pm \sqrt{gH} \frac{\sin k\Delta x}{k\Delta x}, \quad (1.8)$$

or

$$c^* = c \frac{\sin k\Delta x}{k\Delta x}. \quad (1.9)$$

This phase speed is a function of wave number, and, thus, we see that the space differencing again results in computational dispersion. The formula (1.9) is the same as the one obtained in the preceding chapter when considering the advection equation. Therefore, both the phase speed and the group velocity depend on the wave number as shown in Fig. 2.2 of the preceding chapter. The phase speed decreases as the wave length decreases, and the wave with wave length  $2\Delta x$  is stationary.

There is, however, an important difference between this problem and the advection problem because we now have two dependent variables. We have assumed that they are both carried at every grid point, as shown in Fig. 1.1.



Figure 1.1 A grid with two dependent variables that are both carried at every grid point.

As far as the system (1.5) is concerned, however, the underlined variables in the figure depend only on other underlined variables. The same statement holds for the variables that are not underlined. Thus, the grid

in the figure contains two elementary "subgrids", with the solution on one of these subgrids being completely decoupled from the other. Thus, it would be better to calculate only one of these solutions, that is, to use a grid as shown in Fig. 1.2. Such a grid, with variables carried at alternate points in space, is called a *staggered grid*. The computation time needed to solve (1.5) on this grid is reduced by a factor of two, and the truncation error is the same. Furthermore, the waves with  $k\Delta x > \pi/2$  have been eliminated, and these are just the waves associated with large phase speed errors and negative

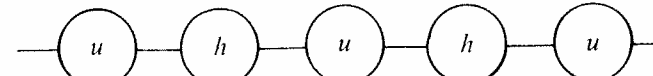


Figure 1.2 A grid with two dependent variables that are carried at alternate grid points.

group velocities. Thus, when using such a staggered grid, the phase speed and group velocity diagram shown in Fig. 2.2 of the preceding chapter is reduced to its left half, covering waves with wave lengths of up to  $4\Delta x$  only. This is a tremendous improvement.

If we wish to have waves with wave lengths between  $4\Delta x$  and  $2\Delta x$  in our calculation we can reduce the grid length by a factor of two and perform a much more accurate integration, using the same amount of computation time than with a grid that is not staggered.

## 2. Two-dimensional gravity waves

We now consider *two-dimensional* gravity waves. Thus, we consider the system of linearized equations

$$\begin{aligned} \frac{\partial u}{\partial t} &= -g \frac{\partial h}{\partial x}, & \frac{\partial v}{\partial t} &= -g \frac{\partial h}{\partial y}, \\ \frac{\partial h}{\partial t} &= -H \nabla \cdot \mathbf{v}. \end{aligned} \quad (2.1)$$

Substituting the wave solutions

$$\begin{aligned} u &= \operatorname{Re}[\hat{u} e^{i(kx+ly-vt)}], & v &= \operatorname{Re}[\hat{v} e^{i(kx+ly-vt)}], \\ h &= \operatorname{Re}[\hat{h} e^{i(kx+ly-vt)}], \end{aligned} \quad (2.2)$$

we now obtain

$$v^2 = gH(k^2 + l^2). \quad (2.3)$$

Thus, in the two-dimensional case the gravity waves propagate with the same constant phase speed  $\sqrt{gH}$ .

Because of the results obtained in the preceding section, we first consider the spatial distribution of the

variables. With two dimensions and three dependent variables, a large number of spatial arrangements of the variables are possible. For the present we consider the three rectangular arrangements shown in Fig. 2.1. The identifying letters (A), (E) and (C) are chosen so as to conform with the symbols used by Winninghoff and

of the area of the admissible region of the wave number plane.

The same standard finite difference approximations can be used for the space derivatives in (2.1) for all three lattices. We write these approximations using the difference operators  $\delta_x$  and  $\delta_y$ , defined by, for example,

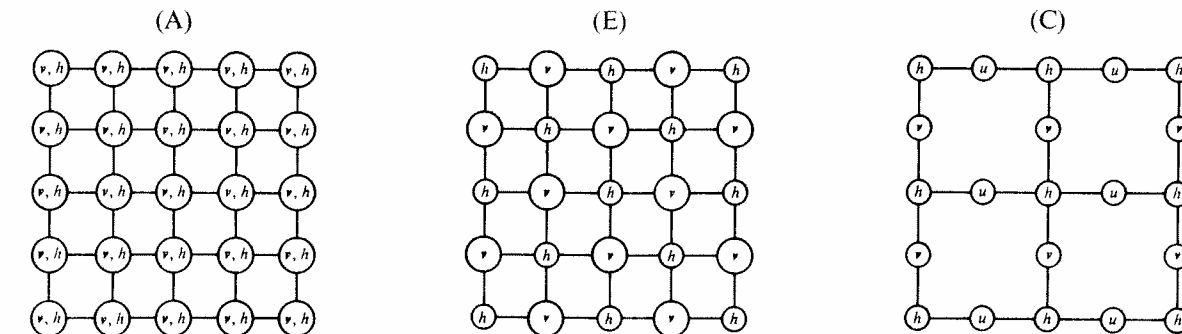


Figure 2.1 Three types of lattice considered for the finite difference solution of 2.1.

$$\delta_x h \equiv \frac{1}{2d^*} [h(x+d^*, y) - h(x-d^*, y)].$$

Thus, (2.1) can be approximated by

$$\begin{aligned} \frac{\partial u}{\partial t} &= -g \delta_x h, & \frac{\partial v}{\partial t} &= -g \delta_y h, \\ \frac{\partial h}{\partial t} &= -H(\delta_x u + \delta_y v). \end{aligned} \quad (2.4)$$

Substituting wave solutions analogous as in (2.2), we obtain

$$v^2 = gH \frac{\sin^2 kd^* + \sin^2 ld^*}{d^{*2}} \quad (2.5)$$

we define

$$X \equiv kd^*, \quad Y \equiv ld^*, \quad (C)$$

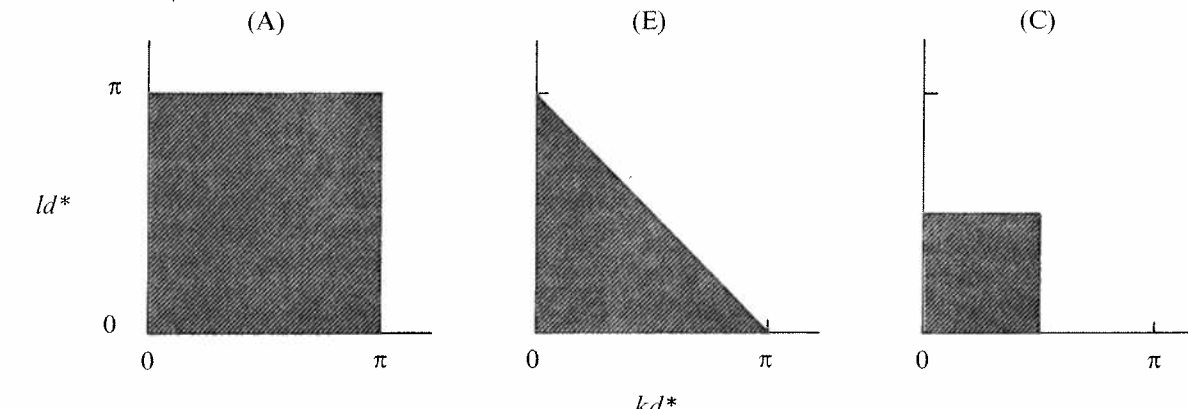


Figure 2.2 Admissible regions of wave numbers for the three types of lattice shown in Figure 2.1.

the ratio of the phase speed given by (2.5),  $c^*$ , to the true phase speed  $\sqrt{gH}$ , can be written as

$$\frac{c^*}{\sqrt{gH}} = \sqrt{\frac{\sin^2 X + \sin^2 Y}{X^2 + Y^2}}. \quad (2.6)$$

This formula reduces to the previous formula, (1.8) or (1.9), when applied to the one-dimensional case.

The values of the relative phase speed (2.6) on the wave number region admitted by lattice (E) are shown in Fig. 2.3. By symmetry about the line  $l = k$  only half of the region needs to be shown. Fig. (2.2) shows that lattice (C) admits only the left half of the triangular region

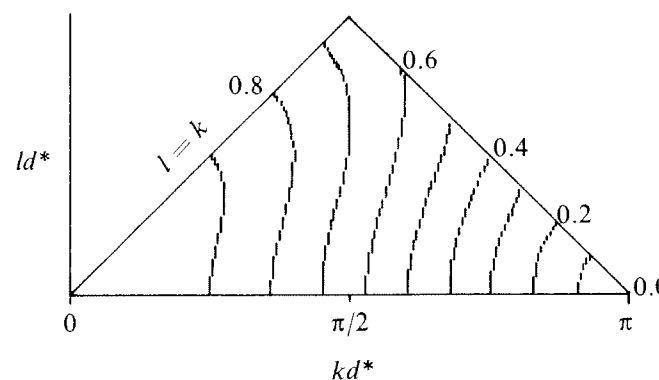


Figure 2.3 Relative phase speed of gravity waves when the space derivatives in (2.1) are approximated by straightforward space-centered finite difference analogues.

shown in the diagram. Clearly lattice (C) gives a more accurate phase speed for gravity waves than the other lattices considered here. Unfortunately, because it does not carry the two velocity components at the same points, there is some difficulty with the Coriolis force term. Of the other lattices, the staggered lattice (E) is much superior to the non-staggered lattice (A). A result with the same truncation error can be achieved in about half of the computation time, (exactly half if the equations are linear), and a sizable fraction of wave numbers that are associated with large phase speed errors and computational dispersion are eliminated. The additional time needed for a calculation on an (A) lattice is spent on waves that can hardly be expected to improve the integration.

As we can see from the phase speed diagram, lattice (E) is not free of computational problems. As with the non-staggered one-dimensional grid discussed in the preceding section, the solutions of (2.4) on each of the two type (C) subgrids forming the (E) lattice are independent and can diverge from each other. This can be a source of serious problems. For example, if the values of the dependent variables on one of these (C) lattices

are constant, they will be a stationary solution on that lattice, no matter what the values of the variables on the other (C) lattice are. Two stationary solutions, with different constant values on each of these complementary lattices, will give a stationary wave represented by the right-hand corner of the triangular region in Fig. 2.3, with a zero phase speed. This wave is usually referred to as the *two-grid-interval wave*. In the same way, the (A) lattice admits four independent stationary solutions, with different constant values on each of its four type (C) subgrids.

The two-grid-interval wave can easily be generated when boundary conditions are artificially described, and, with more complete equations, in cases when gravity waves are generated inside the computational region. These can be caused by heating, for example through the release of latent heat, and by the influence of mountains. When gravity waves are excited involving variables of one of the (C) subgrids only, for example by forcing at individual grid points or lines of points, the gravity wave will propagate through the variables of this subgrid only. The variables of the other (C) subgrid will be influenced only through the Coriolis and advection terms on a much larger time-scale. Thus physical effects which may excite relatively long waves in the atmosphere may excite spurious waves with wave lengths of approximately two grid intervals in a computation. When these reach an excessive amplitude, some remedial measures have to be taken. These will be discussed in a later section.

### 3. Gravity-inertia waves and space distribution of variables

In this section we discuss the effect of centered space differencing on *gravity-inertia waves*. Thus, we consider the system of linearized equations

$$\begin{aligned} \frac{\partial u}{\partial t} &= -g \frac{\partial h}{\partial x} + fv, & \frac{\partial v}{\partial t} &= -g \frac{\partial h}{\partial y} - fu, \\ \frac{\partial h}{\partial t} &= -H \nabla \cdot \mathbf{v}. \end{aligned} \quad (3.1)$$

These equations differ from those of section 2 in the appearance of the two Coriolis terms. The Coriolis terms contain no derivatives. However, they are difficult to calculate on the (C) lattice, which was ideal for pure gravity waves.

Thus, we reconsider the problem of the distribution of the variables.

It is not obvious how we should analyse various arrangements of variables. Our primary concern here is to consider (3.1) as part of the complete system of primitive

equations. We are interested in large-scale motions, otherwise we would not be including the Coriolis terms.

On the large scale, the primitive equations admit two distinct types of motion : low-frequency, quasi-geostrophic and quasi-nondivergent flow ; and high-frequency gravity-inertia waves. Gravity-inertia waves are continually excited in the atmosphere ; however, as they are dispersive, a local accumulation of wave energy disperses with time. This process is known as geostrophic adjustment ; the remaining motion is in approximate geostrophic balance and changes only slowly in time. In this chapter we are concerned with the correct simulation of this process, which is essentially governed by the gravity-inertia wave equations (3.1).

We are interested both in waves caused by physical effects, and in those caused by inadequacies of the initial data and of the numerical procedures.

However, the details of the adjustment process do not matter as much as the correctness of the resulting quasi-geostrophic flow.

We shall therefore investigate the effect of the space distribution of dependent variables on the dispersive properties of the gravity-inertia waves. This will be done using the simplest centered approximations for the space

derivatives, leaving the time derivatives in their differential form.

The discussion is based on that by Winninghoff and Arakawa, as presented by Arakawa (Arakawa, 1972 ; Arakawa *et al.* 1974).

We consider five ways of distributing the dependent variables in space, shown in Fig. 3.1. We denote by  $d$  the shortest distance between neighbouring points carrying the same dependent variable. In the figure  $d$  is the same for each of the five lattices ; thus, all the lattices have the *same number of dependent variables per unit area*. The computation time needed for an integration on each of the lattices will be about the same ; the properties of the solution obtained, though, will differ because of the effect of the space arrangement of variables.

Using the subscripts shown in the figure, we define the centered space differencing operator by

$$(\delta_x a)_{i,j} \equiv \frac{1}{d'} (a_{i+\frac{1}{2},j} - a_{i-\frac{1}{2},j}),$$

this rotation is applicable to all the lattices. Here  $d'$  is the distance between the points between which the finite difference is taken. Thus, for lattices (A) through (D)  $d'$  is equal to the grid size  $d$ , and for the lattice (E) it is

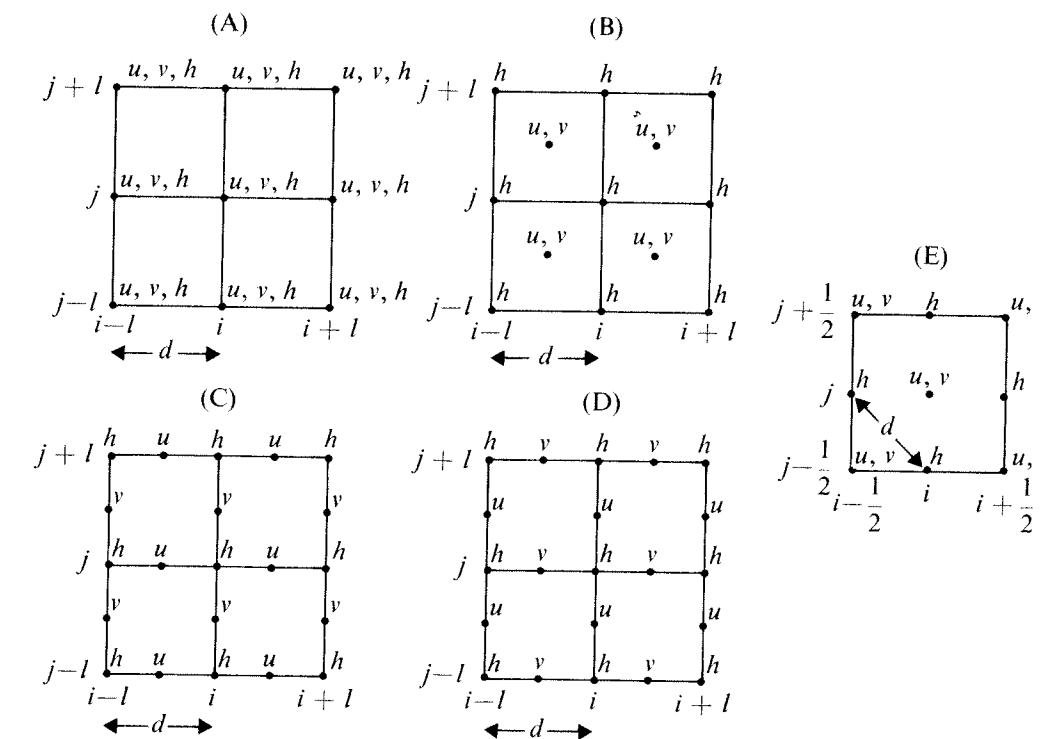


Figure 3.1 Five types of lattice considered for the finite difference solution of (3.1).

equal to  $\sqrt{2}d$ . We also define an average taken over the same two points by

$$(\bar{\alpha}^x)_{i,j} \equiv \frac{1}{2} (\alpha_{i+\frac{1}{2},j} + \alpha_{i-\frac{1}{2},j}).$$

$(\bar{\alpha}_y \alpha)_{i,j}$  and  $(\bar{\alpha}^v)_{i,j}$  are defined in the same way, but with respect to the  $y$  axis. Finally,

$$(\bar{\alpha}^{xy})_{i,j} \equiv (\bar{\alpha}^x)_{i,j}.$$

For each of the five lattices we use the simplest centered approximations for the space derivatives and Coriolis terms (3.1). We obtain the difference systems

$$\begin{aligned} \frac{\partial u}{\partial t} &= -g \bar{\delta}_x^x h + fv, & \frac{\partial v}{\partial t} &= -g \bar{\delta}_y^y h - fu, \\ \frac{\partial h}{\partial t} &= -H (\bar{\delta}_x^x u + \bar{\delta}_y^y v), \end{aligned} \quad (3.2)_A$$

$$\begin{aligned} \frac{\partial u}{\partial t} &= -g \bar{\delta}_x^y h + fv, & \frac{\partial v}{\partial t} &= -g \bar{\delta}_y^x h - fu, \\ \frac{\partial h}{\partial t} &= -H (\bar{\delta}_x^y u + \bar{\delta}_y^x v), \end{aligned} \quad (3.2)_B$$

$$\begin{aligned} \frac{\partial u}{\partial t} &= -g \bar{\delta}_x^x h + f\bar{v}^{xy}, & \frac{\partial v}{\partial t} &= -g \bar{\delta}_y^y h - f\bar{u}^{xy}, \\ \frac{\partial h}{\partial t} &= -H (\bar{\delta}_x^x u + \bar{\delta}_y^y v), \end{aligned} \quad (3.2)_C$$

$$\begin{aligned} \frac{\partial u}{\partial t} &= -g \bar{\delta}_x^{xy} h + f\bar{v}^{xy}, & \frac{\partial v}{\partial t} &= -g \bar{\delta}_y^{xy} h - f\bar{u}^{xy}, \\ \frac{\partial h}{\partial t} &= -H (\bar{\delta}_x^{xy} u + \bar{\delta}_y^{xy} v), \end{aligned} \quad (3.2)_D$$

$$\begin{aligned} \frac{\partial u}{\partial t} &= -g \bar{\delta}_x^x h + fv, & \frac{\partial v}{\partial t} &= -g \bar{\delta}_y^y h - fu, \\ \frac{\partial h}{\partial t} &= -H (\bar{\delta}_x^x u + \bar{\delta}_y^y v). \end{aligned} \quad (3.2)_E$$

We shall first analyze a one-dimensional case, that is in which the variables  $u$ ,  $v$  and  $h$  do not vary with  $y$ . Thus, we have

$$u, v, h = u, v, h(x, t).$$

The system (3.1) then reduces to

$$\begin{aligned} \frac{\partial u}{\partial t} &= -g \frac{\partial h}{\partial x} + fv, & \frac{\partial v}{\partial t} &= -fu, \\ \frac{\partial h}{\partial t} &= -H \frac{\partial u}{\partial x}. \end{aligned} \quad (3.3)$$

Substituting the wave solutions (1.2), we obtain the frequency equation which can be written as

$$\left( \frac{v}{f} \right)^2 = 1 + \frac{gH}{f^2} k^2. \quad (3.4)$$

Thus, as the *radius of deformation*

$$\lambda = \sqrt{gH/f},$$

is never equal to zero, the frequency of the gravity-inertia waves is a monotonically increasing function of  $k$ . Therefore, the group velocity  $\partial v/\partial k$  is never equal to zero. This is very important for the geostrophic adjustment process, as it precludes a local accumulation of wave energy.

We now look at the effect of the finite differencing in space in this case. As the variables are assumed not to depend on  $y$ , the systems (3.2) reduce to

$$\begin{aligned} \frac{\partial u}{\partial t} &= -g \bar{\delta}_x^x h + fv, & \frac{\partial v}{\partial t} &= -fu, \\ \frac{\partial h}{\partial t} &= -H \bar{\delta}_x^x u, \end{aligned} \quad (3.5)_A$$

$$\begin{aligned} \frac{\partial u}{\partial t} &= -g \bar{\delta}_x^y h + fv, & \frac{\partial v}{\partial t} &= -fu, \\ \frac{\partial h}{\partial t} &= -H \bar{\delta}_x^y u, \end{aligned} \quad (3.5)_B$$

$$\begin{aligned} \frac{\partial u}{\partial t} &= -g \bar{\delta}_x^x h + f\bar{v}^{xy}, & \frac{\partial v}{\partial t} &= -fu, \\ \frac{\partial h}{\partial t} &= -H \bar{\delta}_x^x u, \end{aligned} \quad (3.5)_C$$

$$\begin{aligned} \frac{\partial u}{\partial t} &= -g \bar{\delta}_x^{xy} h + f\bar{v}^{xy}, & \frac{\partial v}{\partial t} &= -fu, \\ \frac{\partial h}{\partial t} &= -H \bar{\delta}_x^{xy} u, \end{aligned} \quad (3.5)_D$$

$$\begin{aligned} \frac{\partial u}{\partial t} &= -g \bar{\delta}_x^x h + fv, & \frac{\partial v}{\partial t} &= -fu, \\ \frac{\partial h}{\partial t} &= -H \bar{\delta}_x^x u. \end{aligned} \quad (3.5)_E$$

Substitution of wave solutions into these systems gives the frequency equations

$$\left( \frac{v}{f} \right)^2 = 1 + \left( \frac{\lambda}{d} \right)^2 \sin^2 kd, \quad (3.6)_A$$

$$\left( \frac{v}{f} \right)^2 = 1 + 4 \left( \frac{\lambda}{d} \right)^2 \sin^2 \frac{kd}{2}, \quad (3.6)_B$$

$$\left( \frac{v}{f} \right)^2 = \cos^2 \frac{kd}{2} + 4 \left( \frac{\lambda}{d} \right)^2 \sin^2 \frac{kd}{2}, \quad (3.6)_C$$

$$\left( \frac{v}{f} \right)^2 = \cos^2 \frac{kd}{2} + \left( \frac{\lambda}{d} \right)^2 \sin^2 kd, \quad (3.6)_D$$

$$\left( \frac{v}{f} \right)^2 = 1 + 2 \left( \frac{\lambda}{d} \right)^2 \sin^2 \frac{kd}{\sqrt{2}}. \quad (3.6)_E$$

The non-dimensional frequency  $v/f$  is now seen to depend on two parameters,  $kd$  and  $\lambda/d$ .

We shall analyze the dispersion properties revealed by these expressions for each of the five lattices. The wave length of the shortest resolvable wave along the  $x$  axis is  $2d$  for lattices (A) through (D), and  $\sqrt{2}d$  for the lattice (E). Thus, we have to consider the range  $0 < kd \leq \pi$  for lattices (A) through (D), and the range  $0 < kd \leq \sqrt{2}\pi$  for the lattice (E).

Lattice (A): The frequency reaches a maximum at  $kd = \pi/2$ . Thus, the group velocity is zero for  $k$  equal to  $\pi/(2d)$ . If gravity-inertia waves of approximately that wave number are excited near a point inside the computational region, for example by nonlinear effects or forcing through heating or ground topography, the wave energy stays near that point. Beyond this maximum value, for  $\pi/2 < kd < \pi$ , the frequency decreases as the wave number increases. Thus, for these waves the group velocity has the wrong sign. Finally, the two-grid-interval wave with  $kd = \pi$  behaves like a pure inertia oscillation, and its group velocity is again zero.

Lattice (B): The frequency increases monotonically throughout the range  $0 < kd < \pi$ . However, it reaches a maximum at the end of the range, so that the group velocity is zero for the two-grid-interval wave with  $kd = \pi$ .

Lattice (C): The frequency increases monotonically with  $kd$  if  $\lambda/d > 1/2$  and decreases monotonically with  $kd$  if  $\lambda/d < 1/2$ . It again reaches an extreme value at  $kd = \pi$ ,

associated with a zero group velocity. For  $\lambda/d = 1/2$  the group velocity is equal to zero for all  $k$ .

Lattice (D): The frequency reaches a maximum at  $(\lambda/d)^2 \cos kd = 1/4$ . The two-grid-interval wave at  $kd = \pi$  is stationary.

Lattice (E): The frequency reaches a maximum at  $kd = \pi/\sqrt{2}$ . The shortest resolvable wave with  $kd = \sqrt{2}\pi$  behaves like a pure inertia oscillation, and its group velocity is again zero.

A summary of these results is shown in Fig. 3.2. It shows the functions  $|v|/f$ , in the case  $\lambda/d = 2$ .

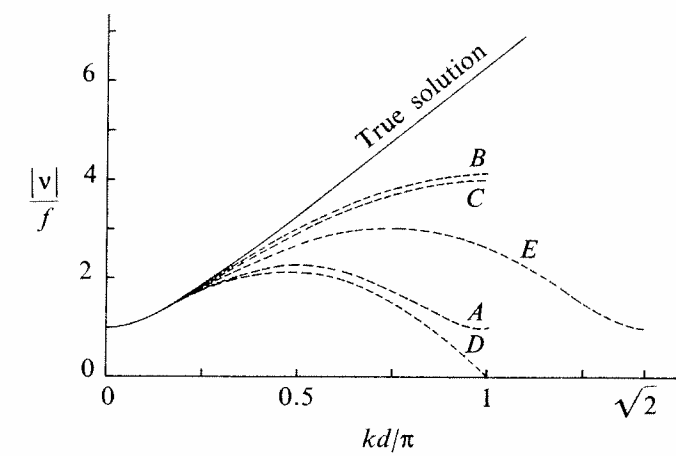


Figure 3.2 The functions  $|v|/f$  given by (3.4) and (3.6), with  $\lambda/d = 2$ .

The figure vividly illustrates the inadequacy of the lattices (D) and (A). The phase speed and dispersion properties of the remaining three lattices are much better: however, zero group velocities occur with every lattice. Thus, with any lattice there will be difficulties in the geostrophic adjustment process.

The difference between the results for lattices (B) and (E) is interesting because these two lattices can be obtained from one another by a rotation through an angle of  $\pi/4$ . If we consider the one-dimensional case in which the dependent variables are constant along the lines  $y = x + c$ , we obtain results for these two lattices that are exactly opposite to those in Fig. 3.2. In general, we define the coordinate system  $x', y'$  by rotating the system  $x, y$  in the positive direction through an angle of  $\pi/4$ , and then, using the relations

$$u' = \frac{\sqrt{2}}{2} (u + v), \quad v' = \frac{\sqrt{2}}{2} (-u + v),$$

change from variables  $u, v, h$  to new dependent variables  $u', v', h$ . We find that this transforms the system (3.2)<sub>B</sub> into (3.2)<sub>E</sub>, and, conversely, (3.2)<sub>B</sub> into (3.2)<sub>E</sub>. Thus, the dispersion properties of the lattices (B) and (E) can be considered equivalent. A gravity-inertia wave in one of these lattices has phase speed and dispersion properties identical to those of the same wave with its front rotated through an angle of  $\pi/4$  in the other lattice.

Obviously, we should also consider the two-dimensional case. The values of  $|v|/f$  that are obtained in the two-dimensional case for the true solution and those using lattices (B) and (C) are shown in Fig. 3.3 with  $\lambda/d' = 2$ . The diagram for lattice (E) can be obtained by a counter-clockwise rotation of the (B) lattice diagram.

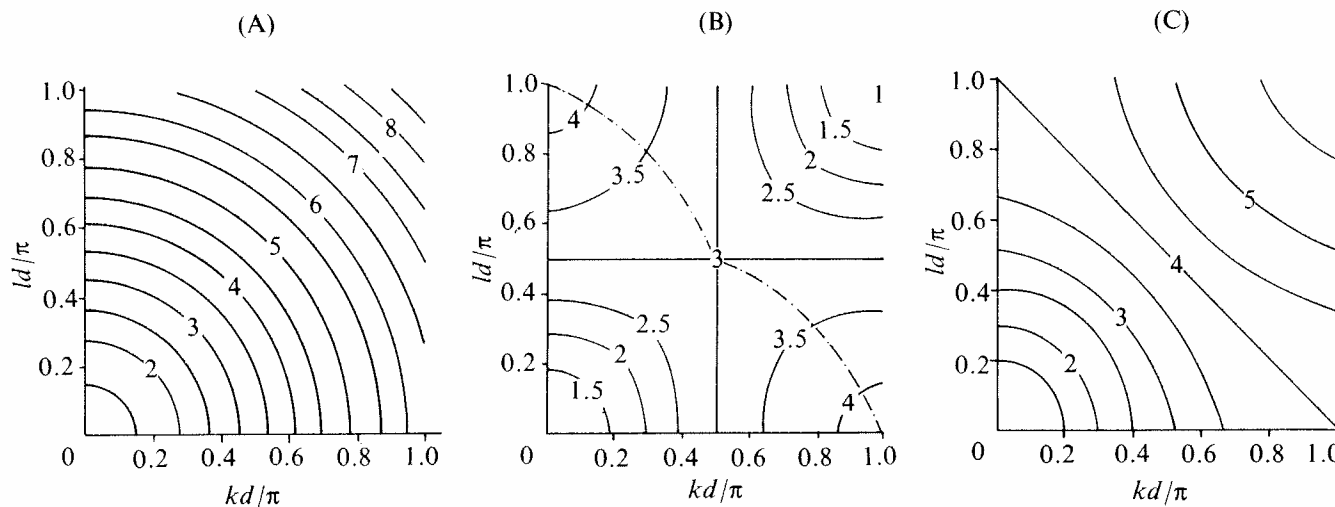


Figure 3.3 The functions  $|v|/f$ , for the true solution and for solutions of systems (3.2)<sub>B</sub> and (3.2)<sub>C</sub>, with  $\lambda/d = 2$ .

The diagram for lattice (C) in the two-dimensional case is seen to be a much better approximation to the exact solution than the (B) or (E) lattice diagram. In the (B) lattice diagram the dot-dashed line shows the maximum  $|v|/f$  for a given ratio  $l/k$ ; note that there is no such line in the (C) lattice diagram and the exact solution. Such a maximum occurs at only two corner points of the (C) lattice diagram. Thus, with the (C) lattice, no waves have a group velocity with the wrong sign. The situation, though, does depend on the parameter  $\lambda/d$ . With a stratified atmosphere the radius of deformation  $\lambda$  depends on the stability; if the stability is so weak as to make  $\lambda/d$  of the order of 1 or less, the (C) lattice loses the advantages shown in Fig. (3.3). However, for typical grid sizes used in atmospheric models this is not the case and therefore Arakawa (Arakawa and Lamb, 1976) concludes that the lattice (C) is the best lattice to simulate the geostrophic adjustment process. Accordingly, it is at present being used in the general circulation model at the University of California at Los Angeles, and also in the British operational model.

We shall demonstrate this for the one-dimensional equations

$$\begin{aligned} \frac{\partial u}{\partial t} + c \frac{\partial u}{\partial x} + g \frac{\partial h}{\partial x} &= 0, \\ \frac{\partial h}{\partial t} + c \frac{\partial h}{\partial x} + H \frac{\partial u}{\partial x} &= 0. \end{aligned} \quad (4.1)$$

We first multiply the second of these equations by an arbitrary parameter  $\lambda$ , and add the result to the first equation. We obtain

$$\frac{\partial}{\partial t} (u + \lambda h) + (c + \lambda H) \frac{\partial u}{\partial x} + (g + \lambda c) \frac{\partial h}{\partial x} = 0. \quad (4.2)$$

We wish to choose  $\lambda$  so that

$$\frac{g + \lambda c}{c + \lambda H} = \lambda, \quad (4.3)$$

The (B) or (E) lattices have a problem with false low frequencies of the shortest waves. The two-grid-interval wave, that was stationary as a pure gravity wave, now behaves like a pure inertia oscillation. The difficulty arises from decoupling of the gravity wave solutions on the two complementary (C) type subgrids. Methods of dealing with this will be discussed later.

#### 4. Time differencing; the leapfrog scheme and the Eliassen grid

Properties of time differencing schemes applied to the gravity wave equations can be deduced from the analysis of Chapter 2, as was done for the advection equation.

to obtain an equation with only one dependent variable,  $u + \lambda h$ . The two solutions of (4.3) are

$$\lambda = \pm \sqrt{\frac{g}{H}}. \quad (4.4)$$

Substituting these into (4.2) we obtain

$$\begin{aligned} \left[ \frac{\partial}{\partial t} + (c + \sqrt{gH}) \frac{\partial}{\partial x} \right] \left( u + \sqrt{\frac{g}{H}} h \right) &= 0, \\ \left[ \frac{\partial}{\partial t} + (c - \sqrt{gH}) \frac{\partial}{\partial x} \right] \left( u - \sqrt{\frac{g}{H}} h \right) &= 0. \end{aligned} \quad (4.5)$$

This is the *normal form* of the system (4.1). It shows that (4.1) is equivalent to a system of two advection equations. The quantity  $u + \sqrt{g/H}h$  is seen to be advected at a velocity  $c + \sqrt{gH}$  in the direction of the  $x$  axis, while, at the same time, the quantity  $u - \sqrt{g/H}h$  is advected in the same direction at a velocity  $c - \sqrt{gH}$ .

Suppose now we choose a grid that carries both  $u$  and  $h$  at every grid point. The systems obtained by using centered space differencing in (4.1) and (4.5) are then equivalent. We can therefore use the same procedure as in Section 1 of Chapter 3 to analyse time differencing schemes. We obtain the same results as before, except that in place of the advection velocity  $c$  we now have  $c + \sqrt{gH}$ . Thus, if the *leapfrog scheme* is used for the time differencing, and  $c$  is considered positive, we obtain the Courant-Friedrichs-Lowy stability criterion for this case as

$$(c + \sqrt{gH}) \frac{\Delta t}{\Delta x} \leq 1. \quad (4.6)$$

The advection velocity in the atmosphere is normally about an order of magnitude less than the phase speed of external gravity waves. Accordingly, in the foregoing criterion  $c$  is often neglected compared with  $\sqrt{gH}$ , giving the stability requirement

$$\sqrt{gH} \frac{\Delta t}{\Delta x} < 1. \quad (4.7)$$

When using the *three-dimensional* primitive equations, external gravity waves are normally eliminated by permitting no vertical velocity at the upper boundary. The highest phase speed admitted by the system is then that of the Lamb waves, which for an isothermal atmosphere is

$$\sqrt{\left(\frac{f}{k}\right)^2 + \gamma RT},$$

where  $\gamma \equiv c_p/c_v$ . If we neglect the first term and recall that the scale height of an isothermal atmosphere is

$$H^* = RT/g,$$

we see that the phase speed of the Lamb waves is of the same order of magnitude as that of the external gravity waves. Thus, in view of the relation between stability and the phase speed, we see that (4.7) should also represent an approximately correct stability requirement in the three-dimensional case. With the highest phase speeds of the order of 300 m sec<sup>-1</sup>, and a grid size of about 100 km, this requirement does not permit time steps longer than about 5 minutes. This time will be smaller by a factor of  $\sqrt{2}$  with two horizontal coordinates. The CFL stability condition thus means that a large amount of computer time is required for integration of the primitive equations, especially when the grid size is small to reduce errors in space differencing. For this reason some investigators prefer using implicit time differencing schemes, so that the choice of time step can be based solely on accuracy and not on stability.

We can also study the stability and other properties of time differencing methods applied to the gravity wave equations by direct substitution of wave solutions. For example, consider the leapfrog scheme with centered space differencing applied to the *two-dimensional* system

$$\begin{aligned} \frac{\partial u}{\partial t} + g \frac{\partial h}{\partial x} &= 0, & \frac{\partial v}{\partial t} + g \frac{\partial h}{\partial y} &= 0, \\ \frac{\partial h}{\partial t} + H \nabla \cdot \mathbf{v} &= 0. \end{aligned} \quad (4.8)$$

Using one of the lattices of Fig. 2.1 as well as the notation of Section 2, we obtain

$$\begin{aligned} u^{n+1} &= u^{n-1} - 2g\Delta t \delta_x h^n, & v^{n+1} &= v^{n-1} - 2g\Delta t \delta_y h^n, \\ h^{n+1} &= h^{n-1} - 2H\Delta t (\delta_x u + \delta_y v)^n. \end{aligned} \quad (4.9)$$

Substituting the wave solutions

$$\begin{aligned} u^n &= Re [\lambda^n \hat{u} e^{i(kx+ly)}], & v^n &= Re [\lambda^n \hat{v} e^{i(kx+ly)}], \\ h^n &= Re [\lambda^n \hat{h} e^{i(kx+ly)}], \end{aligned} \quad (4.10)$$

we obtain the homogeneous system

$$(\lambda^2 - 1) \hat{u} + i\lambda 2\sqrt{2} g \mu \sin X \hat{h} = 0$$

$$(\lambda^2 - 1) \hat{v} + i\lambda 2\sqrt{2} g \mu \sin Y \hat{h} = 0, \quad (4.11)$$

$$i\lambda 2\sqrt{2}H\mu(\sin X \hat{u} + \sin Y \hat{v}) + (\lambda^2 - 1)\hat{h} = 0.$$

Here  $X$  and  $Y$  are defined as in Section 2, while

$$\mu \equiv \Delta t/(\sqrt{2}d^*),$$

that is,  $\mu = \Delta t/d$  when the lattice (E) is chosen.

The properties of the numerical solution can now be studied by analyzing (4.11). The requirement that its determinant be equal to zero gives six solutions for  $\lambda$ . Two of these are

$$\lambda = 1 \quad (4.12)$$

and

$$\lambda = -1. \quad (4.13)$$

The remaining four are given by

$$\lambda^2 = 1 - 4A \pm 2\sqrt{2A(2A-1)} \quad (4.14)$$

where

$$A \equiv gH\mu^2(\sin^2 X + \sin^2 Y).$$

We can now analyze the solutions (4.10) associated with the values found for  $\lambda$ . The first of these values, (4.12), gives a neutral and stationary solution. If either  $\sin X$  or  $\sin Y$  is non-zero in this neutral and stationary case then, according to (4.11), we have  $\hat{h} = 0$ , and the solution represents a physically acceptable translatory motion. If, however,  $\sin X$  and  $\sin Y$  are both equal to zero, the amplitudes of all three dependent variables can take arbitrary values. In addition to the physically acceptable solution where all the dependent variables are constant ( $k = l = 0$ ), there is a solution with one or both of the wave numbers  $k$  and  $l$  equal to  $\pi/d^*$ . This is the two-grid-interval wave, discussed already in Section 2. It again appears as a false computational solution; since it is stationary, it is not affected by the introduction of time differencing.

The second value,  $\lambda = -1$ , represents a false computational mode in time, with a period of  $2\Delta t$ . This computational mode results from using a three time level scheme.

To prove stability of the scheme the behaviour of the remaining solutions given by (4.14) has to be investigated. They will all also be neutral for  $2A < 1$ . To obtain the condition in the form  $B\Delta t \leq 1$  we write

$$\sqrt{2A} \leq 1.$$

Since this has to be satisfied for all the admissible waves, we find that the CFL criterion in the two-dimensional case is now

$$2\sqrt{gH}\mu \leq 1, \quad (4.15)$$

or

$$\sqrt{2gH} \frac{\Delta t}{dx} \leq 1. \quad (4.16)$$

This is in agreement with the previous results. The nondimensional constant on the left side is sometimes called the *Courant number*.

With solutions like (4.10), the frequency  $v$  is given by

$$\lambda = |\lambda| e^{-iv\Delta t}.$$

Thus, the expressions obtained for  $\lambda$  can be used to calculate the *relative phase speed*  $c^*/\sqrt{gH}$  using the relation

$$\frac{c^*}{\sqrt{gH}} = \frac{1}{\Delta t \sqrt{2gH}(k^2 + l^2)} \arctan \frac{-\lambda_{im}}{\lambda_{re}}. \quad (4.17)$$

If we are given  $\lambda^2$  rather than  $\lambda$ , as here, we can express the relative phase speed as a function of  $(\lambda^2)_{im}$  and  $(\lambda^2)_{re}$ . Thus, using (4.14), we find for  $2A \leq 1$ :

$$\begin{aligned} \frac{c^*}{\sqrt{gH}} &= \frac{1}{2\mu \sqrt{2gH}(X^2 + Y^2)} \times \\ &\times \arctan \left( \mp \frac{2\sqrt{2A}(1-2A)}{1-4A} \right). \end{aligned} \quad (4.18)$$

This expression, of course, approaches (2.6) as  $\Delta t$  approaches zero.

For a more explicit illustration of the effect of time differencing, we can perform a series expansion of (4.18). One obtains, for  $\sqrt{2A} < 1/\sqrt{2}$ ,

$$\frac{c^*}{\sqrt{gH}} = \sqrt{\frac{\sin^2 X + \sin^2 Y}{X^2 + Y^2}} \left( 1 + \frac{1}{3} A + \frac{3}{10} A^2 + \dots \right).$$

The factor multiplying the series in parenthesis describes the decelerating effect of space differencing, as given by (2.6). The acceleration resulting from the leapfrog time differencing is beneficial, as it reduces the phase error due to space differencing.

The values of the relative phase speed (4.18) are shown in Fig. 4.1, for the physical mode with  $2\sqrt{gH}\mu = 0.5$ . The wave number region shown here is the same as in Fig. 2.3, where the effect of space differencing alone was considered. Comparison of these figures shows little difference between the two families of isolines. The relative acceleration due to the time differencing has a maximum at the upper corner of the diagram, but the relative phase speed here is still poor.

grid the *Richardson grid*. A single Richardson grid is considered as a time-staggered version of the (C) lattice and suffices for the solution of the pure gravity wave system (4.9); thus, on an Eliassen grid the system (4.9) has two independent solutions. Using the difference system considered above to approximate the differential system (4.19), these solutions are coupled only through the two Coriolis terms.

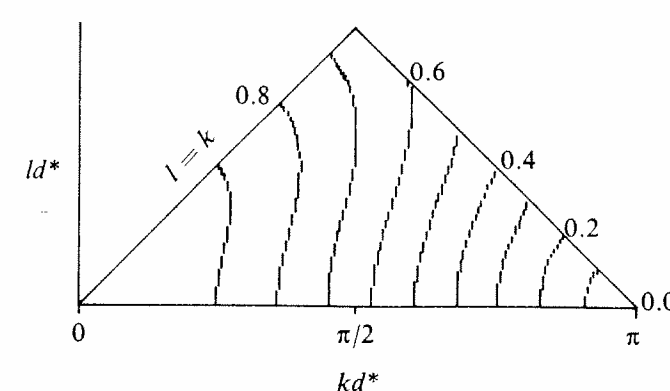


Figure 4.1 Relative phase speed of gravity waves, with centered time and space differencing, and Courant number equal to 0.5.

Finally, we point out that time differencing suggests new ways of distributing the variables, as the grid can now also be time-staggered. A good example is given by the linearized system

$$\begin{aligned} \frac{\partial u}{\partial t} + g \frac{\partial h}{\partial x} - fv &= 0, & \frac{\partial v}{\partial t} + g \frac{\partial h}{\partial y} + fu &= 0, \\ \frac{\partial h}{\partial t} + H \left( \frac{\partial u}{\partial x} + \frac{\partial v}{\partial y} \right) &= 0. \end{aligned} \quad (4.19)$$

approximated using lattice (E), the leapfrog scheme and centered space differencing. If all the variables were calculated at every time level, there would be two independent solutions. The solution involving the variables of the space-time grid shown in Fig. 4.2 would be independent of that involving the variables that are left out in this figure. The second grid can be obtained by shifting the grid a distance  $\sqrt{2d^*}$  along the line  $y = x$ . Thus, as with the space grids discussed in Section 2, the space-time grid formed by using the (E) lattice at every time level can be considered as a superposition of two elementary subgrids of the type shown in Fig. 4.2. Solving the system (4.19) on only one of these saves half the computation time, with no change in the truncation error. In addition the computational mode in time, given by (4.13), is eliminated, as the variables at alternate time levels are missing. Thus, with a more complete system of equations, the gradual separation of solutions at alternate time levels is not possible. The advantages of the space-time grid shown in the figure were pointed out by Eliassen (1956) at an early stage in the study of the primitive equations, and it is called the *Eliassen grid*.

However, as pointed out by Platzman (1958; 1963) the grid in Fig. 4.2 can again be considered as formed by a superposition of two subgrids, where in each of these subgrids only the height is kept at one time level and the velocity components at the next. Platzman calls this sub-

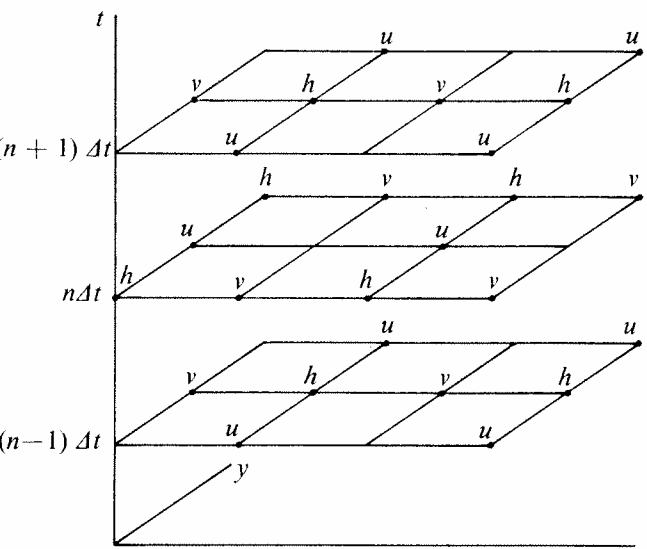


Figure 4.2 A space-time grid staggered both in space and time, convenient for the leapfrog scheme associated with centered space differencing.

##### 5. Economical explicit schemes

The fact that we are now solving *two* equations, the equation of motion and the continuity equation, suggests new ways of constructing time differencing schemes. Some of these have recently attracted the attention of atmospheric modellers.

As seen in the section 4, an inconvenient feature of gravity waves is the high computer time required for a solution using explicit schemes for the time differencing. The time step imposed by the CFL stability criterion is generally considered to be much less than that required for an accurate integration of the slower quasi-geostrophic motions. With these steps, the errors due to space differencing are much greater than those due to time differencing. Robert (1974), for example, estimates that the typical errors due to space differencing in present atmospheric models amount to nearly 40 per cent, and those due to time differencing only to about 1 per cent of the total error. Thus, any economy that can be made in time differencing is welcome, as the time that is saved can usefully be used to increase the accuracy of the space differencing.

Two explicit schemes that are more economical than the standard leapfrog scheme will be given here. They both achieve economy by using a different integration procedure for the height gradient terms of the equation of motion and for the divergence term of the continuity equation. For brevity, we call these terms the *gravity wave terms* of the governing equations.

We shall discuss the properties of one of these "economical" schemes in some detail. It is obtained by first integrating the gravity wave terms of *either* the equation of motion or of the continuity equation forward, and then those of the other equation backward in time. Thus, this scheme could be called the *forward-backward* scheme. With centered space differencing, (4.8) is approximated by

$$\begin{aligned} u^{n+1} &= u^n - g\Delta t \delta_x h^n, & v^{n+1} &= v^n - g\Delta t \delta_y h^n, \\ h^{n+1} &= h^n - H\Delta t (\delta_x u + \delta_y v)^{n+1}, \end{aligned} \quad (5.1)$$

or by an analogous system in which the order of integration is reversed.

Substituting the wave solutions (4.10) we find three solutions for  $\lambda$ . One of these,

$$\lambda = 1, \quad (5.2)$$

gives again a neutral and stationary solution. The remaining two are

$$\lambda = 1 - A \pm \sqrt{A(A-2)}, \quad (5.3)$$

where the quantity  $A$  is defined as in the preceding section. Solutions (5.2) and (5.3) are obtained for both versions of the scheme, that is, no matter which of the two equations — the equation of motion or the continuity equation — is first integrated forward.

Examination of the amplification factors given by (5.3) shows that the scheme is stable and neutral for  $A \leq 2$ , that is, for

$$\sqrt{2A} \leq 2.$$

To satisfy this for all the admissible waves, we must have

$$2\sqrt{gH}\mu \leq 2. \quad (5.4)$$

Thus, the forward-backward scheme is stable and neutral with time steps *twice those allowed by the CFL criterion for the leapfrog scheme* (Ames, 1969).

The amplification factors of the forward-backward and of the leapfrog scheme are equal within their regions of stability. We now compare their effect on the phase speed by comparing the expression (5.3), for the forward-

backward scheme, with (4.14), for the leapfrog scheme. The right-hand side of (5.3), with  $A$  replaced by  $4A$ , is equal to the right-hand side of (4.14). Because of the definition of  $A$ , this means that  $\lambda$  for the forward-backward scheme is identical to  $\lambda^2$  for the leapfrog scheme when time steps are used for the forward-backward scheme *twice as long as* those for the leapfrog scheme! Thus, the forward-backward scheme gives the same result using only half the computation time needed for the leapfrog scheme. In addition, as a two level scheme, it has no computational mode in time.

To understand this advantage of the forward-backward over the leapfrog scheme we compare the finite difference analogues that these two schemes give for the wave equation, since the system of gravity wave equations is equivalent to a single wave equation. Consider the one-dimensional version of this system:

$$\frac{\partial u}{\partial t} + g \frac{\partial h}{\partial x} = 0, \quad \frac{\partial h}{\partial t} + H \frac{\partial u}{\partial x} = 0. \quad (5.5)$$

Eliminating one of the variables  $u, h$  we obtain a wave equation

$$\frac{\partial^2 h}{\partial t^2} - gH \frac{\partial^2 h}{\partial x^2} = 0. \quad (5.6)$$

We can perform the same elimination for each of the finite difference schemes.

The forward-backward and space-centered approximation to (5.5) is

$$\begin{aligned} \frac{u_j^{n+1} - u_j^n}{\Delta t} + g \frac{h_{j+1}^n - h_{j-1}^n}{2\Delta x} &= 0, \\ \frac{h_j^{n+1} - h_j^n}{\Delta t} + H \frac{u_{j+1}^{n+1} - u_{j-1}^{n+1}}{2\Delta x} &= 0, \end{aligned} \quad (5.7)$$

We now subtract from the second of these equations an analogous equation for time level  $n-1$  instead of  $n$ , divide the resulting equation by  $\Delta t$ , and, finally, eliminate all  $u$  values from it using the first of Eqs. (5.7), written for space points  $j+1$  and  $j-1$  instead of  $j$ . We obtain

$$\frac{h_j^{n+1} - 2h_j^n + h_j^{n-1}}{(\Delta t)^2} - gH \frac{h_{j+2}^n - 2h_j^n + h_{j-2}^n}{(2\Delta x)^2} = 0. \quad (5.8)$$

This is a finite difference analogue of the wave equation (5.6). Note that although each of the two equations (5.7) is only of the first order of accuracy in time, the wave equation analogue equivalent to (5.7) is seen to be of the second order of accuracy.

If we use a leapfrog and space-centered approximation to (5.5), and follow an elimination procedure like that used in deriving (5.8), we obtain

$$\begin{aligned} \frac{h_j^{n+1} - 2h_j^n + h_j^{n-1}}{(2\Delta t)^2} - \\ - gH \frac{h_{j+2}^{n-1} - 2h_j^{n-1} + h_{j-2}^{n-1}}{(2\Delta x)^2} = 0. \end{aligned} \quad (5.9)$$

This also is an analogue to the wave equation (5.6) of second-order accuracy. However, in (5.8) the second time derivative was approximated using values at three consecutive time levels; in (5.9) it is approximated by values at every second time level only, that is, at time intervals  $2\Delta t$ . Thus, while the time step required for linear stability with the leapfrog scheme was half that with the forward-backward scheme, (5.9) shows that we can omit the variables at every second time step, and thus achieve the same computation time as using the forward-backward scheme with double the time step. This method was discussed in the previous section for the two-dimensional case, it is the Eliassen grid. Thus, comparing (5.8) and (5.9) shows that *the economy accomplished by the forward-backward scheme is equivalent to that accomplished with leapfrog time differencing by the Eliassen grid*. Both of these methods avoid calculating the false time computational mode, and thus save half of the computation time with no effect on the physical mode of the solution.

Comparing these two methods, the forward-backward scheme has some advantages. With the forward-backward scheme all the variables are defined at all grid points at every time step; this facilitates the programming work. In addition, the forward-backward scheme can be modified to allow propagation of gravity waves between all points of the grid preventing two-grid-interval noise. This modification will be described in Section 8. No analogous method, however, has so far been proposed for the leapfrog scheme with the Eliassen grid.

A disadvantage of the forward-backward scheme is that it is not possible to use the leapfrog scheme for the advection terms. However, the second-order accurate Adams-Basforth scheme can be used for these terms. Its weak instability should cause no trouble because of the relatively slow speed of the advection processes. For example, in experiments of Mesinger and Janic (1974), where a multi-level model was used for simulation of the growth of a baroclinic wave, a forward scheme was used for the advection terms, and no signs of instability were noticed for about a two week period. The forward-backward scheme has been used for the storm surge problem by Fischer (1959) and Sielecki (1968), and,

in meteorology, by Gadd (1974) in experiments with the British operational model.

Another way of constructing an economical explicit scheme was pointed out by Shuman, Brown and Campana (1974), and it is now used in an operational model at the National Meteorological Center. For the shallow water equations with this scheme, the height values at time level  $n+1$  are first calculated using the leapfrog scheme, and then the equation of motion is integrated using the height field averaged over the time interval  $2\Delta t$  by the bi-trapezoidal rule :

$$\frac{1}{4} h^{n-1} + \frac{1}{2} h^n + \frac{1}{4} h^{n+1}.$$

Substitution of wave solutions into the equations of this scheme gives the value (5.3) for  $\lambda$ , in addition to the neutral values. Thus, the stability criterion and the properties of the physical solution are the same as with the forward-backward scheme. Even though this Shuman-Brown-Campana (SBC) scheme is a three level scheme, time staggering of the grid is not possible because of the averaging of the height values. Thus, the economy accomplished by the SBC scheme is again equivalent to that accomplished with leapfrog time differencing by the Eliassen grid. The SBC scheme has somewhat larger storage requirements than the forward-backward scheme. However, it does permit the use of the leapfrog scheme for the advection terms.

## 6. Implicit and semi-implicit schemes

The time step permitted by the economical explicit schemes, twice that prescribed by the CFL criterion, is still considerably shorter than that required for accurate integration of the quasi-geostrophic motions. Even with these schemes the time differencing error is still much less than the space differencing error for typical current atmospheric models. Thus, we consider implicit schemes which are stable for any choice of time step. We shall consider here only the simplest of the implicit schemes, the trapezoidal rule. For brevity it will simply be called *the implicit scheme*.

We shall first discuss the properties of the implicit scheme applied to the system (4.8) in some detail, that is, the case of pure gravity waves. Thus, we consider the finite difference system

$$\begin{aligned} u^{n+1} &= u^n - g\Delta t \frac{1}{2} \left( \delta_x h^n + \delta_x h^{n+1} \right), \\ v^{n+1} &= v^n - g\Delta t \frac{1}{2} \left( \delta_y h^n + \delta_y h^{n+1} \right), \\ h^{n+1} &= h^n - H\Delta t \frac{1}{2} \left[ \left( \delta_x u + \delta_y v \right)^n + \left( \delta_x u + \delta_y v \right)^{n+1} \right]. \end{aligned} \quad (6.1)$$

Substituting the wave solutions (4.10) we find three solutions for  $\lambda$ . One of these,

$$\lambda = 1, \quad (6.2)$$

is again that associated with a neutral and stationary solution. The remaining two are

$$\lambda = \frac{1}{1 + \frac{1}{2} A} \left( 1 - \frac{1}{2} A \pm \sqrt{-2A} \right). \quad (6.3)$$

Examination of (6.3) shows that it always gives amplification factors satisfying

$$|\lambda| = 1, \quad (6.4)$$

and so the scheme is unconditionally stable and neutral. Using (6.3) and (4.17), we find for the relative phase speed of the nonstationary solutions,

$$\frac{c^*}{\sqrt{gH}} = \frac{1}{\mu \sqrt{2gH(X^2 + Y^2)}} \arctan \left( \mp \frac{\sqrt{2A}}{1 - \frac{1}{2} A} \right) \quad (6.5)$$

The numerical values given by (6.5) for the physical mode with  $2\sqrt{gH}\mu = 5$  are shown in Fig. 6.1. The time step is chosen to be of the same order of magnitude as the time steps that are currently used with implicit schemes

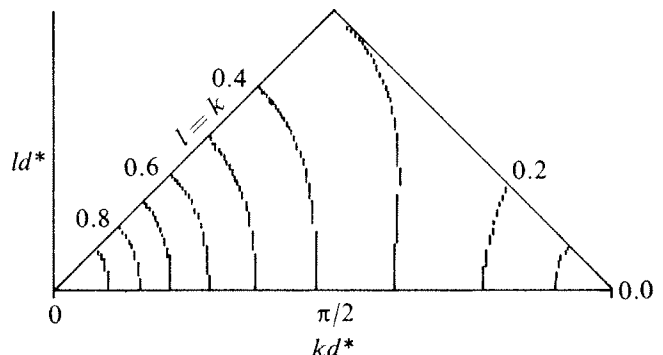


Figure 6.1 Relative phase speed of gravity waves, with implicit time and centered space differencing, and Courant number equal to 5.

in atmospheric models. The wave number region in the figure is the same as in the earlier diagrams, Figs. 2.3 and 4.1. Comparing the isolines of the present figure with those of Fig. 2.3, where the effect of space differencing alone was considered, shows that the effect of time differencing on phase speed is now not negligible. Implicit time differencing is seen to result in a considerable retardation of gravity waves of the same order of magnitude as that due to centered space differencing.

To apply an implicit method it is necessary to solve the difference system for variables at level  $n + 1$ .

With an ordinary oscillation equation, (2.7) in Chapter II, this can be done very simply. For the system (6.1) it is more complex. The quantities  $\delta_x u^{n+1}$  and  $\delta_y v^{n+1}$  can be eliminated from the third equation by applying operators  $\delta_x$  and  $\delta_y$  to the first and second of these equations and substituting the results into the third equation. This gives an equation for the height which can be solved using a number of standard methods: the most popular of these is the *relaxation method* which is discussed later in this section.

Two methods are used to deal with the advection, Coriolis, and other terms of the governing equations, in atmospheric models. One of these, the *splitting method*, will be discussed in the next section. The other is the *semi-implicit method*. There is no advantage in using an implicit method for these additional terms of the governing equations. They are associated with slower phase speeds, and should not require excessively small time steps for linear stability when calculated explicitly. Thus, they can be calculated by an explicit scheme. Since the trapezoidal implicit scheme is a two level scheme like the forward-backward scheme, it is convenient to use the Adams-Basforth scheme for this purpose. Robert (1969) in a spectral model, and subsequently Kwizak and Robert (1971) in a grid point model, chose, however, to use the leapfrog scheme. We then need variables at the middle of the time step used for the implicit differencing, and, therefore, it has to be performed over a time interval of  $2\Delta t$ . However, the scheme is now less economical for gravity waves since these steps have to be made separately for each of the two time levels stored in the leapfrog scheme. In return, we have a differencing for the advection and other additional terms that is neutral and more accurate than Adams-Basforth's. Kwizak and Robert call this combined scheme the *semi-implicit* scheme. It has been used for a number of years in the Canadian operational model, and is becoming increasingly popular in some other operational numerical prediction centres.

The usual procedure used for solving the semi-implicit difference system for variables at time level  $n + 1$  will be illustrated for the shallow water equations. These equations can be written in a compact form

$$\begin{aligned} \frac{\partial u}{\partial t} &= -g \frac{\partial h}{\partial x} + A_u, \quad \frac{\partial v}{\partial t} = -g \frac{\partial h}{\partial y} + A_v, \\ \frac{\partial h}{\partial t} &= -HV \cdot v + A_h, \end{aligned} \quad (6.6)$$

where  $A_u$ ,  $A_v$  and  $A_h$  denote the terms that were omitted in the system (4.8) describing the propagation of pure gravity waves. When we use leapfrog differencing for

these additional terms, and implicit differencing over a time interval  $2\Delta t$  for the gravity wave terms and centered space differencing, (6.6) is replaced by

$$\begin{aligned} u^{n+1} &= u^{n-1} - g\Delta t (\delta_x h^{n-1} + \delta_x h^{n+1}) + 2\Delta t A_u^n, \\ v^{n+1} &= v^{n-1} - g\Delta t (\delta_y h^{n-1} + \delta_y h^{n+1}) + 2\Delta t A_v^n, \\ h^{n+1} &= h^{n-1} - H\Delta t [(\delta_x u + \delta_y v)^{n-1} + (\delta_x u + \delta_y v)^{n+1}] + \\ &\quad + 2\Delta t A_h^n. \end{aligned} \quad (6.7)$$

We now apply the operator  $\delta_x$  to the first, and  $\delta_y$  to the second of these equations, respectively, and add the results. We introduce the notation

$$\delta_{xx} h \equiv \delta_x (\delta_x h) \quad \text{and} \quad \delta_{yy} h \equiv \delta_y (\delta_y h).$$

We obtain

$$\begin{aligned} (\delta_x u + \delta_y v)^{n+1} &= (\delta_x u + \delta_y v)^{n-1} - \\ &- g\Delta t [(\delta_{xx} + \delta_{yy}) h^{n-1} + (\delta_{xx} + \delta_{yy}) h^{n+1}] + \\ &\quad + 2\Delta t (\delta_x A_u + \delta_y A_v)^n. \end{aligned}$$

Substituting the right-hand side into the third of Eqs. (6.7), and defining the "finite difference Laplacian" by

$$\nabla^2 h \equiv (\delta_{xx} + \delta_{yy}) h,$$

we find

$$\begin{aligned} h^{n+1} &= h^{n-1} - 2H\Delta t (\delta_x u + \delta_y v)^{n-1} + \\ &\quad + gH(\Delta t)^2 (\nabla^2 h^{n-1} + \nabla^2 h^{n+1}) + \\ &\quad + 2\Delta t [A_h - H\Delta t (\delta_x A_u + \delta_y A_v)]^n. \end{aligned}$$

Using, in addition, the definitions

$$\begin{aligned} F^{n-1} &\equiv h^{n-1} - 2H\Delta t (\delta_x u + \delta_y v)^{n-1} + gH(\Delta t)^2 \nabla^2 h^{n-1}, \\ G^n &\equiv 2\Delta t [A_h - H\Delta t (\delta_x A_u + \delta_y A_v)]^n, \end{aligned}$$

this can be written as

$$h^{n+1} - gH(\Delta t)^2 \nabla^2 h^{n+1} = F^{n-1} + G^n. \quad (6.8)$$

The terms have been arranged to show that at time level  $n$  the right-hand side is known at all space grid points. Once this equation has been solved for the values  $h^{n+1}$ ,  $u^{n+1}$  and  $v^{n+1}$  can be obtained directly from the first and second of Eqs. (6.7). We now consider ways of solving (6.8).

The quantity  $\nabla^2 h$  on the left side of (6.8) is an approximation to  $\nabla^2 h$ . Using the notation of Fig. 6.2, it can be written as

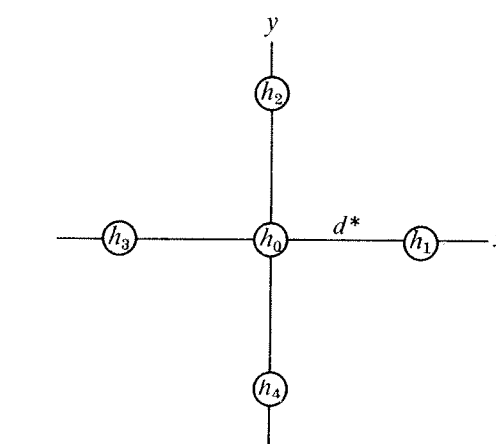


Figure 6.2 Stencil used to calculate the approximation  $\nabla^2 h$ .

Thus, (6.8) is a finite difference approximation to an elliptic equation

$$\nabla^2 h + ah + b(x, y) = 0.$$

To solve such an equation, it is necessary to know the values of  $h(x, y)$  at the boundaries of the computation region. For a numerical solution we write (6.8) at each of the interior grid points where the variable  $h$  is carried. In this way we obtain a system with one equation for each interior grid point. There is one unknown for each grid point. In each of the equations, except the equations for points adjacent to the boundary, there are five of these unknowns. There are no difficulties in principle in solving such a system of linear equations, but, since the number of equations is normally exceedingly large, of the order of 1000 or more, it is not obvious how to set about it.

The method usually used is the relaxation method. This consists of the following steps.

a) An arbitrary guess is made for the field  $h^{n+1}$ . Usually the field of the preceding time step,  $h^n$ , is taken as this *first guess*.

b) At each of the grid points the value  $h^{n+1}$  is changed so as to satisfy the difference equation, in our case (6.8). These changes can be made simultaneously at all grid points (*simultaneous* or *Richardson* relaxation), or sequentially, point by point (*sequential* or *Liebmann* relaxation).

c) The preceding step is repeated as many times as needed to make the change at every point less than some preassigned small value.

The relaxation method always converges. Experience shows that the convergence is faster for sequential relaxation, and also if the changes calculated to satisfy the equation exactly are multiplied by a factor having a value between 1 and 2 (*overrelaxation factor*) before being added on. For a particular problem the optimum value of this overrelaxation factor can easily be found by numerical experiments, in which the number of iterations required is plotted as a function of the value of the overrelaxation factor. This optimum value can be shown to be not much less than 2. More details on the relaxation method can be found in textbooks by Thompson (1961) and by Haltiner (1971).

The algebraic system given by equations of the type (6.8) can also be solved by *direct methods* (e.g. Kreiss and Oliker, 1973, p. 54). Direct method can be more efficient than the relaxation procedure; thus, they are typically used when relaxation requires very large computation time, as may happen, for example, in convection studies. When implicit schemes are used for simulation or prediction of large scale atmospheric motions, the time needed for relaxation is several times less than the time needed for other steps of the integration procedure, so that only a small fraction of the total computer time can be saved by using a faster direct method. For that reason the use of direct methods, requiring a larger programming effort, is not popular in these models.

Generalization to the three-dimensional case of the procedure for solving the semi-implicit system for variables at level  $n + 1$  outlined here is not quite trivial. The reader is referred to the paper by Robert *et al.* (1972).

Implicit schemes were first used extensively in atmospheric models by Marchuk (Марчук, 1957). With the semi-implicit scheme it is also possible to construct an economical grid analogous to the Eliassen grid for the leapfrog scheme; the appropriate space-time staggering of the variables was pointed out by Gerrity and McPherson (1971). A semi-implicit scheme somewhat different from the one outlined here has been developed by Burridge, and is now used in the British operational model (Burridge and Hayes, 1974). Implicit and semi-implicit schemes are undoubtedly the most efficient schemes used in atmospheric models. To achieve this economy we have to put additional effort into solving an elliptic equation. Furthermore they are associated with an appreciable deceleration of gravity waves. Thus, the implicit schemes do not seem suitable for the study of details of the geostrophic adjustment process. However, this deceleration does not appear particularly harmful for the simulation and prediction of the large-scale quasi-geostrophic motions. For example, Kwizak and Robert (1971) have found that barotropic 5-day

forecasts made with explicit differencing and time steps of 10 min are almost identical to those made with semi-implicit differencing and time steps of 60 min. Later Robert *et al.* (1972) have calculated the differences between 5-day forecasts obtained using 30 and 60 min time steps for a baroclinic 5-level semi-implicit model. These differences were found to be insignificant compared to other sources of error normally present in numerical models. However, the model used for these experiments did not include topography, surface friction, and other physical processes; one might expect the deceleration of gravity waves to have a more noticeable effect when these physical processes (e.g. the release of latent heat) are present, since then the gravity waves should be more significant. On the other hand, the computation time saved by the implicit differencing can be used to reduce the grid size on the computation. This would decrease the phase speed error for all the waves, including the gravity waves.

### 7. The splitting or Marchuk method

The complexity of the system of hydrodynamic equations, that is, the simultaneous presence of a number of physical factors, may cause some difficulties. One difficulty was mentioned in the preceding section: if we wanted to approximate (6.6) using a fully implicit scheme we would obtain a system for the variables at level  $n + 1$  that is practically impossible to solve. Also since different physical factors are present in this system we will normally wish to use different schemes for terms associated with them. Thus, considering the linearized system with advection and gravity wave terms,

$$\begin{aligned} \frac{\partial u}{\partial t} + c \frac{\partial u}{\partial x} + g \frac{\partial h}{\partial x} &= 0, \\ \frac{\partial h}{\partial t} + c \frac{\partial h}{\partial x} + H \frac{\partial u}{\partial x} &= 0, \end{aligned} \quad (7.1)$$

we might wish to use one scheme for the advection terms, and another for the gravity wave terms — in much the same way as was done within the semi-implicit scheme. In such a situation, even though both of the schemes to be used are stable considered one at a time, we cannot be certain that the scheme obtained as a combination of the two will also be stable. An example where it is not was given by Kasahara (1965).

These problems can be avoided by using the *splitting method*. The idea of this method is to construct schemes for a complex system of equations so that *within each time step* this system is split into a number of simpler subsystems, which are then solved consecutively one at

a time. In the case of (7.1), within a given time step, we could first solve the system of advection equations

$$\begin{aligned} \frac{\partial u}{\partial t} + c \frac{\partial u}{\partial x} &= 0, \\ \frac{\partial h}{\partial t} + c \frac{\partial h}{\partial x} &= 0. \end{aligned} \quad (7.2)$$

Denote the provisional values  $u^{n+1}, h^{n+1}$  obtained in this way by  $u^*, h^*$ . Use these values at the beginning of the time step for solving the remaining subsystem

$$\begin{aligned} \frac{\partial u}{\partial t} + g \frac{\partial h}{\partial x} &= 0, \\ \frac{\partial h}{\partial t} + H \frac{\partial u}{\partial x} &= 0. \end{aligned} \quad (7.3)$$

The values  $u^{n+1}, h^{n+1}$ , obtained after solving also this other subsystem, are now taken as actual approximate values of these variables at the level  $n + 1$ . The procedure is repeated in each following time step.

A solution obtained by the splitting method will represent a consistent approximation to the true solution. This can be proved easily for a particular choice of schemes for solving the subsystems. The approximate values of the dependent variables then have to approach the true values as the time step approaches zero.

To study the stability of schemes constructed by the splitting method, we consider the example above. Denote by  $\lambda_a$  and  $\lambda_b$  the values of  $\lambda$  of the schemes chosen for the numerical solution of subsystems (7.2) and (7.3), respectively. Then, we have

$$u^* = Re(\lambda_a \lambda^n \hat{u} e^{ikx}), \quad h^* = Re(\lambda_a \lambda^n \hat{h} e^{ikx}),$$

and

$$u^{n+1} = Re(\lambda_b \lambda_a \lambda^n \hat{u} e^{ikx}), \quad h^{n+1} = Re(\lambda_b \lambda_a \lambda^n \hat{h} e^{ikx}).$$

Therefore, we find,

$$\lambda = \lambda_b \lambda_a,$$

and

$$|\lambda| = |\lambda_b| |\lambda_a|.$$

Thus, if both of the schemes chosen for the solution of subsystems (7.2) and (7.3) are stable, the combined scheme constructed by the splitting method will also be stable. This conclusion can be generalized for an arbitrary system of equations and number of subsystems.

When applying the splitting method, we do not necessarily have to use equal time steps for each of the subsystems. This may well be the main advantage of the

splitting method: we can choose a relatively long time step for the subsystem governing a slow process, advection in the present example, and then use a number of smaller steps to calculate the faster process. Since the advection process is the most expensive in computation time within the primitive equations, significant economies can be accomplished in this way. A disadvantage of the method is that calculation of the effects of different physical factors one at a time usually leads to an increase in the truncation error. For example, Burridge and Hayes (1974) suggest that the technique of splitting the governing equations into advection and adjustment stages does not allow time steps longer than 12 to 15 min if the time-truncation is not to become significant.

The splitting method was first used in atmospheric models by Marchuk (Марчук, 1967); thus, in meteorology it is also known as the *Marchuk method*. It would appear that the splitting method is used for most atmospheric models in the Soviet Union. The splitting technique is used also in the British operational model (Burridge and Hayes, 1974), and in a limited area model by Lepas and his collaborators (Lepas *et al.*, 1974).

### 8. Two-grid-interval noise

Unless we are using the lattice (C) shown in Fig. 2.1 we will always have a problem with two-grid-interval waves. These are false stationary waves appearing as neutral solutions of the difference equations for gravity waves. When the Coriolis terms are also present, as seen in Section 3, the two-grid-interval waves appear with false low frequencies as pure inertia waves, or, with lattice (D), as stationary waves.

A number of methods have been used to cope with this. In many models dissipative schemes are used to give maximum damping for the two-grid-interval wave, or lateral diffusion is added with relatively large diffusion coefficients. The appearance of excessive two-grid-interval noise is thereby suppressed. However, instead of attacking the *consequences* of inadequacies in a simulation of a physical process, it is generally better to look for a method that would achieve a physically correct simulation of that process, and thus eliminate the *cause* of the difficulty. One method this kind for dealing with the two-grid-interval wave problem has been suggested and used by Arakawa (1972). It consists of an intermittent use of uncentered space differencing within the gravity wave terms, performed alternately on opposite sides of the central point.

Mesinger (1973) showed how two-grid-interval wave noise could be prevented in some cases even by using cen-

tered differencing; this method will be outlined briefly here. We consider the system of linearized gravity wave equations

$$\frac{\partial u}{\partial t} + g \frac{\partial h}{\partial x} = 0, \quad \frac{\partial v}{\partial t} + g \frac{\partial h}{\partial y} = 0, \quad (8.1)$$

$$\frac{\partial h}{\partial t} + H \nabla \cdot \mathbf{v} = 0.$$

Consider any two neighbouring height points for example within the lattice (E). A height perturbation at one of these points cannot affect the other point because there is no velocity point in between; this velocity is needed to cause a height change at the other point through the divergence term in the continuity equation. To circumvent this difficulty we can introduce auxiliary velocity points midway between the height points. Velocity components at these auxiliary points can be assumed equal to an average of velocities at the two neighbouring velocity points at the beginning of a time step, and the acceleration contributions can then be evaluated and added to these initial values to obtain components at the middle or at the end of the time step. Only the velocity components and accelerations along directions joining the two height points are needed, and these accelerations can be calculated using the height values at the two points. The resulting velocity components can then be used for a more accurate calculation of the divergence term in the continuity equation. In this way schemes are obtained in which a height perturbation at a single grid point is propagated by gravity waves to all the other height grid points. Therefore there can be no grid-splitting and two grid-interval noise in the height field. Since a velocity perturbation can propagate as a gravity wave only by exciting height perturbations, the procedure will prevent false two-grid-interval noise in all the variables.

We shall illustrate this procedure using the implicit scheme, (6.1). The velocity components at regular velocity points are computed in the same way as before, so the first two equations of that system remain unchanged. To calculate the velocity divergence in the continuity equation we define auxiliary velocity points midway between the neighbouring height points, as shown by the circled numbers 5, 6, 7 and 8 in Fig. 8.1. Using the system  $x'$ ,  $y'$  shown in this figure, components  $u'$  are needed at points 5 and 7, and components  $v'$  at points 6 and 8. At the beginning of the time step  $\Delta t$  these components are obtained by

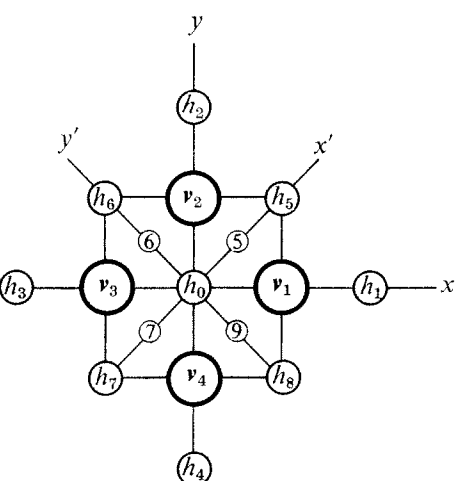


Figure 8.1 Stencil used to denote the height and velocity grid-point values surrounding a height point.

space-averaging, that is

$$u'^n = \frac{\sqrt{2}}{2} (\bar{u}'^n + \bar{v}'^n), \quad v'^n = \frac{\sqrt{2}}{2} (-\bar{u}'^n + \bar{v}'^n).$$

An overbar denotes a two-point average taken along the direction indicated following the bar sign. Acceleration contributions are added to these initial values to obtain values at the end of the time step,

$$u'^{n+1} = u'^n - g \Delta t \frac{1}{2} (\delta_{x'} h^n + \delta_{x'} h^{n+1}),$$

$$v'^{n+1} = v'^n - g \Delta t \frac{1}{2} (\delta_{y'} h^n + \delta_{y'} h^{n+1}).$$

The velocity divergence in the continuity equation can now be approximated by

$$\frac{1}{2} (\delta_x u + \delta_y v) + \frac{1}{2} (\delta_{x'} u' + \delta_{y'} v'),$$

giving equal weight to all eight directions of the lattice. In this way the implicit approximation to the continuity equation may be obtained as

$$h^{n+1} = h^n - H \Delta t (\delta_x u + \delta_y v)^n +$$

$$+ \frac{1}{4} g H (\Delta t)^2 (\nabla_0^2 h^n + \nabla_0^2 h^{n+1}). \quad (8.2)$$

Here the velocity components at level  $n+1$  have already been eliminated using the first two of Eqs. (6.1), and

$$\nabla_0^2 h \equiv \frac{1}{4 d^2} \times \quad (8.3)$$

$$\times [h_1 + h_2 + h_3 + h_4 + 2(h_5 + h_6 + h_7 + h_8) - 12 h_0].$$

This is again a finite difference approximation to  $\nabla^2 h$ , but now it is calculated using the height values of nine neighbouring height points.

Comparing this scheme with the standard implicit scheme of Section 6, the only modification is that this nine-point Laplacian has replaced the five-point Laplacian (6.9) in the continuity equation. This allows propagation of gravity waves between all height points of the grid, thus admitting no false space noise in the height field. A more detailed analysis of the properties of the scheme can be found in Mesinger (1973). The modification, for example, has no effect on the unconditional stability of the implicit scheme; however, instead of being neutral for all waves, the scheme now damps shorter waves to some extent. The modified scheme has a smaller truncation error than the unmodified scheme.

Analogous modifications of some other schemes have been discussed in papers by Janjić (1974) and Mesinger (1974). All of these papers show that the modified schemes are strikingly superior in the case of a stationary circular vortex, forced at a single height grid point. A note by Mesinger and Janjić (1974) provides, furthermore, a dramatic illustration of the advantages of the proposed method in the case of a limited area model, requiring lateral boundary conditions to be prescribed. In a 5-level model using the unmodified forward-backward scheme, intense short-wave noise was generated at the boundaries of the region, a problem noticed also by earlier investigators (e.g. Miller *et al.*, 1972; Krishnamurti *et al.*, 1973). With the scheme modified along these lines, however, there were no difficulties due to the prescribed boundary conditions, even with no lateral diffusion in the model.

It is important to be aware that this method is *not* attempting to improve the calculation of short gravity waves of wave lengths close to two grid intervals. At this scale the finite difference representation is very poor, and significant improvements in accuracy can hardly be expected. The problem is that gravity waves, with longer wave lengths can propagate independently on individual (C) type subgrids, and thus erroneously appear to have wave lengths close to two grid intervals. Thus, we are confronted with a kind of aliasing error. The proposed method enables these waves to appear with wave lengths close to their physical value instead in the noise region with wave lengths close to two grid intervals.

## 9. Time noise and time filtering

In addition to the appearance of spurious short-wave noise in space, spurious short-wave noise in time, that is, high frequency noise can appear in numerical models.

One mechanism causing this when the leapfrog scheme is used for nonlinear equations is the separation of solutions at alternate time steps, generating two-grid-interval noise in time. Such separation is illustrated in a paper by Lilly (1965, p. 23).

High frequency noise appears in atmospheric models also as a result of difficulties in observing initial conditions representative of the large scale atmospheric motions. The observed initial conditions contain instrumental errors, are influenced by meso and small scale motions, are not known at grid points of the model, and, finally, are completely absent over relatively large areas of the globe. As a result of all of these factors, if initial grid point values are interpolated directly from the observed data the numerical forecasts will contain spurious gravity waves of unrealistically large amplitudes.

In the early successful integrations of the primitive equations these problems were partially bypassed by obtaining the initial winds from the initial geopotential fields as a solution of the *balance equation* — the equation obtained by assuming the initial velocity divergence and its time derivative to be equal to zero. Initial conditions prepared in this way (e.g. Haltiner, 1971) prevent excessive high-frequency gravity wave noise.

It is now generally accepted that this is not the best way of preparing the initial conditions. First, the wind data are not used when solving the balance equation, and some information is lost. It has also been shown (e.g. Phillips, 1960b; Winninghoff, 1968) that the presence of a realistic initial divergent wind field should have a beneficial effect on the forecast. Finally, an increasing fraction of the observations are now continuous, and in time not obtained at specific times. The methods being used to extract the maximum information from this type of data rely more on running a prediction model to adjust the data in space and time (e.g. Bengtsson, 1975). In such an integration relatively intense high frequency noise is generated.

The first of the mechanisms mentioned here, separation of solutions at alternate time steps, has to be suppressed in some way — otherwise it may lead to a complete breakdown of the integration. One method that is used for this purpose is an intermittent step made with a two level scheme. A weakness of such a procedure is that the choice of the solution that is eliminated is arbitrary.

Experience shows that the noise generated by assimilation of the observed data typically dies out to an acceptable level in about 24 hours of simulated time due to geostrophic adjustment. However, it may be desirable to accelerate this adjustment by appropriate numerical techniques. The Matsuno scheme can be used for this purpose.

Another method that can be used to increase the damping of high frequency noise in atmospheric models is *time filtering* originally proposed by Roberts (1966). To apply this at least three consecutive values of the function to be filtered are needed. We shall consider the simplest case where this minimum number of three values is used. It suffices to consider one function only, which we assume to be a solution of the oscillation equation. Thus, we consider the function

$$U(t) = U(0) e^{i\omega t}, \quad (9.1)$$

where the values  $U(t-\Delta t)$ ,  $U(t)$  and  $U(t+\Delta t)$  are known.

We shall first examine the effect of changing only the middle of these three values using the relation

$$\bar{U}(t) = U(t) + \frac{1}{2} S \times \\ \times [U(t-\Delta t) - 2U(t) + U(t+\Delta t)], \quad (9.2)$$

known as the *centered filter*. The overbar now denotes the filtered value of a function, and  $S$  is the *filter parameter*. The expression within the square bracket in (9.2) is proportional to the simplest approximation to the second derivative in time; thus, for sufficiently small positive values of  $S$  application of the filter (9.2) will decrease the curvature in a graph of the three values of  $U(t)$ .

For a quantitative analysis of the effect of the filter we define

$$\bar{U}(t) \equiv R U(t), \quad (9.3)$$

where the complex factor  $R$  is called the *response* of the filter. When this is substituted into (9.2) and we use (9.1), we obtain

$$R = 1 - S(1 - \cos \omega \Delta t). \quad (9.4)$$

It is convenient to define  $R \equiv |R| e^{i\delta}$ .

We can then say that the phase change  $\delta$  resulting from the centered filter is zero, and that within the CFL stability criterion and for small positive values of  $S$  the amplitude factor  $|R|$  exerts a damping effect increasing with increasing frequencies.

When, however, a filter is continually applied during a numerical integration, the value  $U(t-\Delta t)$  has already

been changed prior to changing  $U(t)$ . It is then appropriate to consider the filter

$$\bar{U}(t) = U(t) + \frac{1}{2} S \times \\ \times [U(t-\Delta t) - 2U(t) + U(t+\Delta t)]. \quad (9.5)$$

Asselin (1972) calls this the *basic time filter*. A procedure like the one used in deriving (9.4) now gives

$$R = \frac{(2-S)^2 + 2S^2(1 - \cos \omega \Delta t)}{(2-S)^2 + 4S(1 - \cos \omega \Delta t)} e^{i\omega \Delta t}. \quad (9.6)$$

Thus, there is now a phase change that is different from zero; however, it is small for small values of  $\omega \Delta t$ . The amplitude factor is not much different from that of the centered filter for small values of  $S$ . More details can be found in the paper by Asselin.

An analysis of the effect of the time filter for some particular choices of time differencing schemes — the leapfrog, implicit and semi-implicit schemes — can also be found in the paper by Asselin. We find, for example, that the time filter in conjunction with the leapfrog scheme can give a procedure damping the high frequencies in a more selective way than the Matsuno scheme — less for low frequencies and more for high frequencies. Since the computer time needed for application of the filter is relatively small, this means that one obtains a better result with only about half of the computer time. However, the application of the filter does require the storage of the time dependent variables at three time levels, that is, at one level more than with the standard leapfrog scheme.

Using an analogous approach one can analyze the effect of smoothing and filtering in space. The reader is referred to a review article by Shapiro (1970) or the textbook by Haltiner (1971). It is, however, not obvious that there are physical or computational reasons for using two-dimensional space filtering in atmospheric models.

## 10. Dissipation in numerical schemes

In concluding this chapter we add, following Arakawa (1970), a few remarks regarding the role of dissipation that may be inherent in numerical schemes. The discussion of the preceding chapter shows that the use of dissipative schemes for the *advection process* should be avoided — provided care is taken to avoid a false cascade of energy to short waves. However, such short waves can still be generated as a result of false reflections at boundaries on the down-stream side of the region (Matsuno, 1966c), or false reflections at sudden jumps in the grid size, or at places where coefficients change rapidly. The use of dissipative advection schemes at those places, and only at those places, is justified.

The situation is different when we are now considering the gravity-inertia wave terms, governing the geostrophic adjustment process. This process is a result of the dispersion of high frequency waves. Use of a frequency-selective dissipative scheme will make these high frequency waves damp out at a faster rate, and thus accelerate the adjustment process, although the actual physical process is dispersive rather than dissipative. This gives an effect much the same as that of time filtering. Therefore, if we are only interested in the final result of the geostrophic adjustment process, dissipation in the gravity-inertia wave terms may be helpful, especially when the high frequency waves are predominantly unphysical. If we are interested in the high frequency waves themselves, the use of a dissipative scheme must, of course, be avoided.

## REFERENCES

- Марчук, Г. И., 1967. Численные методы в прогнозе погоды. Ленинград. Гидрометеорологическое издательство, 356 стр.
- Ames, W. F., 1969. *Numerical Methods for Partial Differential Equations*. London, Nelson. 291 pp.
- Anderson, D. and Fattah, B., 1974. *A comparison of numerical solutions of the advective equation*. J. Atmos. Sci., 31, 1500–1506.
- Arakawa, A., 1966. *Computational design for long-term numerical integration of the equations of fluid motion: Two dimensional incompressible flow. Part I*. J. Comput. Phys., 1, 119–143.
- 1970. *Numerical simulation of large-scale atmospheric motions. Numerical Solution of Field Problems in Continuum Physics*, Proc. Symp. Appl. Math., Durham, N. C., 1968. SIAM-AMS Proc., 2, 24–40.
- 1972. *Design of the UCLA general circulation model. Numerical Simulation of Weather and Climate*, Dept. of Meteorology, Univ. of California, Los Angeles, Tech. Rept. 7, 116 pp.
- and Lamb, V. R., 1976. *Computational design of the UCLA General Circulation Model*. To be published in *Methods in Computational Physics*, Academic Press, New York.
- Asselin, R., 1972. *Frequency filter for time integrations*. Mon. Wea. Rev., 100, 487–490.
- Bengtsson, L., 1975. *4-dimensional assimilation of meteorological observations*. WMO/ICSU Joint Organizing Committee, GARP Publications Series No. 15, 76 pp.
- Bjerknes, V., 1904. *Das Problem der Wettervorhersage, betrachtet vom Standpunkte der Mechanik und der Physik*. Meteor. Zeitschr., 21, 1–7.
- Burridge, D. M. and Hayes, F. R., 1974. *Development of the British operational model*. The GARP Programme on Numerical Experimentation, Rept. 4, 102–104.
- Charney, J. G., 1966. *Some remaining problems in numerical weather prediction*. Advances in Numerical Weather Prediction, Hartford, Conn., Travelers Research Center, Inc., 61–70.
- , Fjørtoft, R. and von Neumann, J., 1950. *Numerical integration of the barotropic vorticity equation*. Tellus, 2, 237–254.
- Courant, R., Friedrichs, K. and Lewy, H., 1928. *Über die partiellen Differenzengleichungen der mathematischen Physik*. Math. Annalen, 100, 32–74.
- and Hilbert, D., 1953. *Methods of Mathematical Physics, Vol. I*. New York, Interscience. 562 pp.
- Cullen, M. J. P., 1974. *Integration of the primitive equations on a sphere using the finite element method*. Quart. J. Roy. Meteor. Soc., 100, 555–562.
- Deardorff, J. W., 1974. *Three-dimensional numerical study of the height and mean structure of a heated planetary boundary layer*. Boundary-Layer Meteor., 7, 81–106.
- Egger, J., 1971. *Mindestgrösse von Gebirgen und Konvektionsgebieten, die in den Modellen der numerischen Vorhersage berücksichtigt werden können*. Beitr. Phys. Atmos., 44, 245–271.
- Eliassen, A., 1956. *A procedure for numerical integration of the primitive equations of the two-parameter model of the atmosphere*. Large-Scale Synoptic Processes, Dept. of Meteorology, Univ. of California, Los Angeles, Sci. Rept. 4, 53 pp.
- Fischer, G., 1959. *Ein numerisches Verfahren zur Errechnung von Windstau und Gezeiten in Randmeeren*. Tellus, 11, 60–76.
- Fjørtoft, R., 1953. *On the changes in the spectral distribution of kinetic energy for two-dimensional, nondivergent flow*. Tellus, 5, 225–230.
- Gadd, A. J., 1974a. *An economical explicit integration scheme*. Meteorological Office Tech. Note 44, 7 pp.
- 1974b. *Fourth order advection schemes for the 10 level model*. Meteorological Office Tech. Note 45, 8 pp.
- Gerrity, J. P., Jr. and McPherson, R. D., 1971. *On an efficient scheme for the numerical integration of a primitive-equation barotropic model*. J. Appl. Meteor., 10, 353–363.
- Haltiner, G. J., 1971. *Numerical Weather Prediction*. New York, Wiley, 317 pp.
- Harlow, F. H. and Amsden, A. A., 1971. *Fluid dynamics*. Los Alamos Scientific Laboratory of the Univ. of California, Monograph LA-4700, 115 pp.
- Hinkelmann, K., 1959. *Ein numerisches Experiment mit den primitiven Gleichungen*. The Atmosphere and the Sea in Motion, Rossby Memorial Volume, New York, Rockefeller Institute Press, 486–500.
- Janjić, Z. I., 1974. *A stable centered difference scheme free of two-grid interval noise*. Mon. Wea. Rev., 102, 319–323.
- Jespersen, D. C., 1974. *Arakawa's method is a finite-element method*. J. Comput. Phys., 16, 383–390.
- Kasahara, A., 1965. *On certain finite-difference methods for fluid dynamics*. Mon. Wea. Rev., 93, 27–31.
- 1969. *Simulation of the earth's atmosphere*. National Center for Atmospheric Research, Boulder, Colo., NCAR Manuscript 69–27, 42 pp.
- Kreiss, H. and Oliker J., 1973. *Methods for the approximate solution of time dependent problems*. WMO/ICSU Joint Organizing Committee, GARP Publications Series No. 10, 107 pp.
- Krishnamurti, T. N., Kanamitsu, M., Ceselski, B. and Mathur, M. B., 1973. *Florida State University's Tropical Prediction Model*. Tellus, 25, 523–535.
- Kurihara, Y., 1965. *On the use of implicit and iterative methods for the time integration of the wave equation*. Mon. Wea. Rev., 93, 33–46.

- Kwizak, M. and Robert, A. J., 1971. *A semi-implicit scheme for grid point atmospheric models of the primitive equations*. Mon. Wea. Rev., 99, 32-36.
- Lax, P. D. and Wendroff, B., 1960. *Systems of conservation laws*. Commun. Pure Appl. Math., 13, 217-237.
- Leith, C., 1965. *Lagrangian advection in an atmospheric model*. WMO-IUGG Symposium on Research and Development Aspects of Long Range Forecasting, Boulder, Colo., 1964. WMO Tech. Note 66, 168-176.
- Lepas, J., Benlareche, M., Coiffier, J., Finke, L. and Tagnit-Hammou, A., 1974. *Primitive equations model — implicit method for numerical integration*. The GARP Programme on Numerical Experimentation, Rept. 4, 65.
- Lilly, D. K., 1965. *On the computational stability of numerical solutions of time-dependent non-linear geophysical fluid dynamics problems*. Mon. Wea. Rev., 93, 11-26.
- Matsuno, T., 1966a. *Numerical integrations of the primitive equations by a simulated backward difference method*. J. Meteor. Soc. Japan, Ser. 2, 44, 76-84.
- 1966b. *A finite difference scheme for time integrations of oscillatory equations with second order accuracy and sharp cut-off for high frequencies*. J. Meteor. Soc. Japan, Ser. 2, 44, 85-88.
- 1966c. *False reflection of waves at the boundary due to the use of finite differences*. J. Meteor. Soc. Japan, Ser. 2, 44, 145-157.
- Mesinger, F., 1971. *Numerical integration of the primitive equations with a floating set of computation points : Experiments with a barotropic global model*. Mon. Wea. Rev., 99, 15-29.
- 1973. *A method for construction of second-order accuracy difference schemes permitting no false two-grid-interval wave in the height field*. Tellus, 25, 444-458.
- 1974. *An economical explicit scheme which inherently prevents the false two-grid-interval wave in the forecast fields*. Difference and Spectral Methods for Atmosphere and Ocean Dynamics Problems, Proc. Symp., Novosibirsk, 1973, Part II, 18-34.
- and Janjić Z. I., 1974. *Noise due to time-dependent boundary conditions in limited area models*. The GARP Programme on Numerical Experimentation, Rept. 4, 31-32.
- Miller, B. I., Chase, P. P. and Jarvinen, B. R., 1972. *Numerical prediction of tropical weather systems*. Mon. Wea. Rev., 100, 825-835.
- Orszag, S. A., 1971. *On the elimination of aliasing in finite-difference schemes by filtering high-wavenumber components*. J. Atmos. Sci., 28, 1074.
- Phillips, N. A., 1956. *The general circulation of the atmosphere : a numerical experiment*. Quart. J. Roy. Meteor. Soc., 82, 123-164.
- 1959. *An example of non-linear computational instability*. The Atmosphere and the Sea in Motion, Rossby Memorial Volume, New York, Rockefeller Institute Press, 501-504.
- 1960a. *Numerical weather prediction*. Advances in Computers, New York, Academic Press, 1, 43-90.
- 1960b. *On the problem of initial data for the primitive equations*. Tellus, 12, 121-126.
- Platzman, G. W., 1958. *The lattice structure of the finite-difference primitive and vorticity equations*. Mon. Wea. Rev., 86, 285-292.
- 1963. *The dynamical prediction of wind tides on Lake Erie*. Meteor. Monogr., 4, No. 26, 44 pp.
- 1964. *An exact integral of complete spectral equations for unsteady one-dimensional flow*. Dynamical Prediction Group, Dept. of the Geophysical Sciences, Univ. of Chicago, Tech. Rept. 16, 28 pp.
- Richardson, L. F., 1922. *Weather Prediction by Numerical Process*. London, Cambridge University Press/reprinted : Dover, 1965/. 236 pp.
- Richtmyer, R. D., 1963. *A survey of difference methods for non-steady fluid dynamics*. National Center for Atmospheric Research, Boulder, Colo., NCAR Tech. Notes 63-2, 25 pp.
- and Morton, K. W., 1967. *Difference Methods for Initial Value Problems*. New York, Interscience. 406 pp.
- Robert, A. J., 1966. *The integration of a low order spectral form of the primitive meteorological equations*. J. Meteor. Soc. Japan, Ser. 2, 44, 237-245.
- 1969. *The integration of a spectral model of the atmosphere by the implicit method*. Proc. WMO/IUGG Symposium on Numerical Weather Prediction in Tokyo, 1968. Meteor. Soc. Japan. VII-19-VII-24.
- Henderson, J. and Turnbull, C., 1972. *An implicit time integration scheme for baroclinic models of the atmosphere*. Mon. Wea. Rev., 100, 329-335.
- 1974. *Computational resolution requirements for accurate medium-range numerical predictions*. Difference and Spectral Methods for Atmosphere and Ocean Dynamics Problems, Proc. Symp., Novosibirsk, 1973, Part I, 82-102.
- Sawyer, J. S., 1972. *Numerical weather prediction within World Weather Watch—past, present and future*. Tenth Anniversary of the World Weather Watch, Geneva, WMO Publ. No. 342, 33-44.
- Shapiro, R., 1970. *Smoothing, filtering, and boundary effects*. Rev. Geophys. Space Phys., 8, 359-387.
- Shuman, F. G., 1974. *Analysis and experiment in nonlinear computational stability*. Difference and Spectral Methods for Atmosphere and Ocean Dynamics Problems, Proc. Symp., Novosibirsk, Part I, 51-81.
- Brown, J. A. and Campana, K., 1975. *A new explicit differencing system for primitive equations*. In preparation.
- Sielecki, A., 1968. *An energy-conserving difference scheme for the storm surge equations*. Mon. Wea. Rev., 96, 150-156.
- Thompson, P. D., 1961. *Numerical Weather Analysis and Prediction*. New York, Macmillan. 170 pp.
- Winninghoff, F. J., 1968. *On the adjustment toward a geostrophic balance in a simple primitive equation model with application to the problems of initialization and objective analysis*. Ph. D. thesis, Dept. of Meteorology, Univ. of California, Los Angeles, 161 pp.
- Wurtele, M. G., 1961. *On the problem of truncation error*. Tellus, 13, 379-391.
- Young, J. A., 1968. *Comparative properties of some time differencing schemes for linear and non-linear oscillations*. Mon. Wea. Rev., 96, 357-364.

## GARP PUBLICATIONS SERIES

- No. 1 An Introduction to GARP
- No. 2 COSPAR Working Group VI Report to JOC—Systems Possibilities for an Early GARP Experiment (out of print)
- No. 3 The Planning of the First GARP Global Experiment (out of print)
- No. 4 The Planning of GARP Tropical Experiments (out of print)
- No. 5 Problems of Atmospheric Radiation in GARP
- No. 6 Numerical Experimentation Related to GARP
- No. 7 The GARP Programme on Numerical Experimentation
- No. 8 Parameterization of Sub-Grid Scale Processes
- No. 9 The Basic Data Set Project
- No. 10 Methods for the Approximate Solution of Time-Dependent Problems
- No. 11 The First GARP Global Experiment — Objectives and Plans
- No. 12 The Complete Atmospheric Energetics Experiment (CAENEX)
- No. 13 The Air Mass Transformation Experiment (AMTEX)
- No. 14 Modelling for the First GARP Global Experiment
- No. 15 Four-Dimensional Assimilation of Meteorological Observations
- No. 16 The Physical Basis of Climate and Climate Modelling
- No. 17 Numerical Methods Used in Atmospheric Models
- No. 18 The Monsoon Experiment (MONEX)

## GARP SPECIAL REPORTS

- No. 1 Report of Planning Conference on GARP — Brussels, March 1970
- No. 2 Report of Interim Planning Group on GARP Tropical Experiment in the Atlantic — London, July 1970
- No. 3 Report of the First Session of the Tropical Experiment Council — Geneva, February 1971
- No. 4 Report of the First Session of the Tropical Experiment Board — Geneva, February 1971
- No. 5 Report of the Second Session of the Tropical Experiment Board — Geneva, December 1971
- No. 6 Report of the Third Session of the Tropical Experiment Board — Geneva, April 1972 (out of print)
- No. 7 Report of the Second Session of the Tropical Experiment Council — Geneva, September 1972
- No. 8 Report of the Planning Conference on the First GARP Global Experiment — Geneva, September 1972
- No. 9 Report of the Fourth Session of the Tropical Experiment Board — Geneva, March 1973 (out of print)
- No. 10 Report on Special Observing Systems for the First GARP Global Experiment — Geneva, February 1973
- No. 11 Report of the Fifth Session of the Tropical Experiment Board — Geneva, December 1973
- No. 12 Report of the Sixth Session of the Tropical Experiment Board — Geneva, April 1974
- No. 13 Report of the Meeting on Drifting Buoys for the First GARP Global Experiment — Geneva, March 1974
- No. 14 Report of the First Session of WMO Executive Committee Inter-Governmental Panel on the First GARP Global Experiment — Geneva, October 1974
- No. 15 Report of the Seventh Session of the Tropical Experiment Board — Geneva, February 1975
- No. 16 Report of the Meeting of Experts for the Development of a Data Management Plan for the FGGE — Washington, April 1975
- No. 17 Report of the Second Session of WMO Executive Committee Inter-Governmental Panel on the First GARP Global Experiment — Geneva, September 1975 (in preparation)
- No. 18 Report of the Inter-Governmental Planning Meeting for the First GARP Global Experiment — Geneva, February 1976
- No. 19 Report of the Extraordinary Session of WMO Executive Committee Inter-Governmental Panel on the First GARP Global Experiment — Geneva, February 1976
- No. 20 Report of the Eighth Session of the Tropical Experiment Board — Geneva, May 1976
- No. 21 Report of the Planning Meeting for the Monsoon-77 Experiment — Colombo, Sri Lanka, May 1976
- No. 22 Report of the Third Session of WMO Executive Committee Inter-Governmental Panel on the First GARP Global Experiment — Geneva, July 1976

By arrangement between ICSU and WMO, these publications are on sale and copies can be obtained from the Secretariat of the World Meteorological Organization, Case postale No. 5, CH-1211 Geneva 20, Switzerland.